Appendix A.7:

50 Eureka St – VsVp 57195

Table 1: Site Description for 50 Eureka Street (v_Sv_P 57195).

Attribute	Yes/No 10-m Buffer	Yes/No 20-m Buffer	Yes/No 50-m Buffer	Description/Date	Symbol in Figure 1
Near a body of surface water or other free face features?	No	No	No	The center of the site is 530 meters away from the Avon River.	NA
Lateral spreading observed during the CES?	No	No	No	Ground cracks indicating lateral spreading were not observed by the mapping team.[1]	NA
Nearby buildings or structures?	Yes	Yes	Yes	Residential buildings cover 24% of the 10-m buffer, 21% of the 20-m buffer, and 23% of the 50-m buffer, affecting all quadrants of the buffers.	White Fill + Brown Outline
Sloping land?	No	No	No	Flat residential area.	NA
Step changes in the ground surface?	No	No	No	NA	NA
Retaining walls?	No	No	No	NA	NA
Vegetation?	Yes	Yes	Yes	Trees and bushes cover 24% of the 10-m buffer, 9% of the 20-m buffer, and 15% of the 50-m buffer. They affect all quadrants of the buffers.	White Fill + Green Outline
Manmade changes to the site between the LiDAR surveys?	Yes	Yes	Yes	Removal of a dwelling in the NE, SE, and SW quadrants sometime between Sep 2014 and Jan 2015, affecting the 10-m and 20-m buffers.	Orange Crossline
Other important factors?	Yes	Yes	Yes	Road covers 9% of the 10-m buffer, 21% of the 20-m buffer, and 10% of the 50-m buffer. Cars are often parked on the road.	Road: White Fill + Gray Outline

Note: Buffer is the area within a circle of a specified radius with VsVp investigations done at its center (172.706500°, -43.509273°).

[1] Canterbury Geotechnical Database. (2012). "Observed Ground Crack Locations", Map Layer CGD0400 - 23 July 2012, retrieved July 09, 2018 from https://canterburygeotechnicaldatabase.projectorbit.com/

Figure 1: Site plan with areas where LiDAR survey data is considered.

Note 1: The areas selected for settlement assessment (Patch A and Road) are free of vegetation, structures, manmade changes, and other important factors that have the potential to influence LiDAR measurements.

Table 2: LiDAR flight error adjustments, global adjustments for the difference between average LiDAR point elevations and benchmark survey elevations, and vertical tectonic movement adjustments.

	Adjustments (mm)		
Earthquake Event(s)	LiDAR Flight Error	Global Offset[2]	Tectonic Vertical Movement
Sep-10	0	-3	0
Feb-11	0	16	-25
Jun-11	0	38	-50
Dec-11	0	-65	10
CES	0	-14	-65
Any LiDAR survey affected by ejecta?			No

Note: The negative sign indicates the subtraction from the ground surface subsidence, while the positive sign indicates the addition to the ground surface subsidence.

[2] Russell, J., & van Ballegooy, S. (2015). *Canterbury Earthquake Sequence: Increased liquefaction vulnerability assessment methodology*. New Zealand: Tonkin & Taylor Ltd.

Table 3a: LiDAR Measurement Error for Patch A.

Surveys	Buffer	Area-Averaged Difference Indicating Repeat Measurement Error (mm)	$\sigma^{*}_{\text{individual LiDAR points}}$ (mm)	%Reduction in σ due to Area Averaging of LiDAR Points
Post Feb 2011: Mar 2011 and May 2011	10-m	NA	59	[181,181]
	20-m	NA		
	50-m	107		
Post Dec 2011: Feb 2012 and Oct 2015	10-m	NA	70	[23,23]
	20-m	NA		
	50-m	16		

*Standard deviation.

Table 3b: LiDAR Measurement Error for Road.

Surveys	Buffer	Area-Averaged Difference Indicating Repeat Measurement Error (mm)	$\sigma^{*}_{\text{individual LiDAR points}}$ (mm)	%Reduction in σ due to Area Averaging of LiDAR Points
Post Feb 2011: Mar 2011 and May 2011	10-m	127	59	[198,220]
	20-m	117		
	50-m	130		
Post Dec 2011: Feb 2012 and Oct 2015	10-m	27	70	[6,39]
	20-m	13		
	50-m	4		

*Standard deviation.

Table 4a: Ground surface subsidence adjustments due to LiDAR measurement error for Patch A.

Earthquake Event(s)	$\sigma^2_{\text{pre-EQ LiDAR survey}}$ (mm)	$\sigma^2_{\text{post-EQ LiDAR survey}}$ (mm)	σ_{total} (mm)	Area Average Adjusted σ (mm) **
Sep-10	158	56	134	±243
Feb-11	56	59	59	±107
Jun-11	59	61	62	±113
Dec-11	61	70	87	±157
CES	158	70	124	±226

**Based on the highest %Reduction in Table 3a.

Table 4b: Ground surface subsidence adjustments due to LiDAR measurement error for Road.

Earthquake Event(s)	$\sigma^2_{\text{pre-EQ LiDAR survey}}$ (mm)	$\sigma^2_{\text{post-EQ LiDAR survey}}$ (mm)	σ_{total} (mm)	Area Average Adjusted σ (mm) **
Sep-10	158	56	134	±295
Feb-11	56	59	59	±130
Jun-11	59	61	62	±137
Dec-11	61	70	87	±191
CES	158	70	124	±274

**Based on the highest %Reduction in Table 3b.

Table 5a: Raw liquefaction-related ground surface subsidence for Patch A using original LiDAR points.

	Average Ground Surface Subsidence (mm)		
Earthquake Event(s)	10-m Buffer	20-m Buffer	50-m Buffer
Sep-10	NA	NA	-76
Feb-11	NA	NA	182
Jun-11	NA	NA	99
Dec-11	NA	NA	23
CES	NA	NA	228

Table 5b: Raw liquefaction-related ground surface subsidence for Road using original LiDAR points.

	Average Ground Surface Subsidence (mm)		
Earthquake Event(s)	10-m Buffer	20-m Buffer	50-m Buffer
Sep-10	-4	-51	-11
Feb-11	162	207	165
Jun-11	122	134	134
Dec-11	6	6	9
CES	286	295	297

Table 6a: Corrected liquefaction-related ground surface subsidence for Patch A using original LiDAR points with the calculated adjustments in Table 2.

	Average Calculated Ground Surface Subsidence (mm)		
Earthquake Event(s)	10-m Buffer	20-m Buffer	50-m Buffer
Sep-10	NA	NA	-79±250
Feb-11	NA	NA	173±100
Jun-11	NA	NA	87±125
Dec-11	NA	NA	-32±150
CES	NA	NA	149±225

Notes: Plus/minus values are same as those in Table 4, but rounded to the nearest 25; Positive overall values indicate ground surface subsidence, while negative overall values indicate ground surface uplift.

Table 6b: Corrected liquefaction-related ground surface subsidence for Road using original LiDAR points with the calculated adjustments in Table 2.

	Average Calculated Ground Surface Subsidence (mm)		
Earthquake Event(s)	10-m Buffer	20-m Buffer	50-m Buffer
Sep-10	-7±300	-54±300	-14±300
Feb-11	153±125	198±125	156±125
Jun-11	110±125	122±125	122±125
Dec-11	-49±175	-49±175	-46±200
CES	207±275	216±275	218±275

Notes: Plus/minus values are same as those in Table 4, but rounded to the nearest 25; Positive overall values indicate ground surface subsidence, while negative overall values indicate ground surface uplift.

Table 7a: Corrected liquefaction-related ground surface subsidence for Patch A using LiDAR DEMs.

	Estimated Ground Surface Subsidence (mm)								
	10-m Buffer			20-m Buffer			50-m Buffer		
Earthquake Event(s)	16th %ile	50th %ile	84th %ile	16th %ile	50th %ile	84th %ile	16th %ile	50th %ile	84th %ile
Sep-10	NA	NA	NA	NA	NA	NA	50	50	50
Feb-11	NA	NA	NA	NA	NA	NA	150	250	250
Jun-11	NA	NA	NA	NA	NA	NA	50	50	50
Dec-11	NA	NA	NA	NA	NA	NA	50	50	50
CES	NA	NA	NA	NA	NA	NA	250	350	350

Note: These percentiles are not the exact statistical measures; they indicate the spatial variability of ground surface subsidence.

Table 7b: Corrected liquefaction-related ground surface subsidence for Road using LiDAR DEMs.

	Estimated Ground Surface Subsidence (mm)								
	10-m Buffer			20-m Buffer			50-m Buffer		
Earthquake Event(s)	16th %ile	50th %ile	84th %ile	16th %ile	50th %ile	84th %ile	16th %ile	50th %ile	84th %ile
Sep-10	50	50	50	50	50	50	50	50	50
Feb-11	150	150	250	150	250	250	150	150	250
Jun-11	50	50	50	50	50	50	50	50	50
Dec-11	50	50	50	50	50	50	50	50	50
CES	350	350	350	350	350	350	350	350	350

Note: These percentiles are not the exact statistical measures; they indicate the spatial variability of ground surface subsidence.

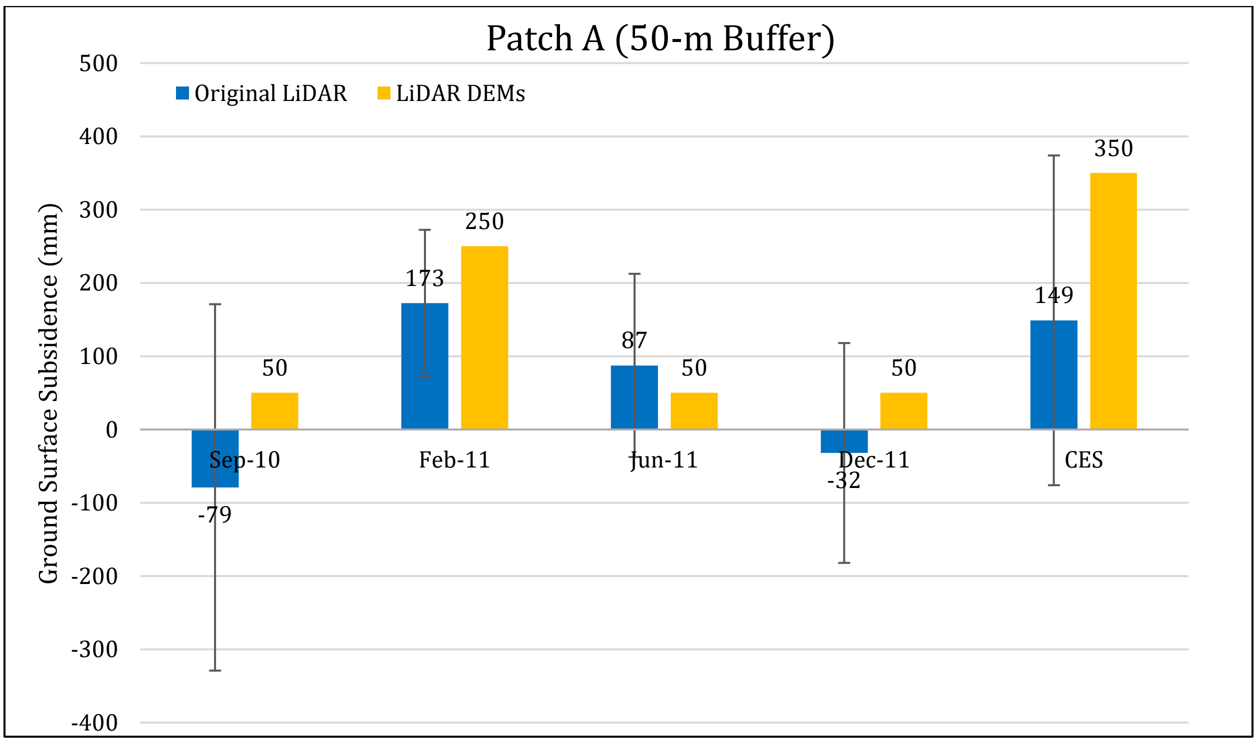

Figure 2: Comparison between ground surface subsidence determined from original LiDAR survey points and ground surface subsidence (50th %ile) estimated using LiDAR DEMs for Patch A within the 50-m buffer.

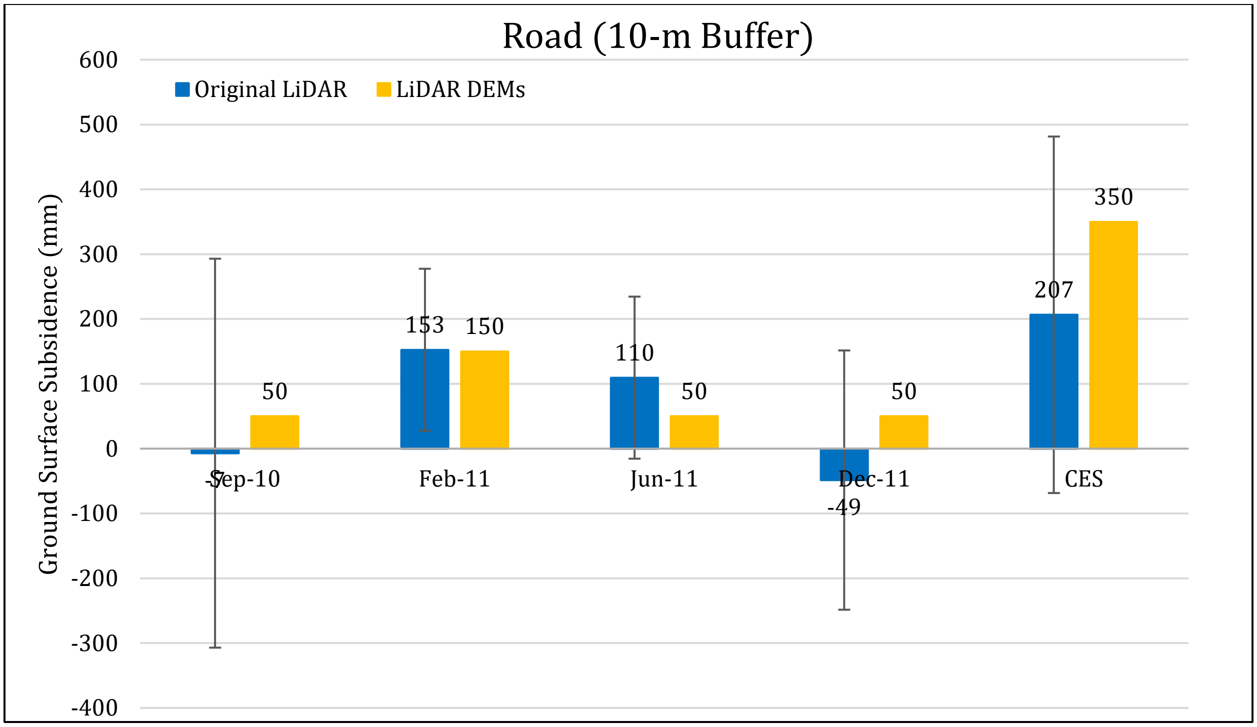

Figure 3: Comparison between ground surface subsidence determined from original LiDAR survey points and ground surface subsidence (50th %ile) estimated using LiDAR DEMs for Road within the 10-m buffer.

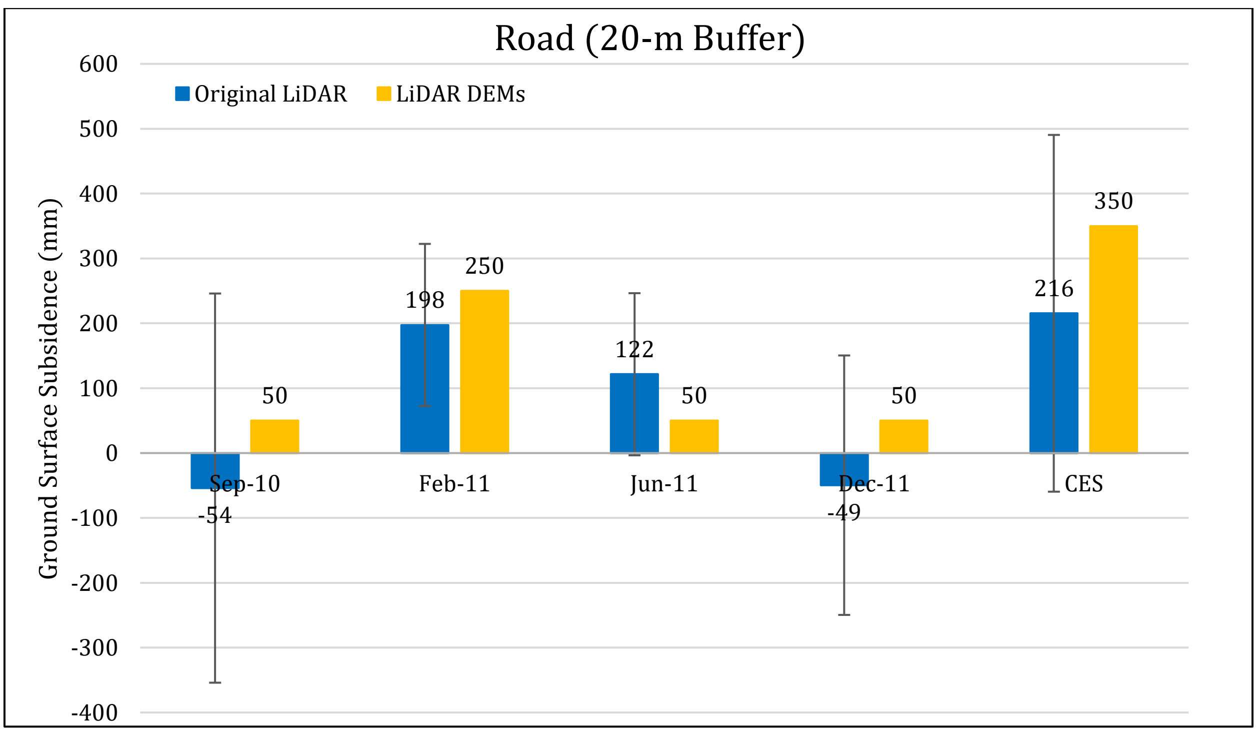

Figure 4: Comparison between ground surface subsidence determined from original LiDAR survey points and ground surface subsidence (50th %ile) estimated using LiDAR DEMs for Road within the 20-m buffer.

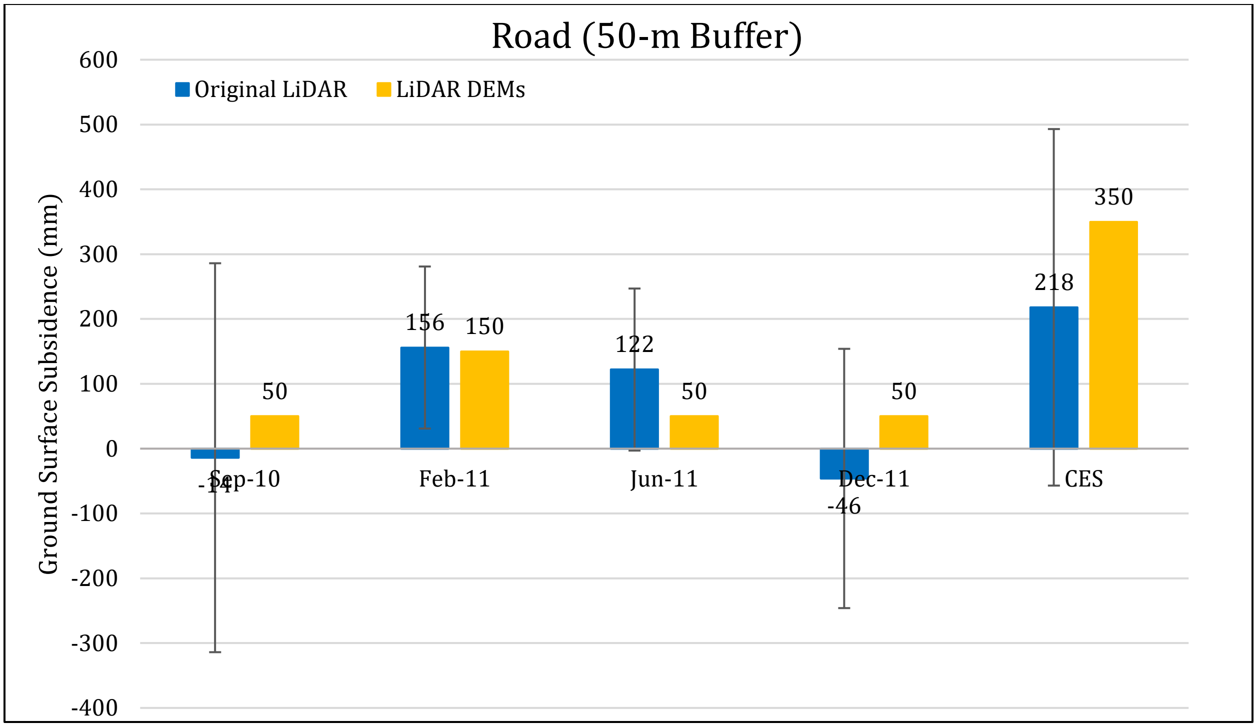

Figure 5: Comparison between ground surface subsidence determined from original LiDAR survey points and ground surface subsidence (50th %ile) estimated using LiDAR DEMs for Road within the 50-m buffer.

Note 2: The ground surface subsidence values determined from original LiDAR survey points for Road are similar to the ground surface subsidence values estimated using LiDAR DEMs for all earthquake events. Some discrepancy between the two methods is observed for Patch A, specifically the Sep-10 EQ and consequently the CES. However, the values determined by the two methods are comparable when the standard deviations are accounted for.

Table 8a: Ejecta-Induced settlement for the top 20 m of the soil profile for Patch A within the 50-m buffer for the 50th %ile PGA, P_L=50%, and C_{FC}=0.13 using BI-2014, ZRB-2002, and I_C cutoff of 2.6.

Earthquake Event	M_W	PGA (g)	Depth to Groundwater (m)	S_T (mm)	S_{V1D} (mm)	$S_{E,L}$ (mm)
Sep-10	7.1	0.18	2.5	-79±250	1±20	-80±251
Feb-11	6.2	0.43	2.5	173±100	15±50	158±112
Jun-11	6.2	0.27	2.5	87±125	6±25	81±128
Dec-11	6.1	0.33	2.0	-32±150	11±50	-43±158

Notes: S_T = Total settlement (Table 6a); S_{V1D} = Average vertical settlement due to volumetric compression using Boulanger and Idriss (2014) (BI-2014) and Zhang et al. (2002) (ZRB-2002) procedures and de Greef and Lengkeek (2018) thin-layer correction; $S_{E,L}$ = Ejecta-induced settlement as the difference between the LiDAR-based S_T and S_{V1D}.

Table 8b: Ejecta-Induced settlement for the top 20 m of the soil profile for Road within the 10-m buffer for the 50th %ile PGA, P_L=50%, and C_{FC}=0.13 using BI-2014, ZRB-2002, and I_C cutoff of 2.6.

Earthquake Event	M_W	PGA (g)	Depth to Groundwater (m)	S_T (mm)	S_{V1D} (mm)	$S_{E,L}$ (mm)
Sep-10	7.1	0.18	2.5	-7±300	4±20	-11±301
Feb-11	6.2	0.43	2.5	153±125	59±50	94±135
Jun-11	6.2	0.27	2.5	110±125	19±25	90±128
Dec-11	6.1	0.33	2.0	-49±200	38±50	-86±206

Notes: S_T = Total settlement (Table 6b); S_{V1D} = Average vertical settlement due to volumetric compression using Boulanger and Idriss (2014) (BI-2014) and Zhang et al. (2002) (ZRB-2002) procedures and de Greef and Lengkeek (2018) thin-layer correction; $S_{E,L}$ = Ejecta-induced settlement as the difference between the LiDAR-based S_T and S_{V1D}.

Table 8c: Ejecta-Induced settlement for the top 20 m of the soil profile for Road within the 20-m buffer for the 50th %ile PGA, P_L=50%, and C_{FC}=0.13 using BI-2014, ZRB-2002, and I_C cutoff of 2.6.

Earthquake Event	M_W	PGA (g)	Depth to Groundwater (m)	S_T (mm)	S_{V1D} (mm)	$S_{E,L}$ (mm)
Sep-10	7.1	0.18	2.5	-54±300	4±20	-58±301
Feb-11	6.2	0.43	2.5	198±125	59±50	139±135
Jun-11	6.2	0.27	2.5	122±125	19±25	103±128
Dec-11	6.1	0.33	2.0	-49±200	38±50	-87±206

Notes: S_T = Total settlement (Table 6b); S_{V1D} = Average vertical settlement due to volumetric compression using Boulanger and Idriss (2014) (BI-2014) and Zhang et al. (2002) (ZRB-2002) procedures and de Greef and Lengkeek (2018) thin-layer correction; $S_{E,L}$ = Ejecta-induced settlement as the difference between the LiDAR-based S_T and S_{V1D}.

Table 8d: Ejecta-Induced settlement for the top 20 m of the soil profile for Road within the 50-m buffer for the 50th %ile PGA, P_L=50%, and C_{FC}=0.13 using BI-2014, ZRB-2002, and I_C cutoff of 2.6.

Earthquake Event	M_W	PGA (g)	Depth to Groundwater (m)	S_T (mm)	S_{V1D} (mm)	$S_{E,L}$ (mm)
Sep-10	7.1	0.18	2.5	-14±300	3±20	-17±301
Feb-11	6.2	0.43	2.5	156±125	53±50	103±135
Jun-11	6.2	0.27	2.5	122±125	14±25	108±128
Dec-11	6.1	0.33	2.0	-46±200	31±50	-77±206

Notes: S_T = Total settlement (Table 6b); S_{V1D} = Average vertical settlement due to volumetric compression using Boulanger and Idriss (2014) (BI-2014) and Zhang et al. (2002) (ZRB-2002) procedures and de Greef and Lengkeek (2018) thin-layer correction; $S_{E,L}$ = Ejecta-induced settlement as the difference between the LiDAR-based S_T and S_{V1D}.

Note 3: The uncertainty for volumetric settlement was derived based on the sensitivity of volumetric settlement to PGA, C_{FC}, and P_L for each earthquake event for VsVp 57203 *Shirley Intermediate School* and CC LIQ 1 – CPT 5586 – *Vivian St* sites. Taking the 50th percentile as the baseline case, the minimum and maximum values corresponding to the difference between the 25th percentile and the 50th percentile and the 75th percentile and the 50th percentile were determined. The arithmetic mean of the range of the minimum and maximum difference was evaluated for each patch at the two sites. The maximum arithmetic mean for each earthquake event was rounded to the nearest five and used as the uncertainty value. Accordingly, the 1-D volumetric settlement uncertainties of ±20, ±50, ±25, and ±50 mm for the Sep-10, Feb-11, Jun-11, and Dec-11 earthquake events, respectively, were used for all sites in this study.

Table 9a: Coverage area and height of ejecta estimates for Patch A (50-m buffer) using photographs.

Earthquake Event	$A_{E,thick}$ (m²)	$H_{E,thick}$ (mm)	$A_{E,thin}$ (m²)	$H_{E,thin}$ (mm)	A_T (m²)
Sep-10	0	0	0	0	92
Feb-11	8	40-80	0	0	92
Jun-11	0	0	0	0	92
Dec-11	0	0	0	0	92

Notes: $A_{E,thick/thin}$ = Coverage area of thick/thin ejecta layers; $H_{E,thick/thin}$ = Lower-upper estimate of height of thick/thin ejecta layers; A_T= Total assessment area of a buffer being considered; Thin and thick layers correspond to light gray and dark gray colors of ejecta observed in aerial photographs.

Table 9b: Coverage area and height of ejecta estimates for Road (10-m buffer) using photographs.

Earthquake Event	H_E (mm)	$V_{E,pyramid}$ (m³)	$V_{E,prism}$ (m³)	A_T (m²)
Sep-10	0	0	0	34.2
Feb-11	55-124	0.557-1.12	0.437-0.874	34.2
Jun-11	0	0	0	34.2
Dec-11	0	0	0	34.2

Notes: H_E = Range of lower and upper estimates of ejecta height near the curb based on 2-4% cross slope of normal crown; $V_{E,pyramid}$ = Lower-upper estimate of total volume of pyramidal-shape ejecta; $V_{E,prism}$ = Lower-upper estimate of total volume of prismatic-shape ejecta; A_T= Total assessment area of a buffer being considered.

Table 9c: Coverage area and height of ejecta estimates for Road (20-m buffer) using photographs.

Earthquake Event	H_E (mm)	$V_{E,pyramid}$ (m^3)	$V_{E,prism}$ (m^3)	A_T (m^2)
Sep-10	0	0	0	258
Feb-11	32-158	1.74-3.47	4.26-8.51	258
Jun-11	0	0	0	258
Dec-11	0	0	0	258

Notes: H_E = Range of lower and upper estimates of ejecta height near the curb based on 2-4% cross slope of normal crown; $V_{E,pyramid}$ = Lower-upper estimate of total volume of pyramidal-shape ejecta; $V_{E,prism}$ = Lower-upper estimate of total volume of prismatic-shape ejecta; A_T= Total assessment area of a buffer being considered.

Table 9d: Coverage area and height of ejecta estimates for Road (50-m buffer) using photographs.

Earthquake Event	H_E (mm)	$V_{E,pyramid}$ (m^3)	$V_{E,prism}$ (m^3)	A_T (m^2)
Sep-10	0	0	0	782
Feb-11	10-165	2.24-4.48	16.4-32.7	782
Jun-11	41-82	0.016-0.032	0.670-1.40	782
Dec-11	0	0	0	782

Note: H_E = Range of lower and upper estimates of ejecta height near the curb based on 2-4% cross slope of normal crown; $V_{E,pyramid}$ = Lower-upper estimate of total volume of pyramidal-shape ejecta; $V_{E,prism}$ = Lower-upper estimate of total volume of prismatic-shape ejecta; A_T= Total assessment area of a buffer being considered.

Note 4:

- The values in Table 9a correspond to the coverage area of ejecta outlined in aerial photographs (Figure 70) and the lower and upper estimates of ejecta height based on ground photographs taken nearby and LDAT property inspection notes (Figure 75). The ejecta-induced settlement using photographs and engineering judgment, $S_{E,P}$, is estimated as

$$S_{E,P} = \frac{\sum_{i=1}^{n} A_{E,thick,i} * H_{E,thick,i} + \sum_{j=1}^{m} A_{E,thin,j} * H_{E,thin,j}}{A_T}$$

  where $A_{E,thick,i}$ and $H_{E,thick,i}$ are the area and the height of a thick ejecta layer, respectively, $A_{E,thin,j}$ and $H_{E,thin,j}$ are the area and the height of a thin ejecta layer, respectively, and A_T is the total assessment area for a buffer being considered (Figure 1).

- The values in Tables 9b, c, and d correspond to the coverage area of ejecta outlined in aerial photographs (Figures 70 and 72) and the lower and upper estimates of ejecta height based on typical 2-4% cross slope of normal road crown, EQC LDAT property inspection reports and ground photographs. The ejecta-induced settlement using photographs and engineering judgment, $S_{E,P}$, is estimated as

$$S_{E,P} = \frac{\sum_{k=1}^{a} \frac{W_{E,k} * H_{E,k} * L_{E,k}}{2} + \sum_{l=1}^{b} \frac{W_{E,l} * H_{E,l} * L_{E,l}}{3}}{A_T} = \frac{\sum_{k=1}^{a} V_{E,prism,k} + \sum_{l=1}^{b} V_{E,pyramid,l}}{A_T}$$

where $W_{E,k}$ and $L_{E,k}$ are the width and the length of the coverage area of a prismatic-shape ejecta layer, respectively, $H_{E,k}$ is the height of a prismatic-shape ejecta layer, $W_{E,l}$ and $L_{E,l}$ are the width and the length of the coverage area of a pyramidal-shape ejecta layer, respectively, $H_{E,l}$ is the height of a pyramidal-shape ejecta layer, and A_T is the total assessment area for a buffer being considered (Figure 1).

Table 10a: Ejecta-induced settlement estimates based on photographs for Patch A.

Earthquake Event	10-m buffer		20-m buffer		50-m buffer	
	$S_{E,P,lower}$ (mm)	$S_{E,P,upper}$ (mm)	$S_{E,P,lower}$ (mm)	$S_{E,P,upper}$ (mm)	$S_{E,P,lower}$ (mm)	$S_{E,P,upper}$ (mm)
Sep-10	NA	NA	NA	NA	0	0
Feb-11	NA	NA	NA	NA	4	7
Jun-11	NA	NA	NA	NA	0	0
Dec-11	NA	NA	NA	NA	0	0

Note: $S_{E,P,lower}$ and $S_{E,P,upper}$ correspond to lower and upper estimates of $S_{E,P}$ (Table 9a), respectively.

Table 10b: Ejecta-induced settlement estimates based on photographs for Road.

Earthquake Event	10-m buffer		20-m buffer		50-m buffer	
	$S_{E,P,lower}$ (mm)	$S_{E,P,upper}$ (mm)	$S_{E,P,lower}$ (mm)	$S_{E,P,upper}$ (mm)	$S_{E,P,lower}$ (mm)	$S_{E,P,upper}$ (mm)
Sep-10	0	0	0	0	0	0
Feb-11	29	58	23	47	24	48
Jun-11	0	0	0	0	1	2
Dec-11	0	0	0	0	0	0

Note: $S_{E,P,lower}$ and $S_{E,P,upper}$ correspond to lower and upper estimates of $S_{E,P}$ (Tables 9b, c, and d), respectively.

Table 11a: Best final estimates of ejecta-induced settlement for Patch A.

EQ Event	10-m buffer			20-m buffer			50-m buffer		
	$S_{E,L}$ (mm)	$S_{E,P}$ (mm)	$S_{E,final}$ (mm)	$S_{E,L}$ (mm)	$S_{E,P}$ (mm)	$S_{E,final}$ (mm)	$S_{E,L}$ (mm)	$S_{E,P}$ (mm)	$S_{E,final}$ (mm)
Sep-10	NA	NA	NA	NA	NA	NA	-80±251	0	0
Feb-11	NA	NA	NA	NA	NA	NA	158±112	5.5±1.5	5±5
Jun-11	NA	NA	NA	NA	NA	NA	81±128	0	0
Dec-11	NA	NA	NA	NA	NA	NA	-43±158	0	0

Notes: $S_{E,L}$ = Ejecta-induced settlement based on LiDAR data reported in Table 8a; $S_{E,P}$ = Median ejecta-induced settlement for the range of values reported in Table 10a; $S_{E,final}$ = Best final estimate of ejecta-induced settlement rounded to the nearest 5; Final plus/minus values are also rounded to the nearest 5.

Table 11b: Best final estimates of ejecta-induced settlement for Road.

EQ Event	10-m buffer			20-m buffer			50-m buffer		
	$S_{E,L}$ (mm)	$S_{E,P}$ (mm)	$S_{E,final}$ (mm)	$S_{E,L}$ (mm)	$S_{E,P}$ (mm)	$S_{E,final}$ (mm)	$S_{E,L}$ (mm)	$S_{E,P}$ (mm)	$S_{E,final}$ (mm)
Sep-10	-11±301	0	0	-58±301	0	0	-17±301	0	0
Feb-11	94±135	44±14	70±70	139±135	35±12	90±70	103±135	36±12	70±70
Jun-11	90±128	0	0	103±128	0	0	108±128	1.5±0.5	<5
Dec-11	-86±206	0	0	-87±206	0	0	-77±206	0	0

Notes: $S_{E,L}$ = Ejecta-induced settlement based on LiDAR data reported in Tables 8b, c, and d; $S_{E,P}$ = Median ejecta-induced settlement for the range of values reported in Table 10b; $S_{E,final}$ = Best final estimate of ejecta-induced settlement rounded to the nearest 5; Final plus/minus values are also rounded to the nearest 5.

Note 5:

- For Sep-10, Jun-11, and Dec-11, $S_{E,final}$ is based solely on $S_{E,P}$ for both Patch A and Road.
- For Patch A, $S_{E,final}$ for Feb-11 EQ is equal to $S_{E,P}$. For Road, $S_{E,final}$ for Feb-11 EQ is a weighted average of $S_{E,L}$ and $S_{E,P}$, both with weights of 1/2. The uncertainty associated with $S_{E,final}$ is also a weighted average of uncertainties associated with $S_{E,L}$ and $S_{E,P}$ with the same weights of 1/10 and 9/10, respectively, for Patch A, and 1/2 and 1/2, respectively, for Road.
- The weights are based on the LiDAR error bands, LPI prediction error (Maurer et al. 2014[3]), completeness of visual evidence (i.e., ground and aerial photographs and EQC LDAT property inspection reports for the site), presence of ejecta at the time of LiDAR surveys, density of July 2003 LiDAR points, and agreement between visual evidence and LiDAR-based ejecta-induced settlement estimates. The negative $S_{E,L}$ is given the weight of zero. The 50 Eureka St site is not in the apparent zone of higher/lower ground surface subsidence compared to the adjacent areas. The post-earthquake LiDAR surveys for the site are not affected by ejecta. The site is in the zone of moderate to severe LPI overprediction of liquefaction severity for the Feb-11 EQ. For Sep-10 EQ, the site is in the zone of accurate LPI prediction to slight LPI overprediction of liquefaction severity. The property at which Patch A is located was inspected by the EQC LDAT property inspection team on 30 Aug 2011. The team did not observe any ejecta at the time of the inspection, but did not talk with a claimant/occupier to hear their story (e.g., the possible removal of the ejected material outlined in Patch A in Figure 70). The presence of a small amount of ejected material within Patch A following the Feb-11 EQ is evident in Figure 75. There are no ground photographs of ejecta only the high-resolution aerial photographs for all four earthquake events.

<u>Summary 1</u>:

- **The best estimate of the ejecta-induced free-field settlement at the 50 Eureka St site for the SEP 2010, JUN 2011, and DEC 2011 earthquake is 0 mm, 0 mm, and 0 mm, respectively. For the FEB 2011 earthquake, ejecta were predominantly located on the road and most properties had the ejecta-induced free-field settlement of 0 mm. However, for properties with ejecta (<5% of the unobstructed area of the site), the best estimate of the ejecta-induced free-field settlement for the FEB 2011 earthquake is 5±5 mm.**

[3] Maurer, B. W., Green, R. A., Cubrinovski, M., & Bradley, B. A. (2014). Evaluation of the Liquefaction Potential Index for Assessing Liquefaction Hazard in Christchurch, New Zealand. *Journal of Geotechnical and Geoenvironmental Engineering*, 140(7), 04014032-1-11. doi:10.1061/(asce)gt.1943-5606.0001117

- **The best estimate of the ejecta-induced free-field settlement of the road at the 50 Eureka St site for the SEP 2010, FEB 2011, JUN 2011, and DEC 2011 earthquake is 0 mm, 70±70 mm, <5 mm, and 0 mm, respectively.**

Figure 6: Location of the site.

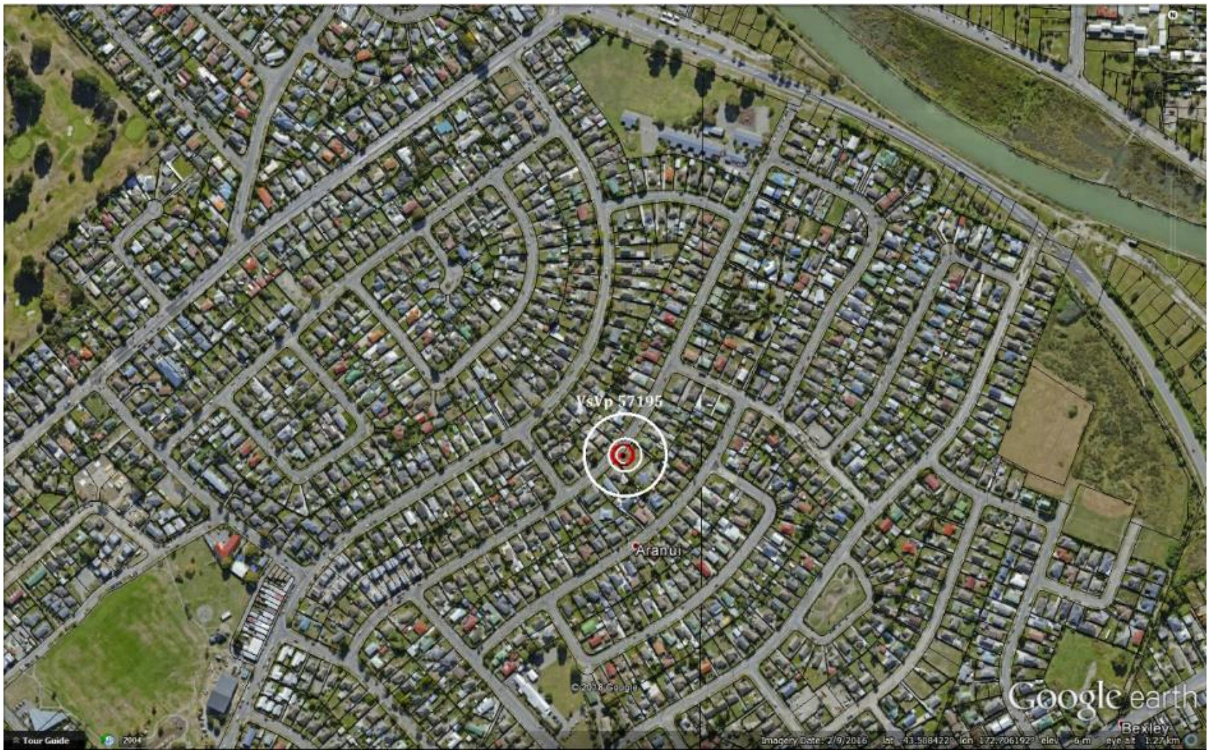

Figure 7: Position of the site relative to nearby buildings, vegetation, and free-face features.

Figure 8: Street view of the flat land.

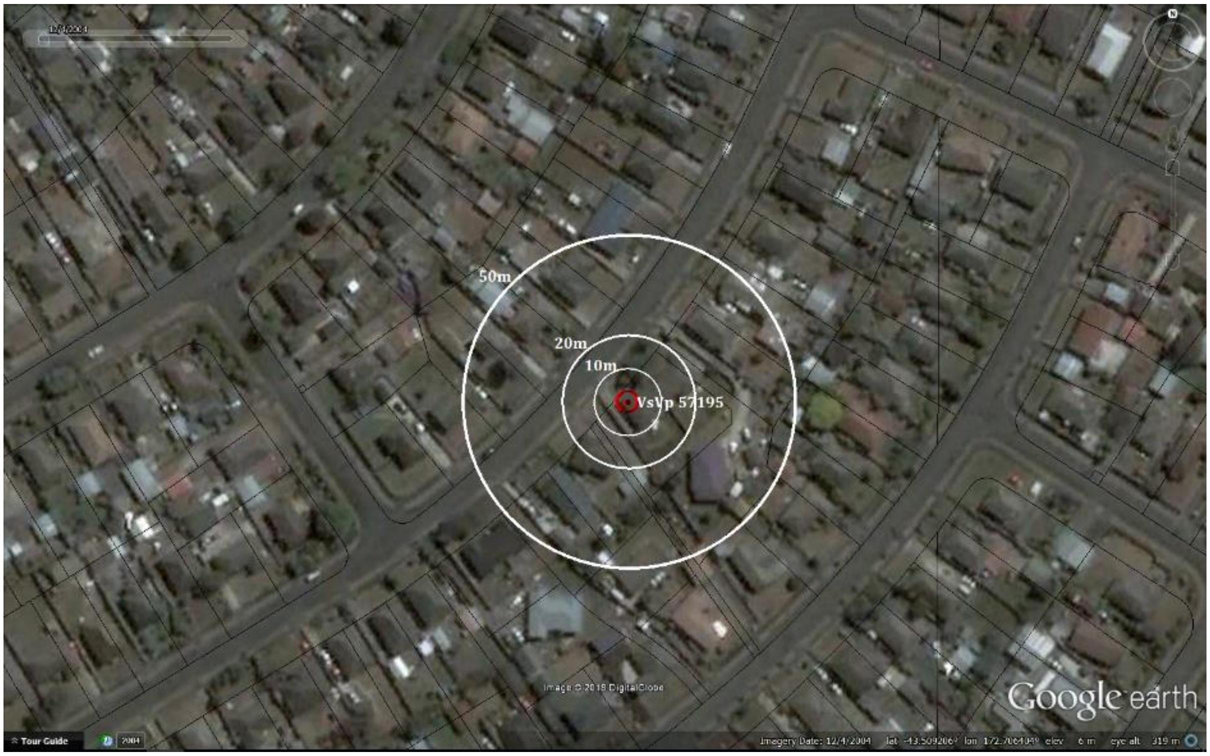

Figure 9: Satellite image of the site taken in Dec 2004.

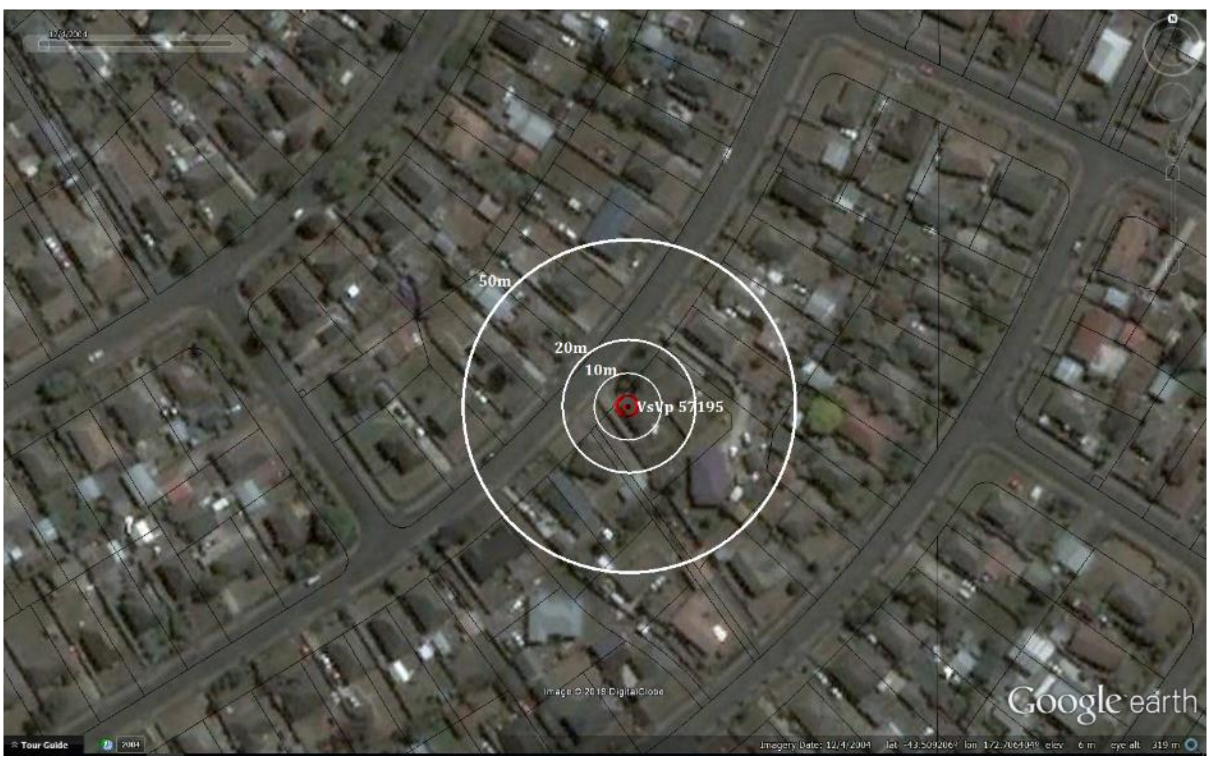

Figure 10: Satellite image of the site taken in Sep 2010.

Figure 11: Satellite image of the site taken in Feb 2011.

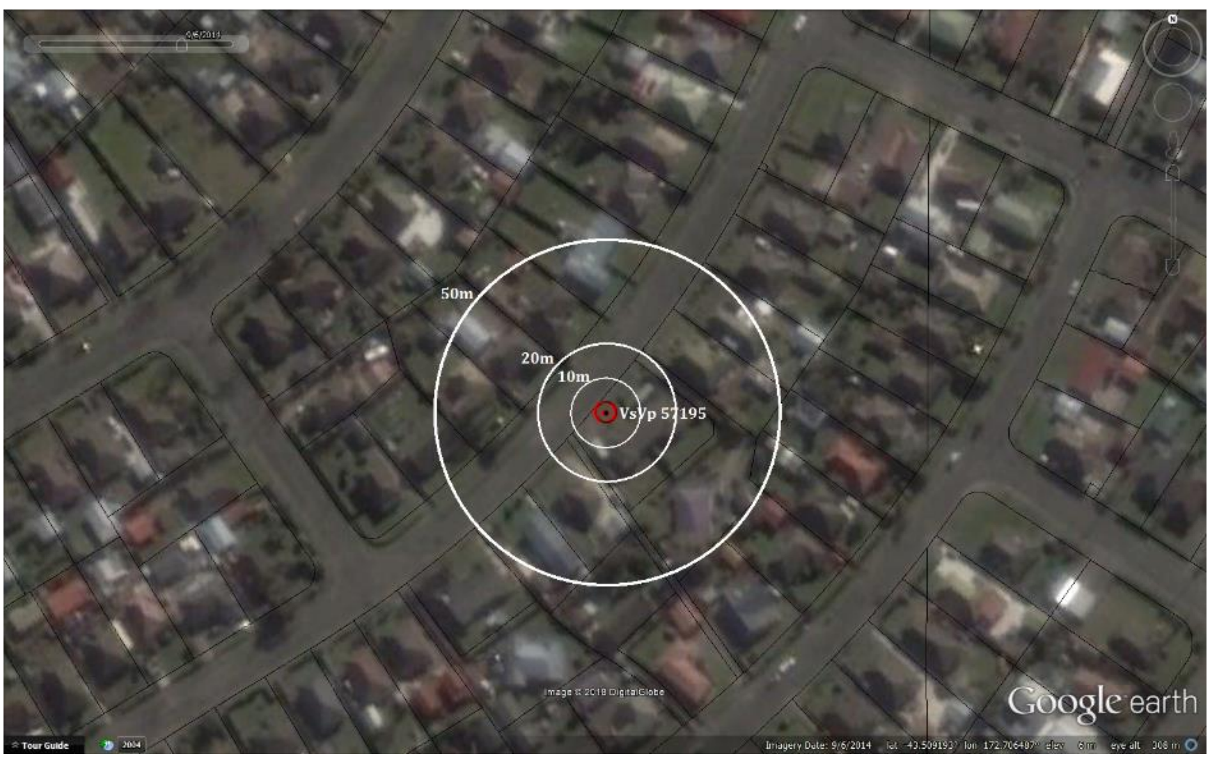

Figure 12: Satellite image of the site taken in Sep 2014.

Figure 13: Satellite image of the site taken in Jan 2015.

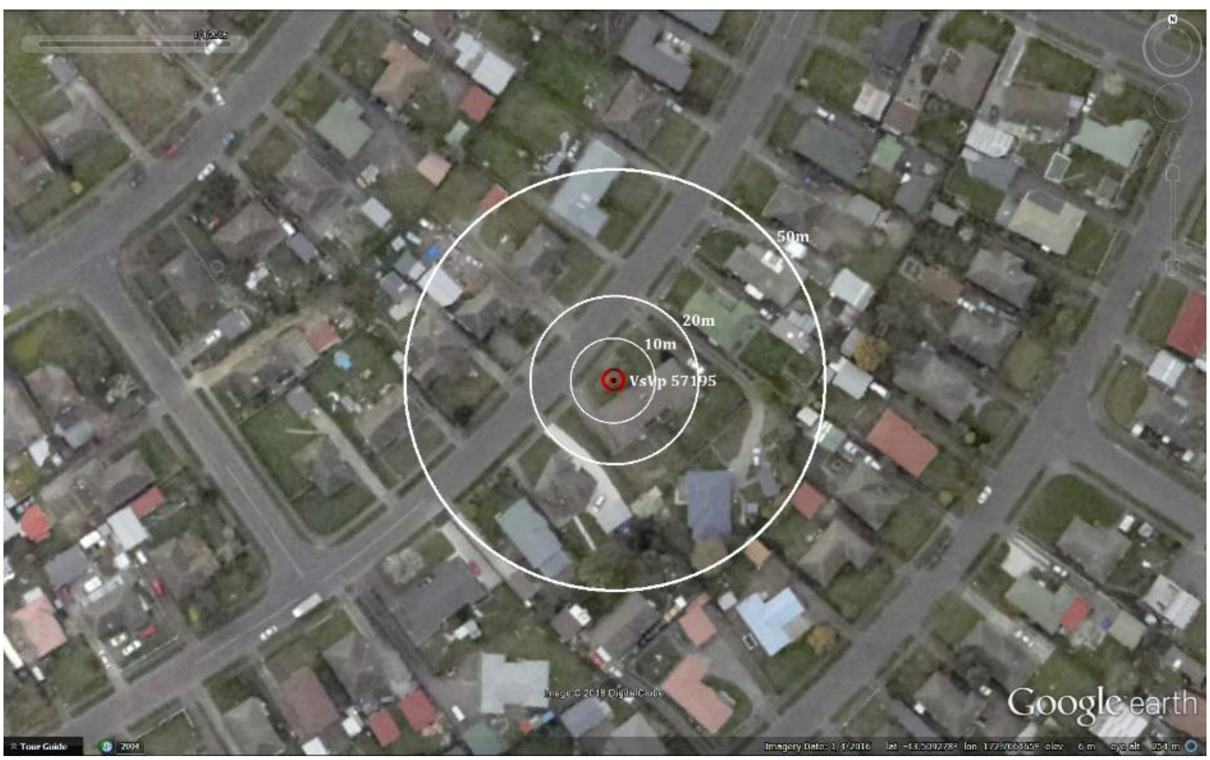

Figure 14: EQC Aerial Photograph of the site taken Sep 4, 2010.

Figure 15: EQC Aerial Photograph of the site taken on Feb 24, 2011.

Figure 16: EQC Aerial Photograph of the site taken on June 16, 2011.

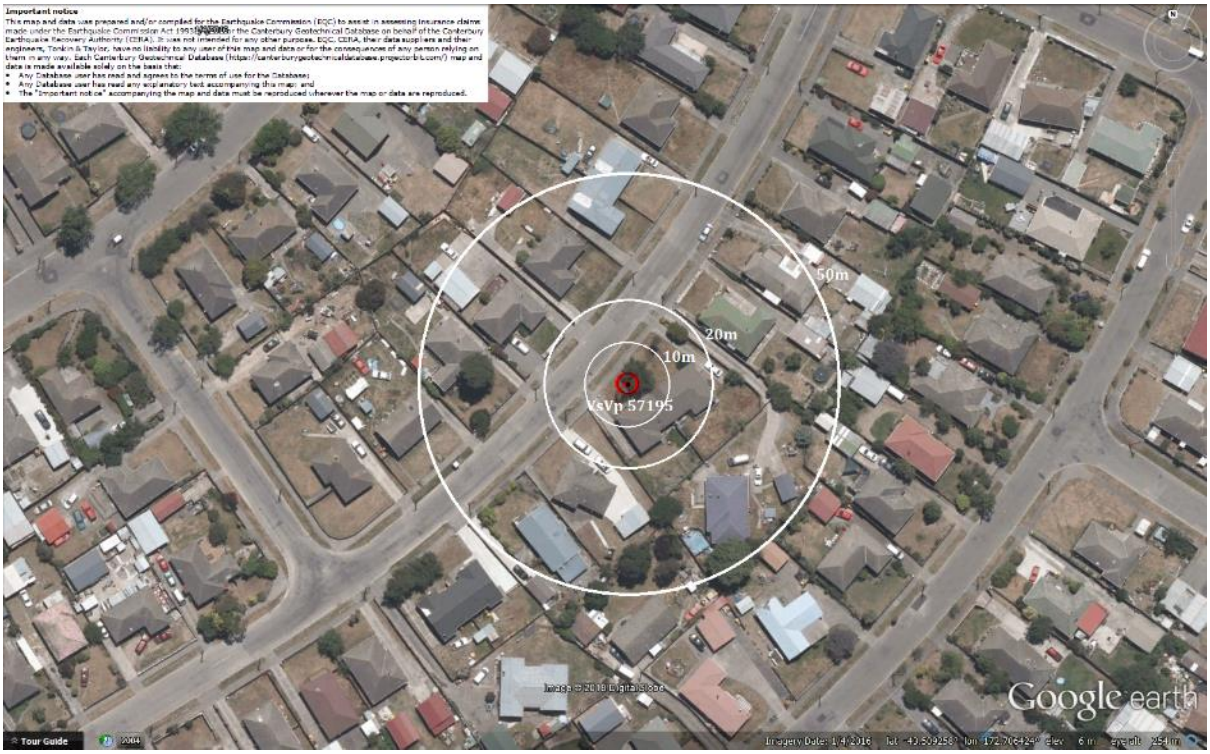

Figure 17: EQC Aerial Photograph of the site taken on Dec 24, 2012.

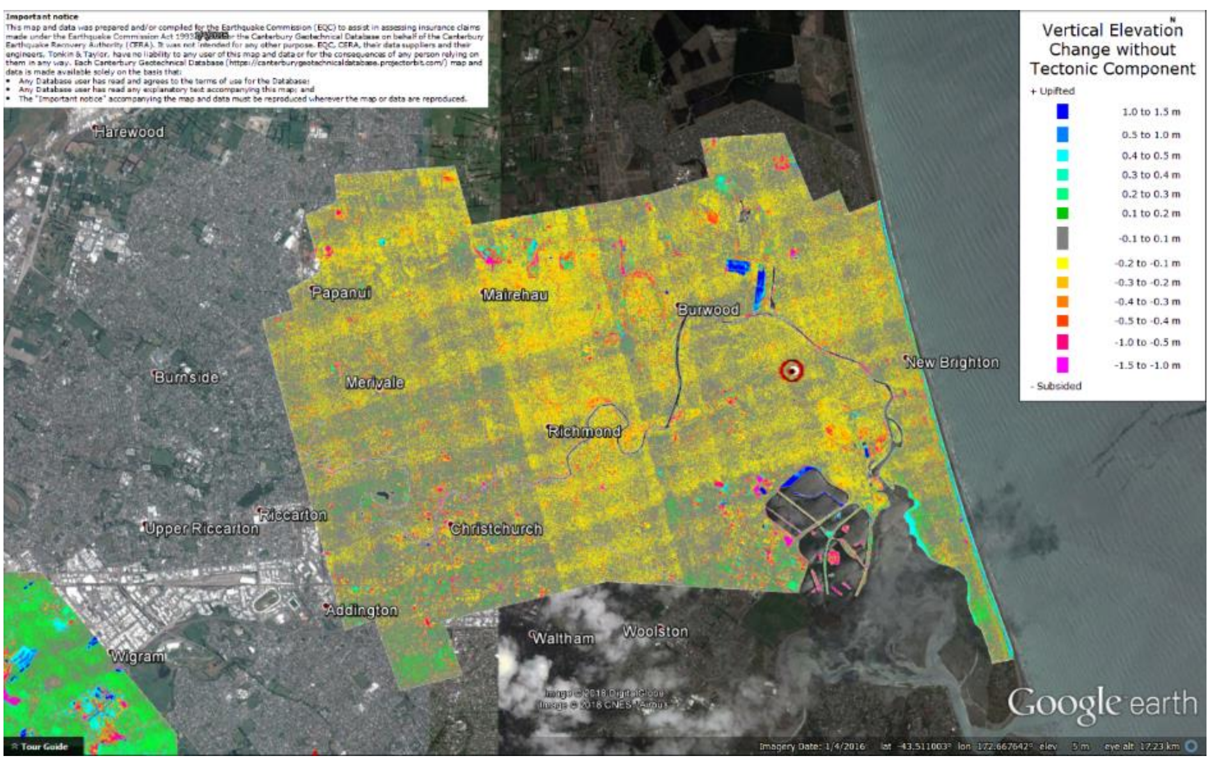

Figure 18: Vertical Ground Movements (Surface – Tectonic) for Sep 2010 Earthquake – the site is not in the apparent zone of overestimated ground surface subsidence.

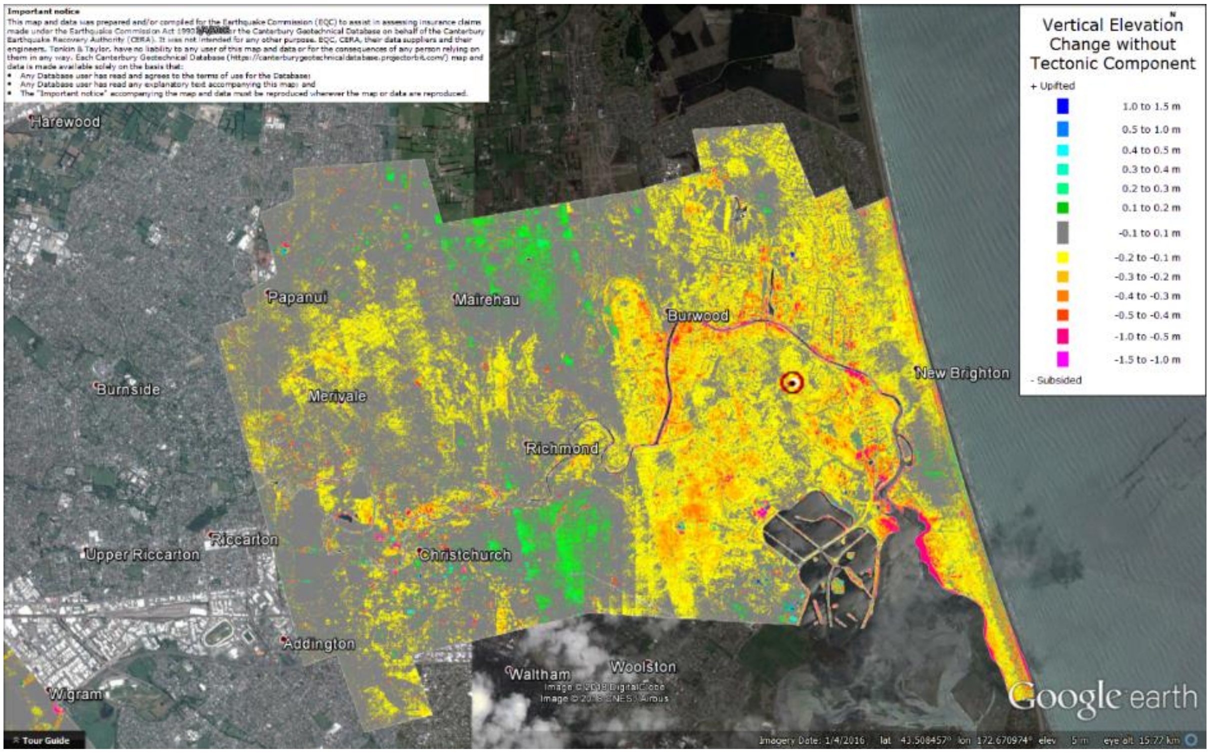

Figure 19: Vertical Ground Movements (Surface – Tectonic) for Feb 2011 Earthquake – the site is not in the apparent zone of underestimated ground surface subsidence.

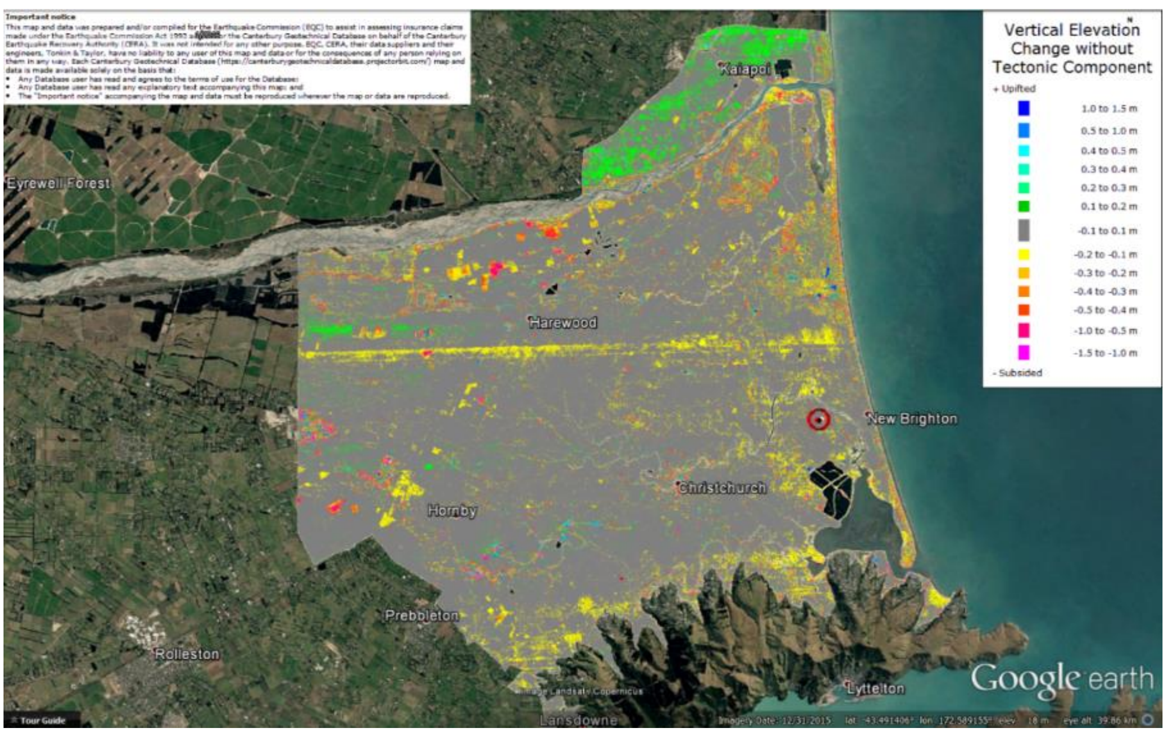

Figure 20: Vertical Ground Movements (Surface – Tectonic) for June 2011 Earthquake – the site is not in the apparent zone of overestimated or underestimated ground surface subsidence.

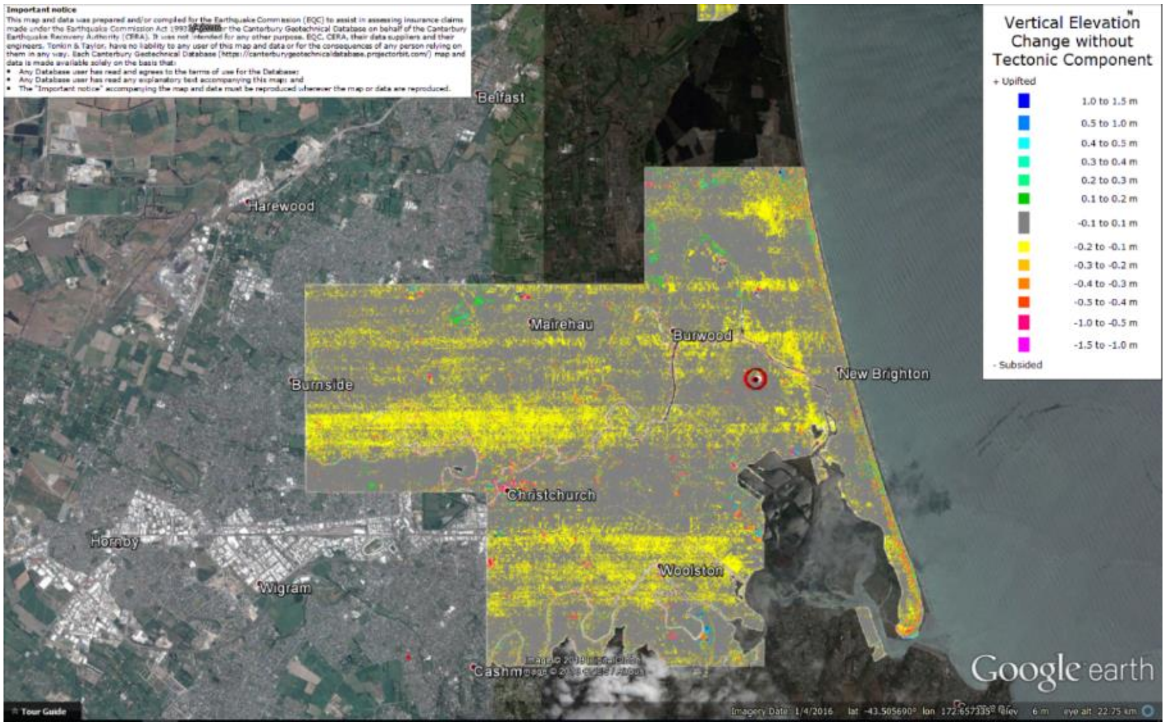

Figure 21: Vertical Ground Movements (Surface – Tectonic) for Dec 2011 Earthquake – the site is not in the apparent zone of overestimated or underestimated ground surface subsidence.

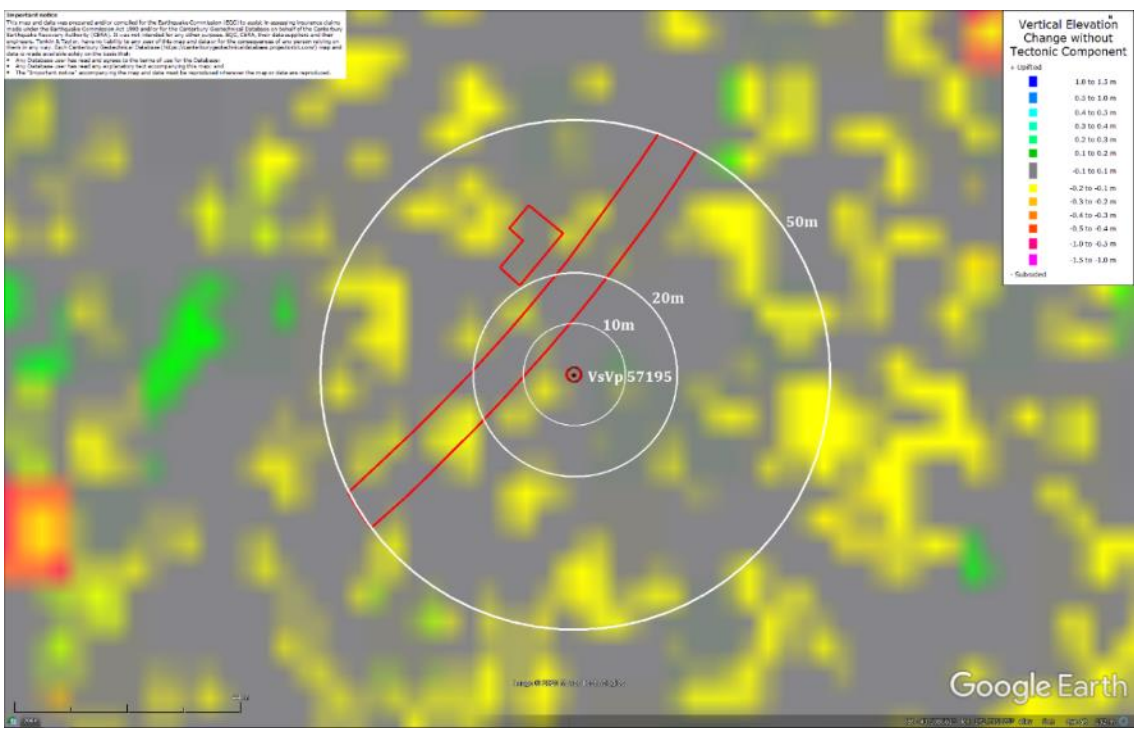

Figure 22: Ground surface subsidence without tectonic component for Sep 2010 Earthquake according to the LiDAR DEM.

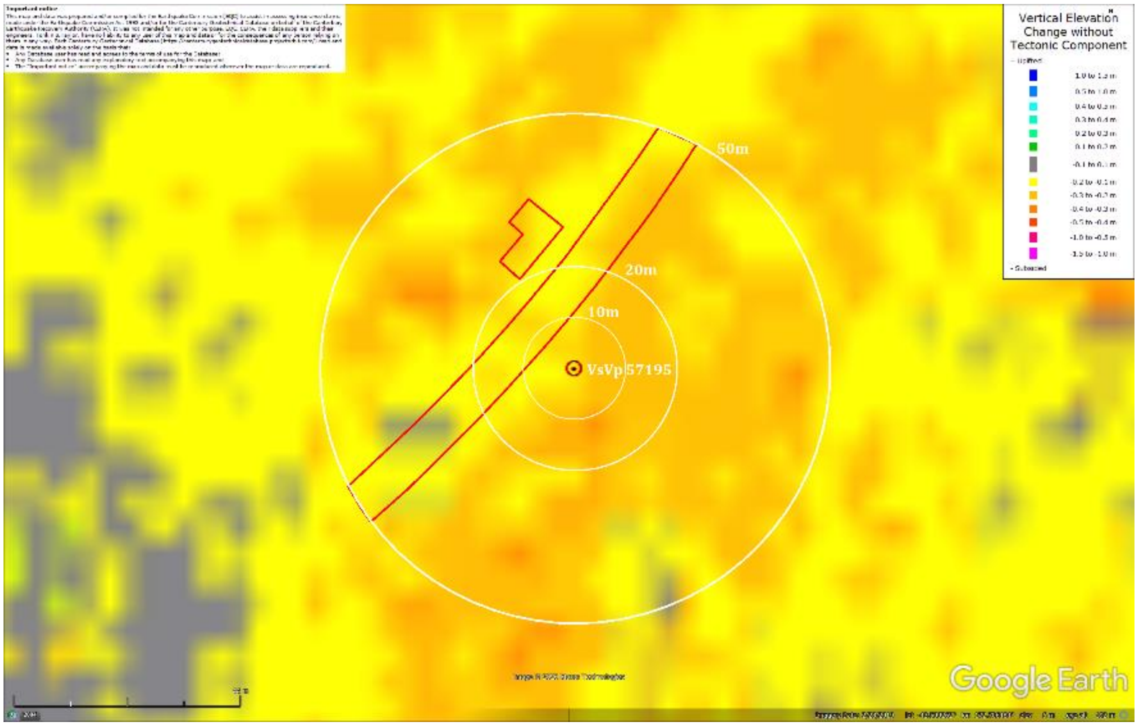

Figure 23: Ground surface subsidence without tectonic component for Feb 2011 Earthquake according to the LiDAR DEM.

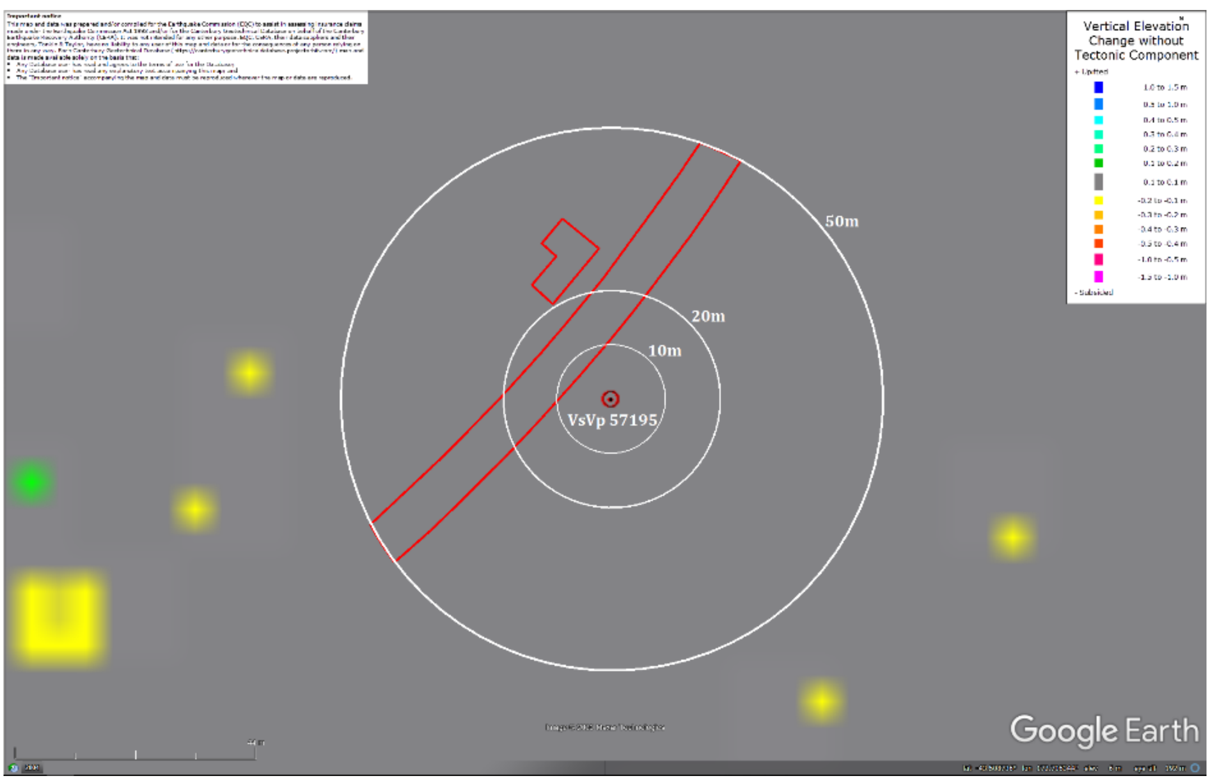

Figure 24: Ground surface subsidence without tectonic component for June 2011 Earthquake according to the LiDAR DEM.

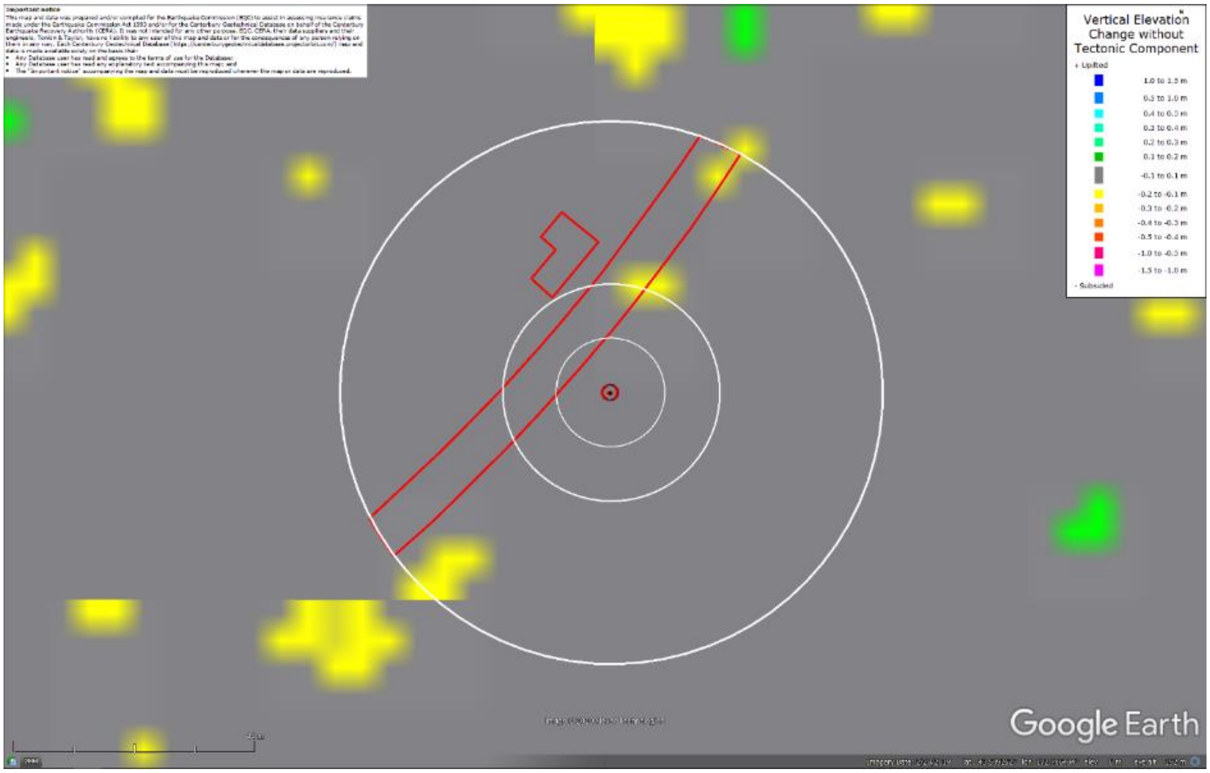

Figure 25: Ground surface subsidence without tectonic component for Dec 2011 Earthquake according to the LiDAR DEM.

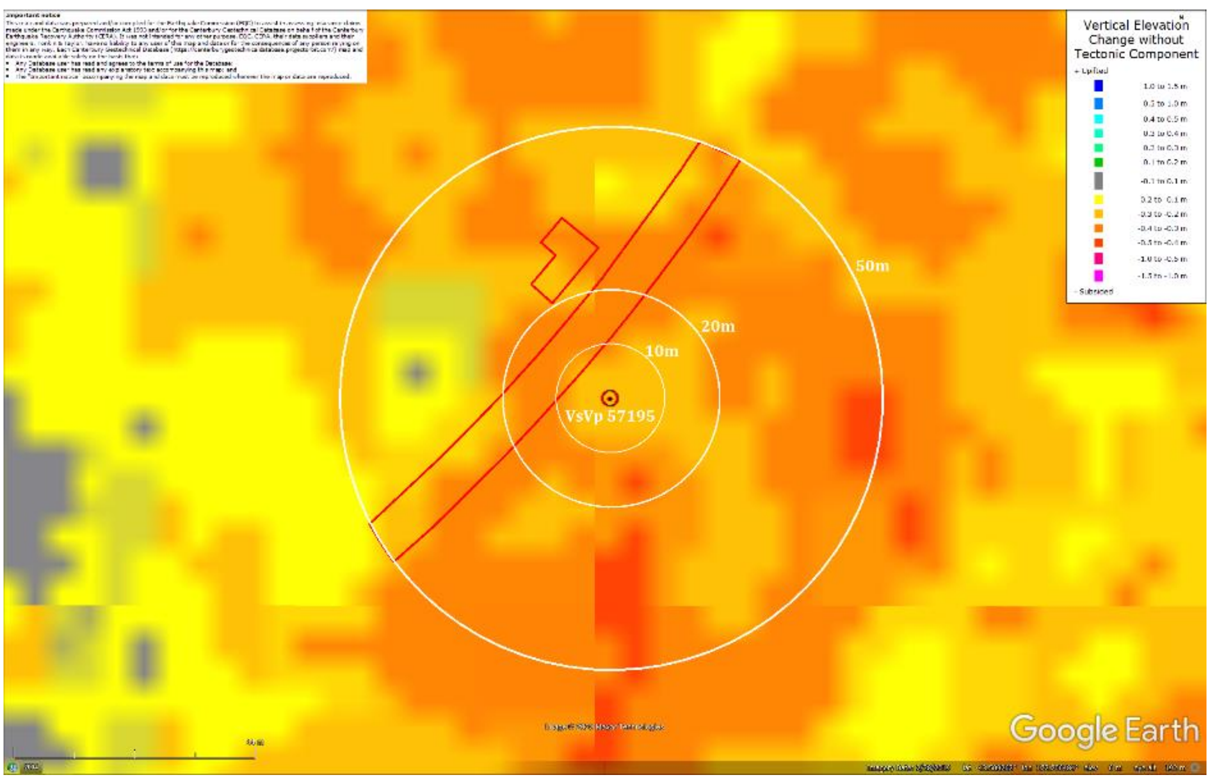

Figure 26: Ground surface subsidence without tectonic component for Canterbury Earthquake Sequence according to the LiDAR DEM.

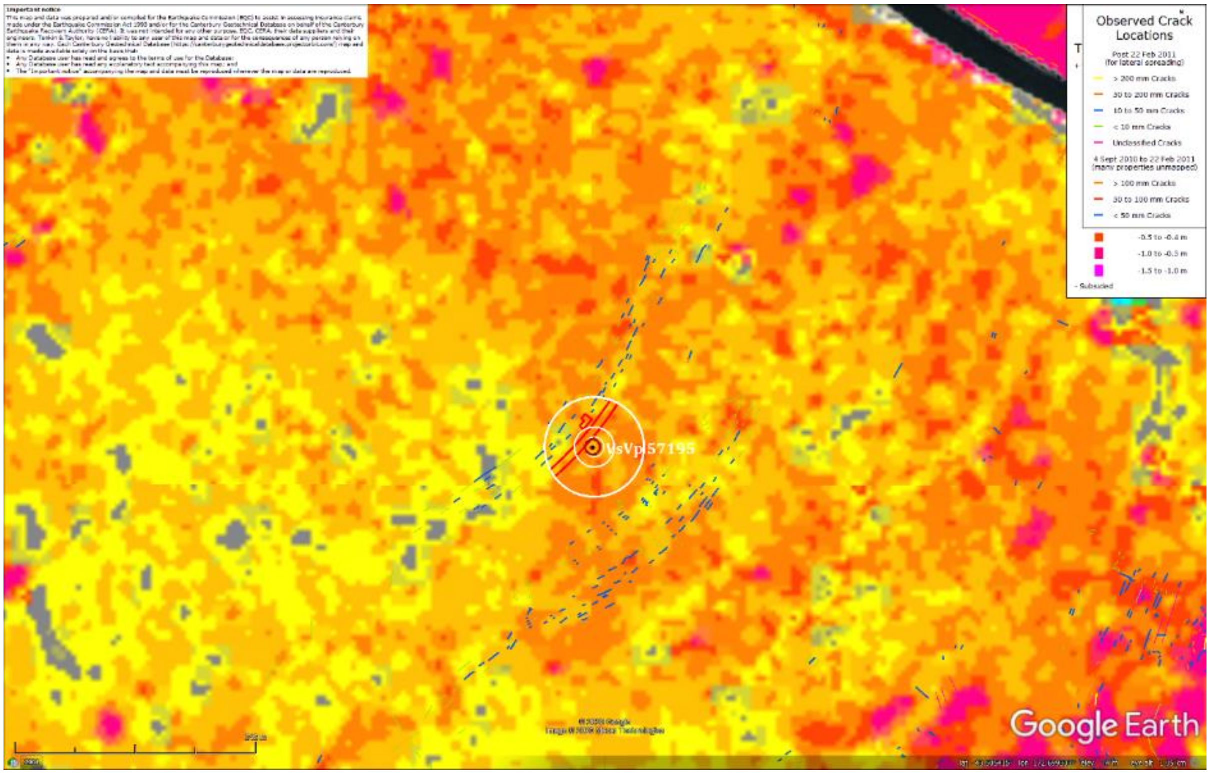

Figure 27: Absence of significant ground cracks indicating no lateral spreading for Canterbury Earthquake Sequence.

Figure 28: Vertical tectonic movements for Sep 2010 Earthquake.

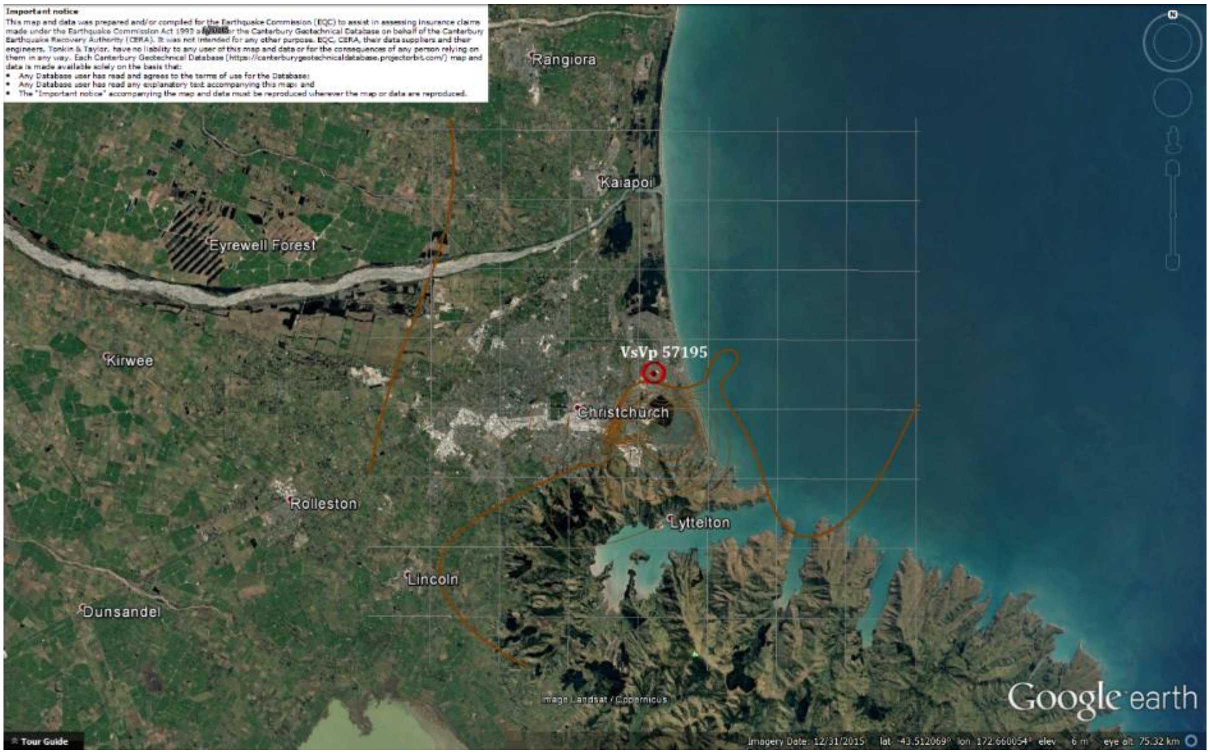

Figure 29: Vertical tectonic movements for Feb 2011 Earthquake.

Figure 30: Vertical tectonic movements for June 2011 Earthquake.

Figure 31: Vertical tectonic movements for Dec 2011 Earthquake.

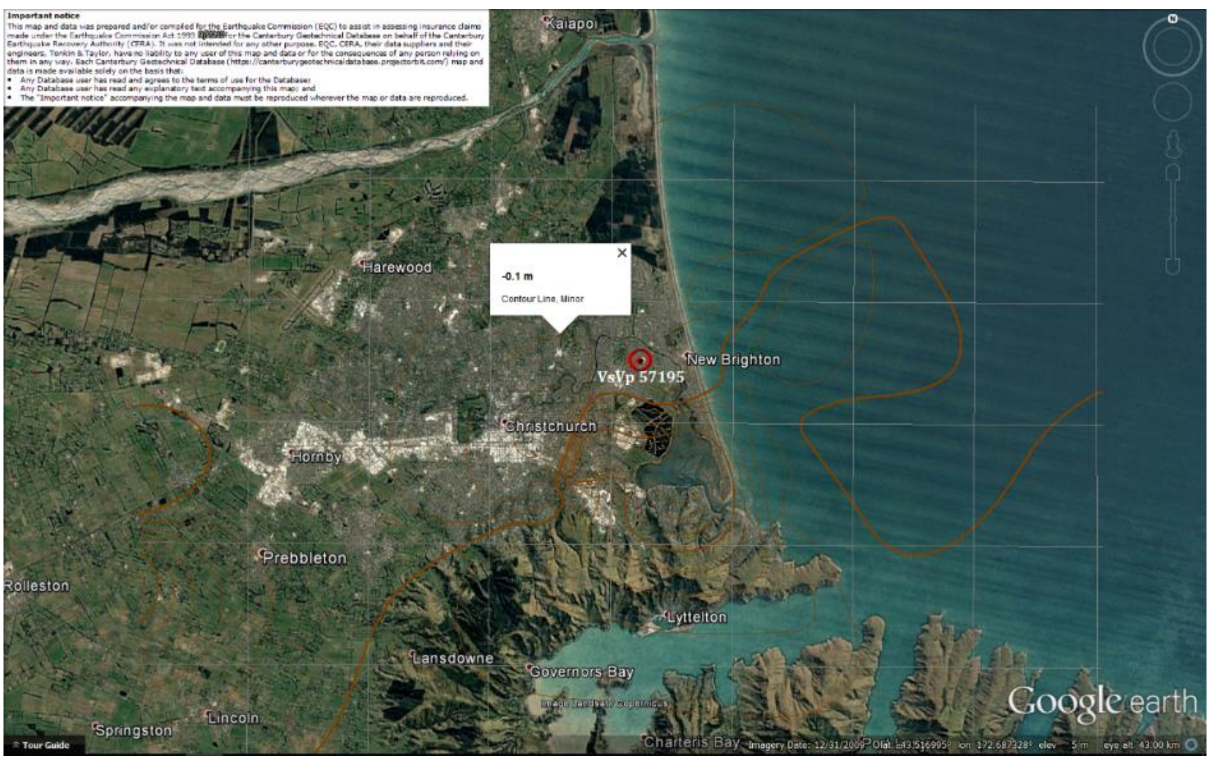

Figure 32: Vertical tectonic movements for Canterbury Earthquake Sequence.

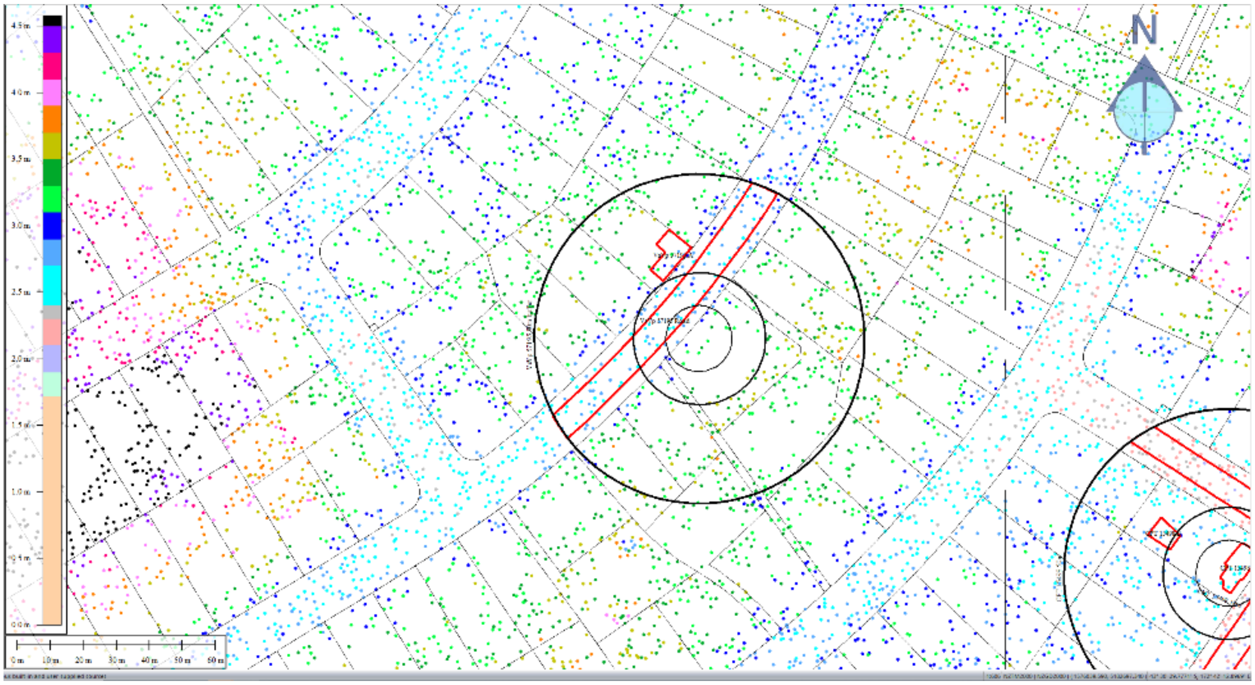

Figure 33: Jul 2003 LiDAR survey.

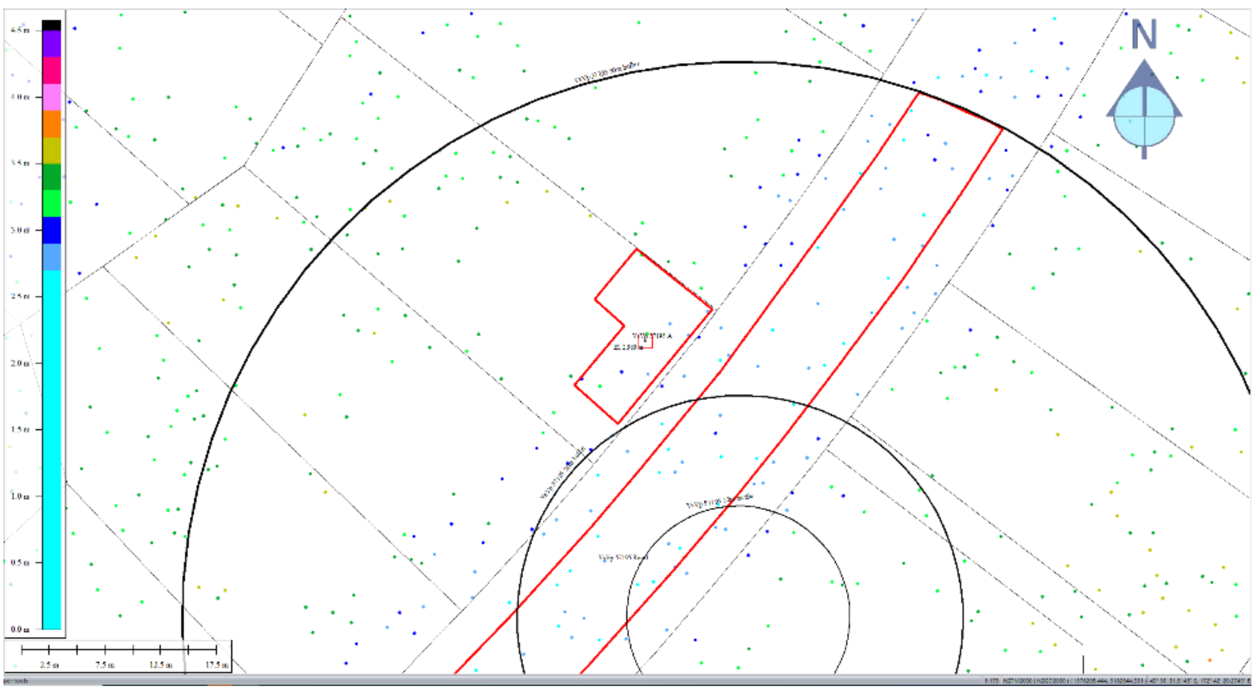

Figure 34: Ground surface elevation averaged over 50-m buffer for Patch A for Jul 2003 LiDAR survey.

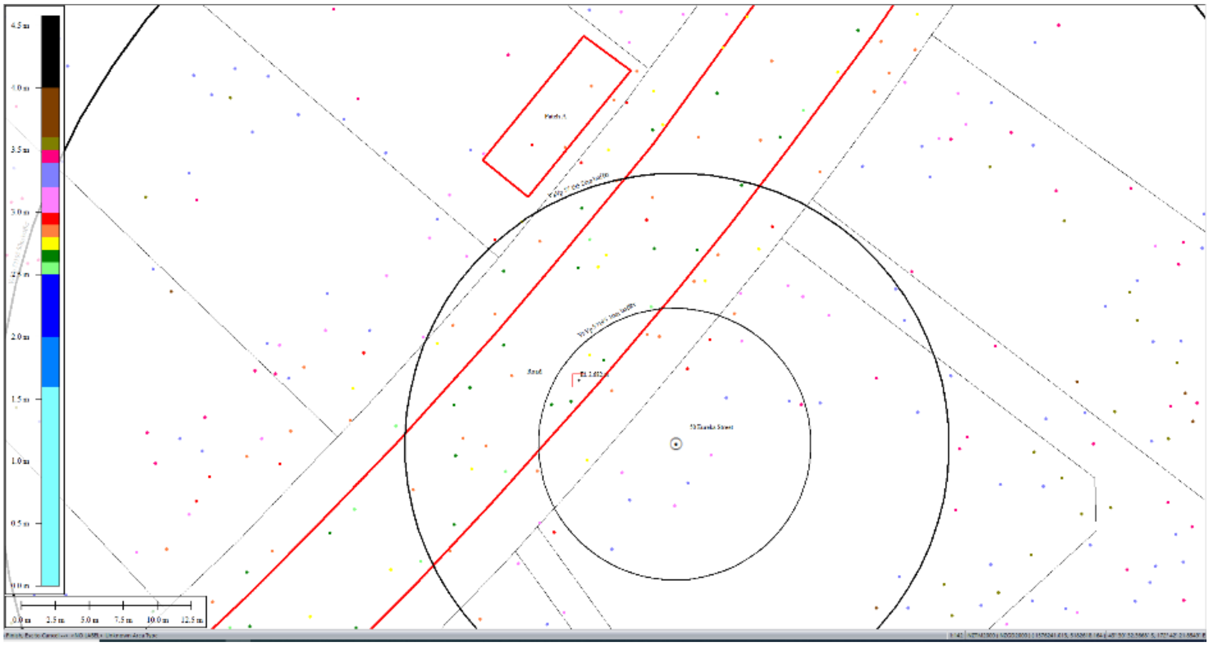

Figure 35: Ground surface elevation averaged over 10-m buffer for Road for Jul 2003 LiDAR survey.

Note 6: The rectangular shape of Patch A was later changed to L shape due to the presence of ejecta as seen in the aerial photograph for the Feb-11 EQ.

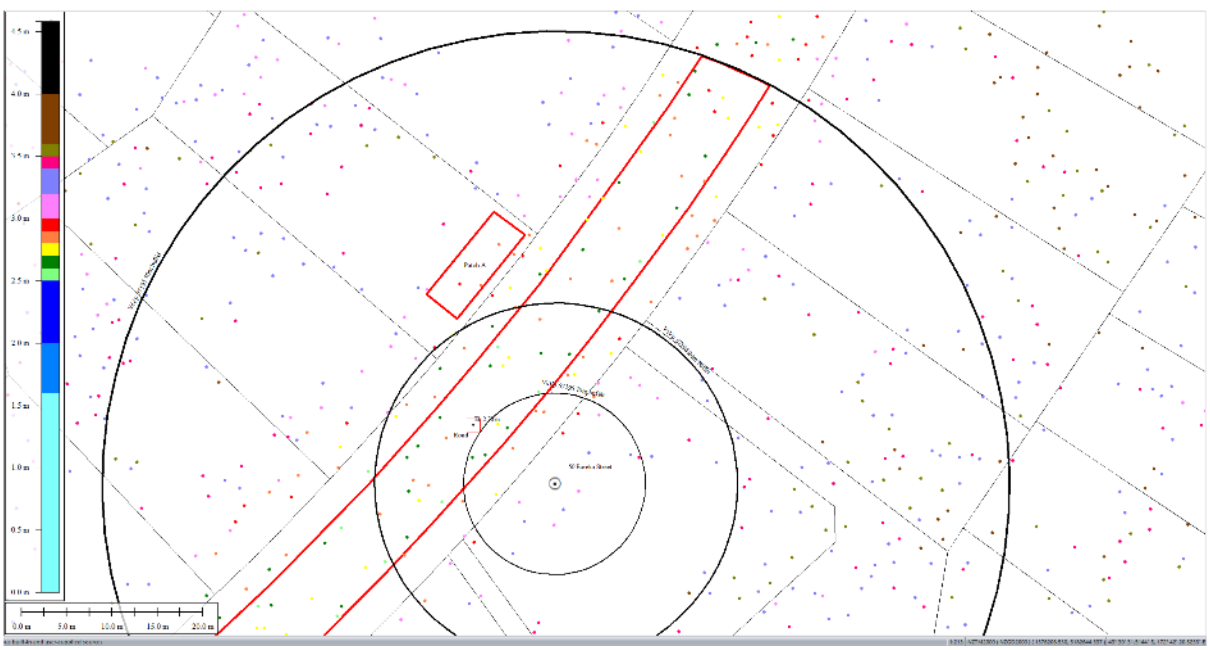

Figure 36: Ground surface elevation averaged over 20-m buffer for Road for Jul 2003 LiDAR survey.

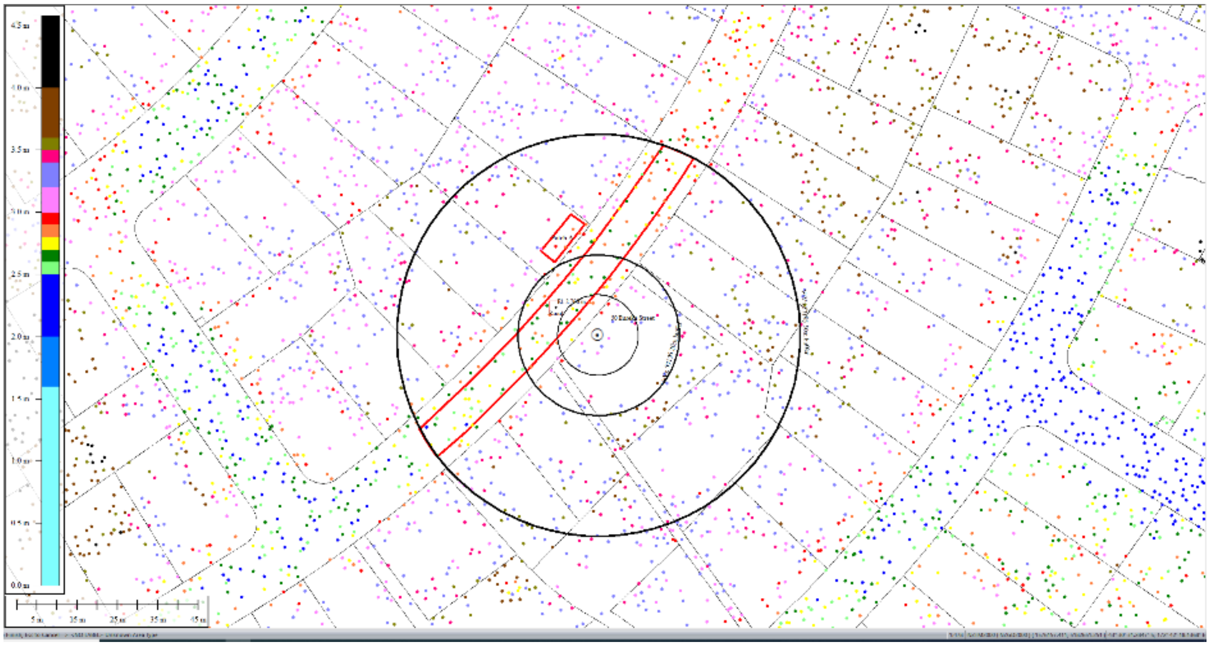

Figure 37: Ground surface elevation averaged over 50-m buffer for Road for Jul 2003 LiDAR survey.

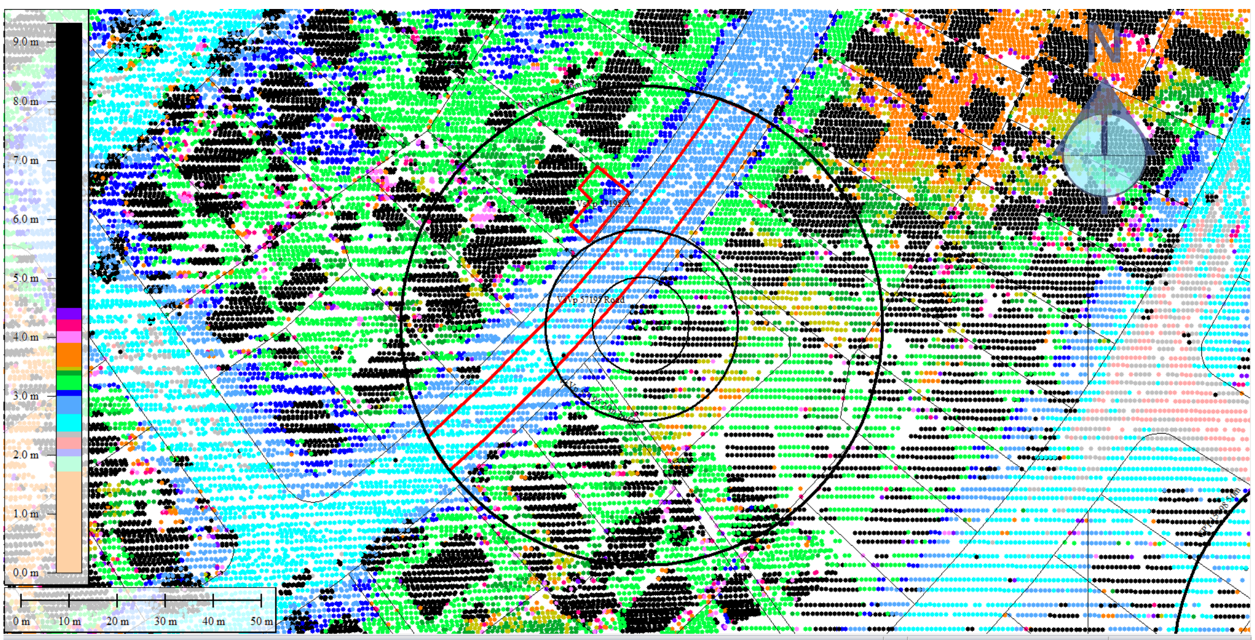

Figure 38: Sep 5, 2010 LiDAR survey.

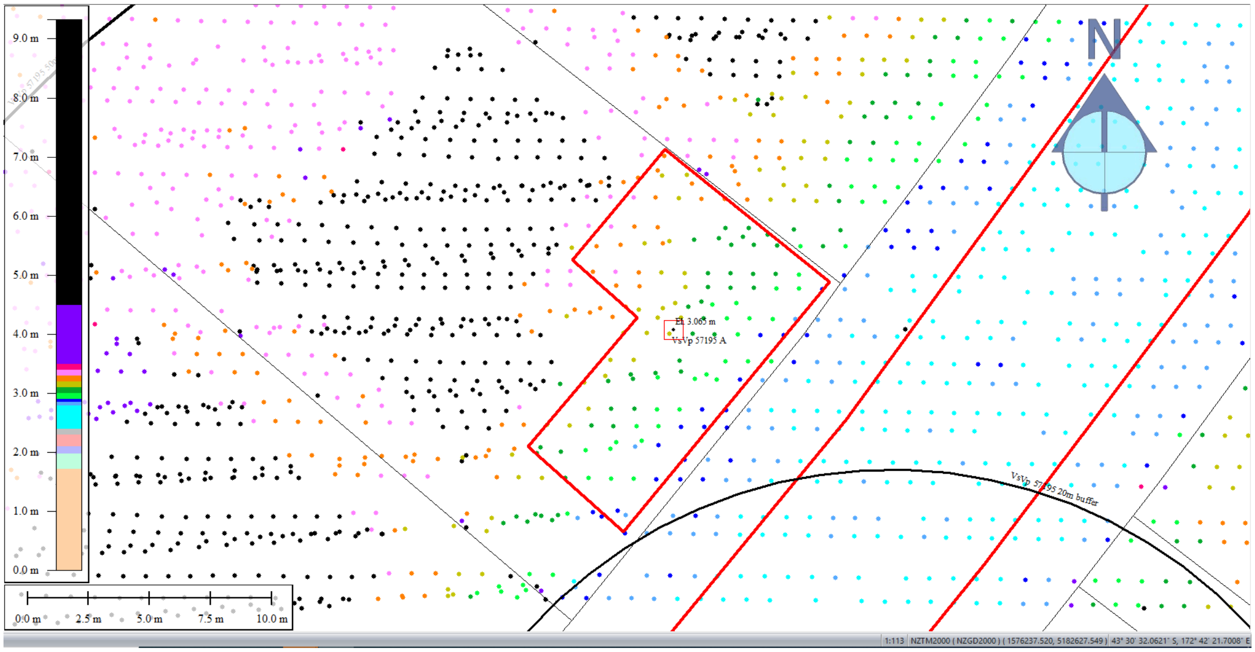

Figure 39: Ground surface elevation averaged over 50-m buffer for Patch A for Sep 5, 2010 LiDAR survey.

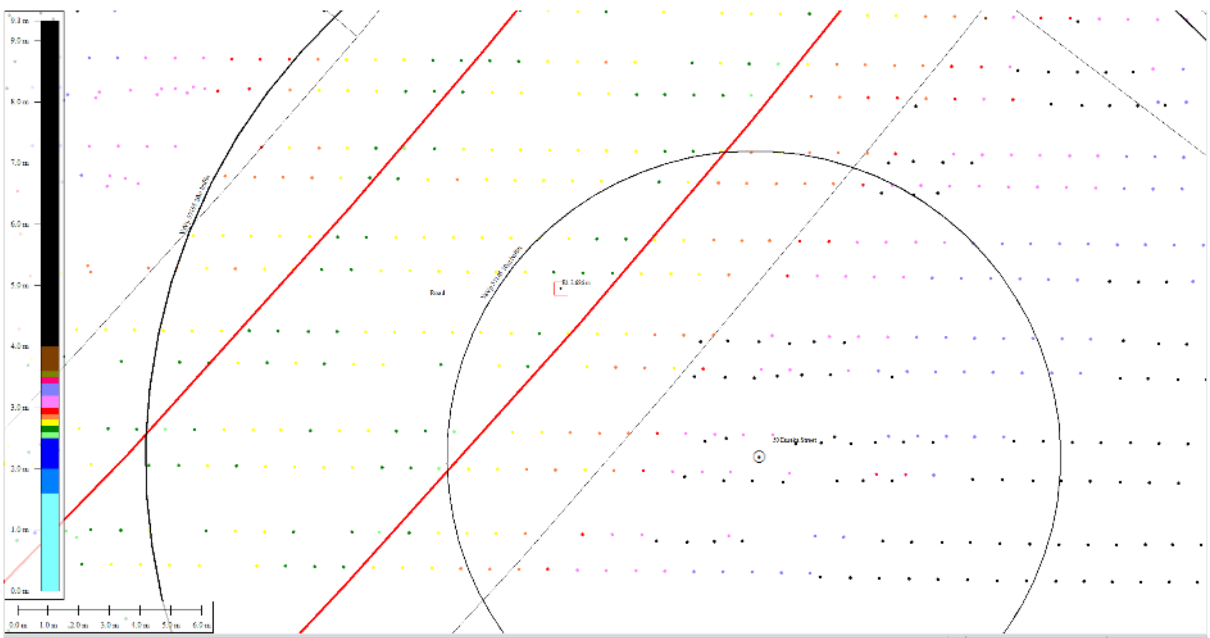

Figure 40: Ground surface elevation averaged over 10-m buffer for Road for Sep 5, 2010 LiDAR survey.

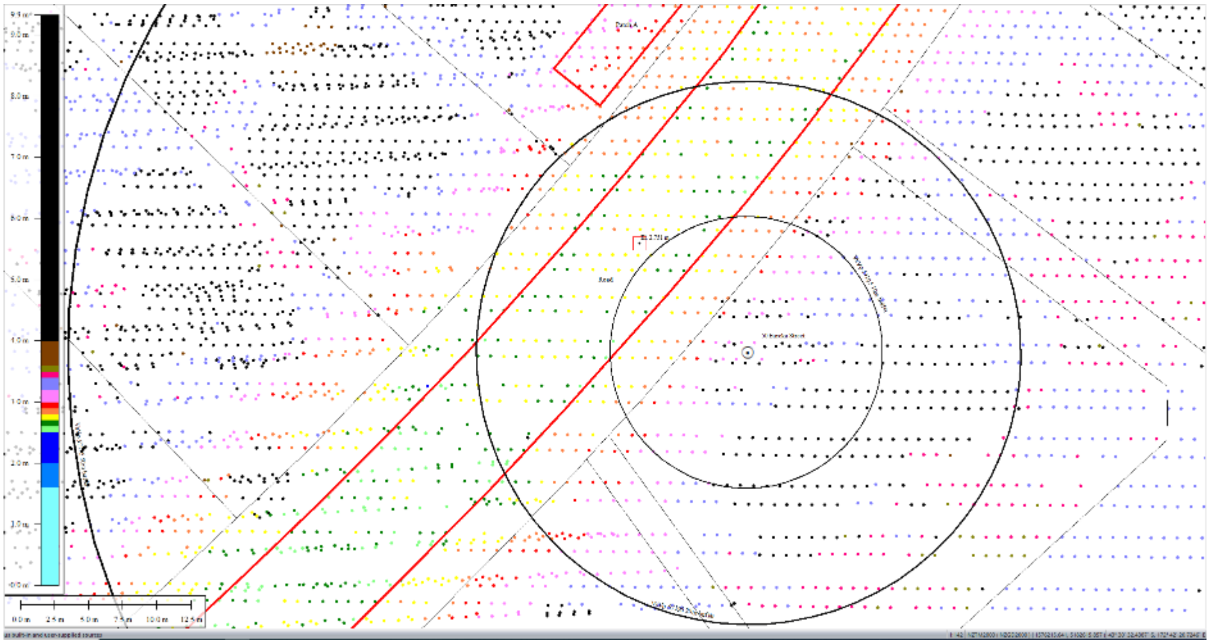

Figure 41: Ground surface elevation averaged over 20-m buffer for Road for Sep 5, 2010 LiDAR survey.

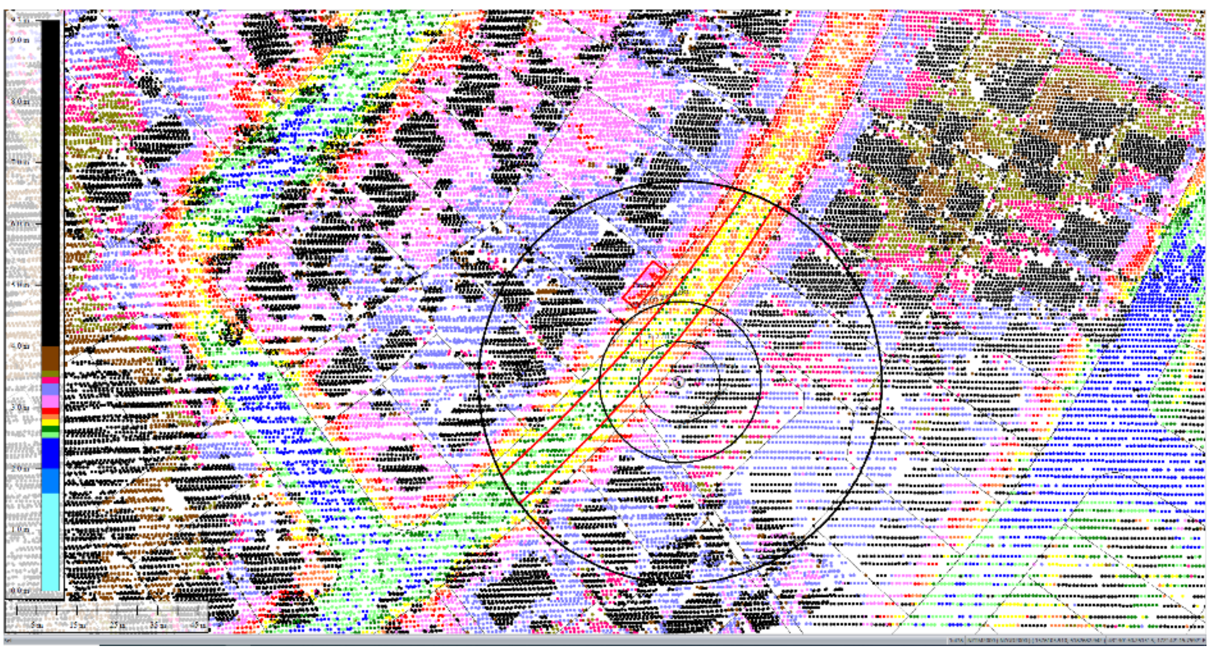

Figure 42: Ground surface elevation averaged over 50-m buffer for Road for Sep 5, 2010 LiDAR survey.

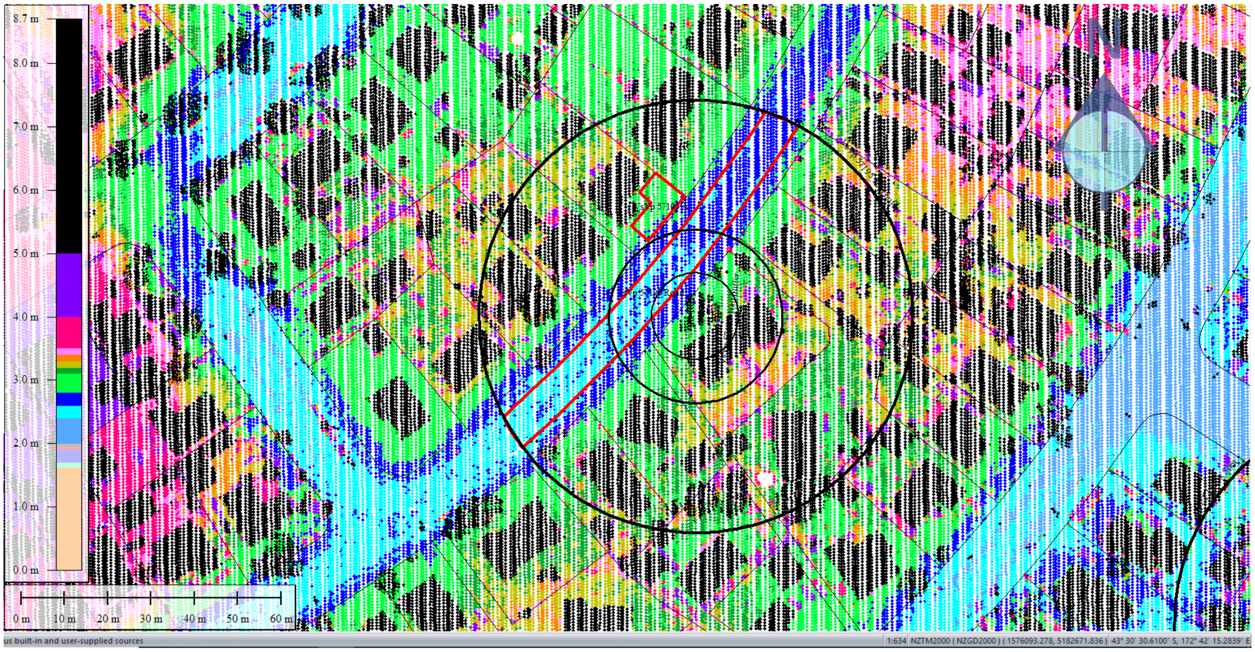

Figure 43: Mar 2011 LiDAR survey.

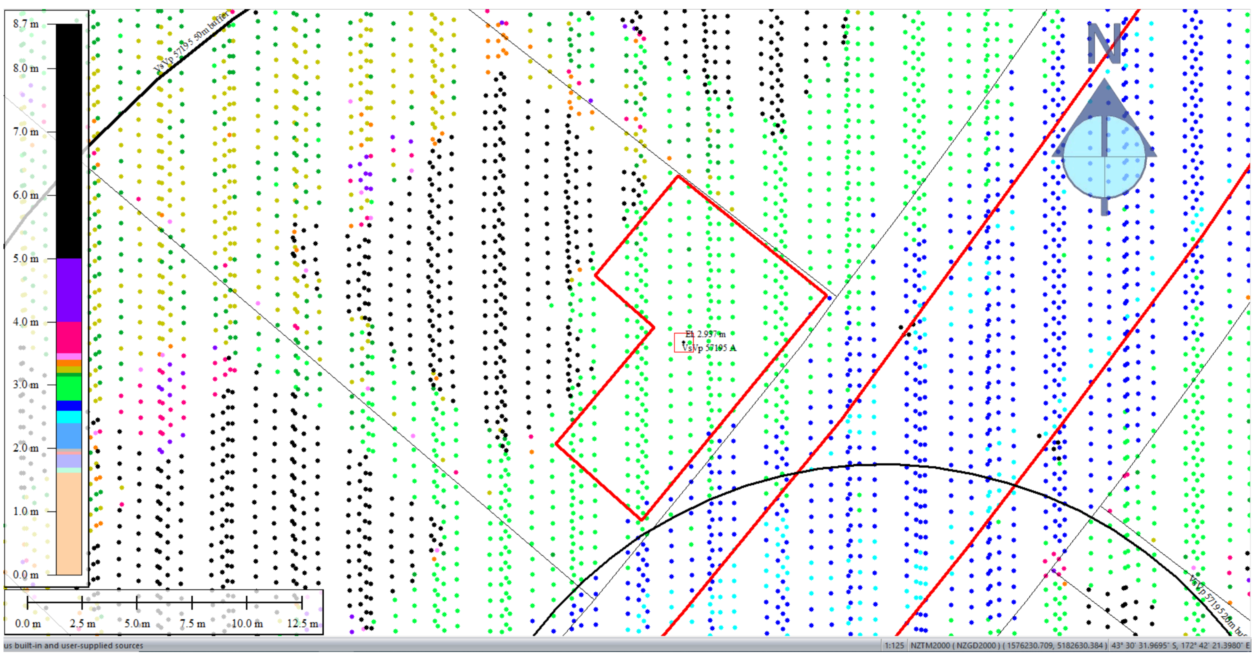

Figure 44: Ground surface elevation averaged over 50-m buffer for Patch A for Mar 2011 LiDAR survey.

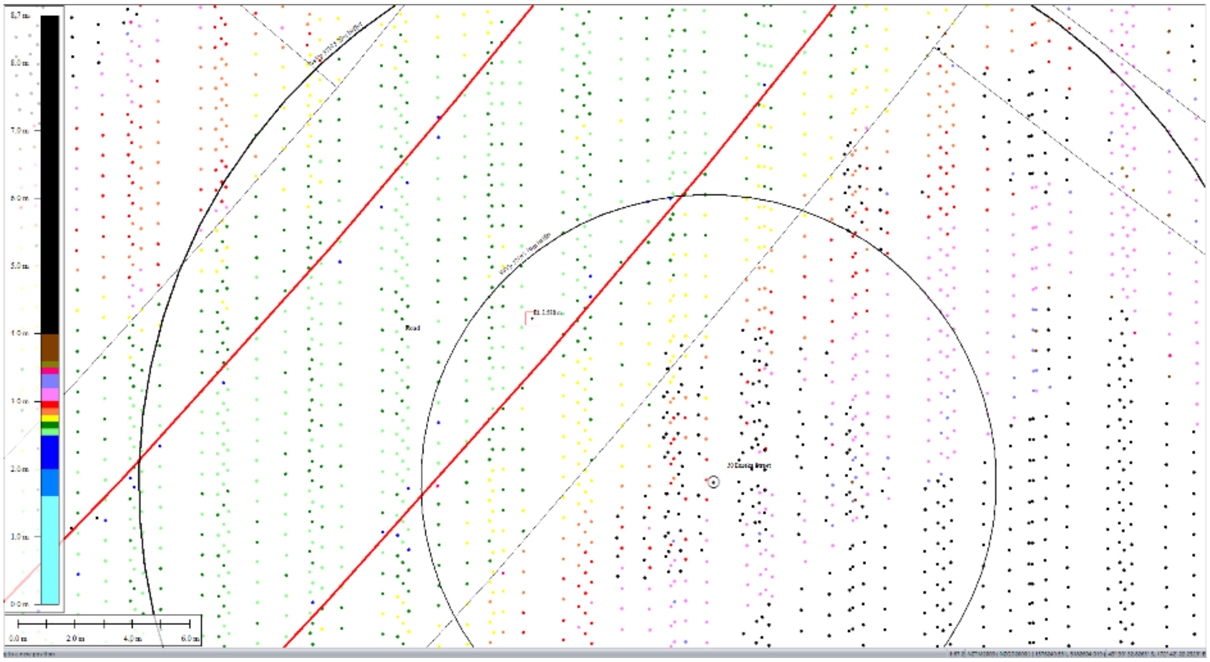

Figure 45: Ground surface elevation averaged over 10-m buffer for Road for Mar 2011 LiDAR survey.

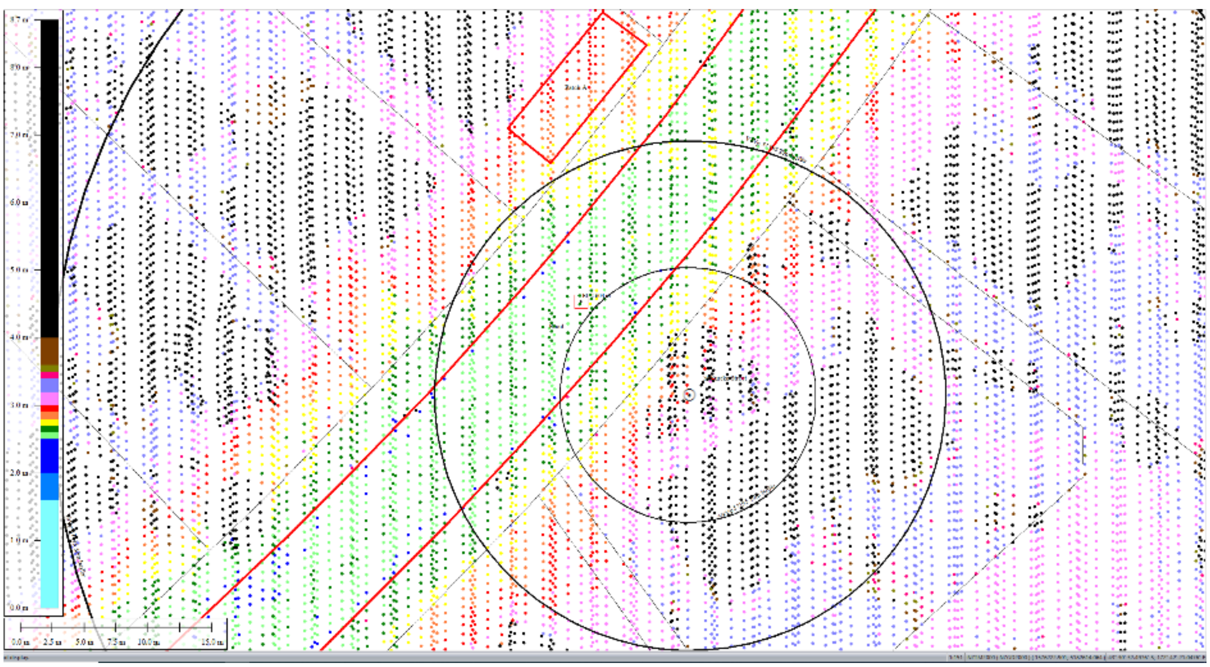

Figure 46: Ground surface elevation averaged over 20-m buffer for Road for Mar 2011 LiDAR survey.

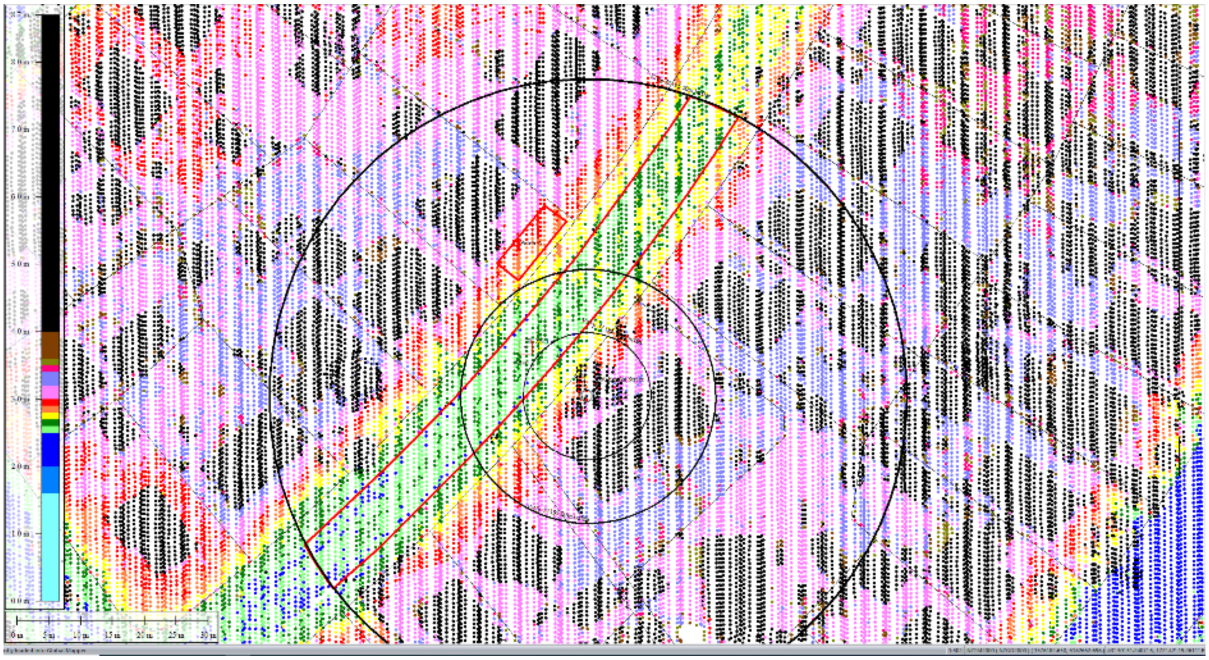

Figure 47: Ground surface elevation averaged over 50-m buffer for Road for Mar 2011 LiDAR survey.

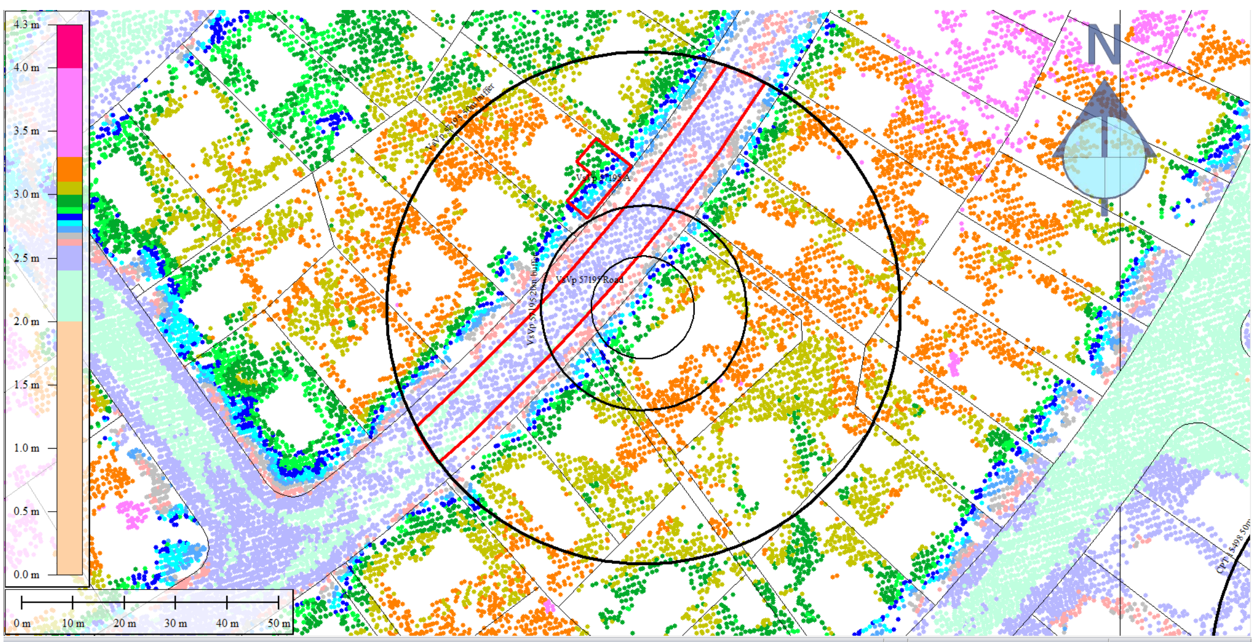

Figure 48: May 2011 LiDAR survey.

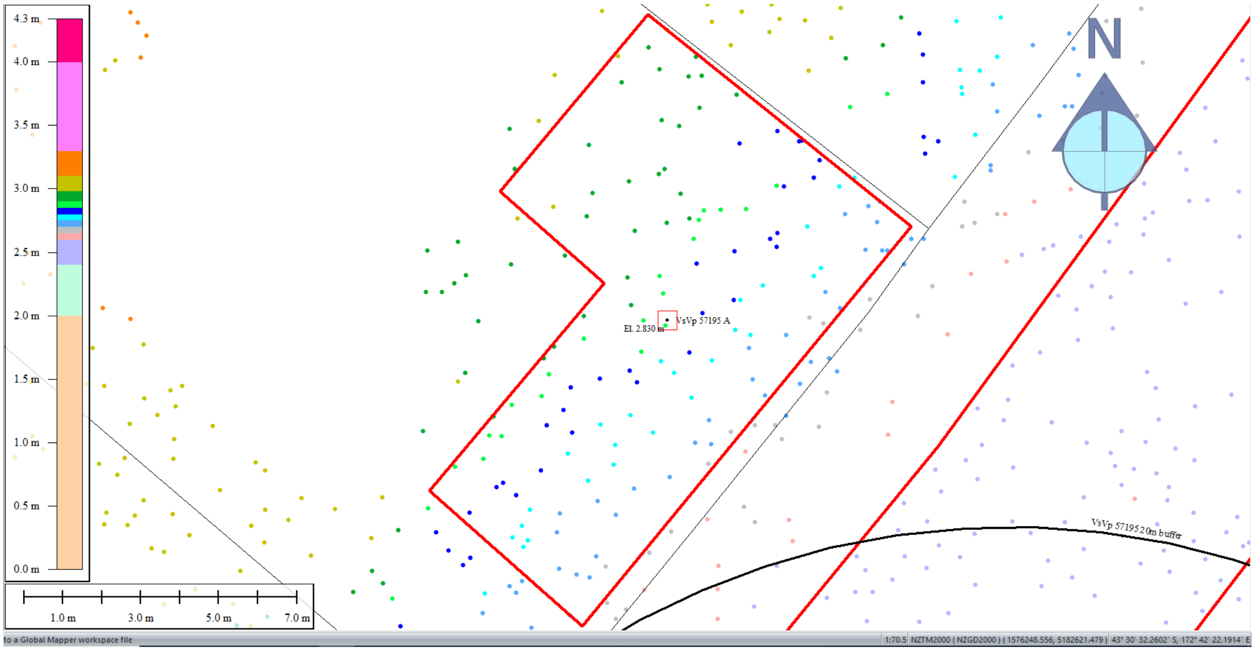

Figure 49: Ground surface elevation averaged over 50-m buffer for Patch A for May 2011 LiDAR survey.

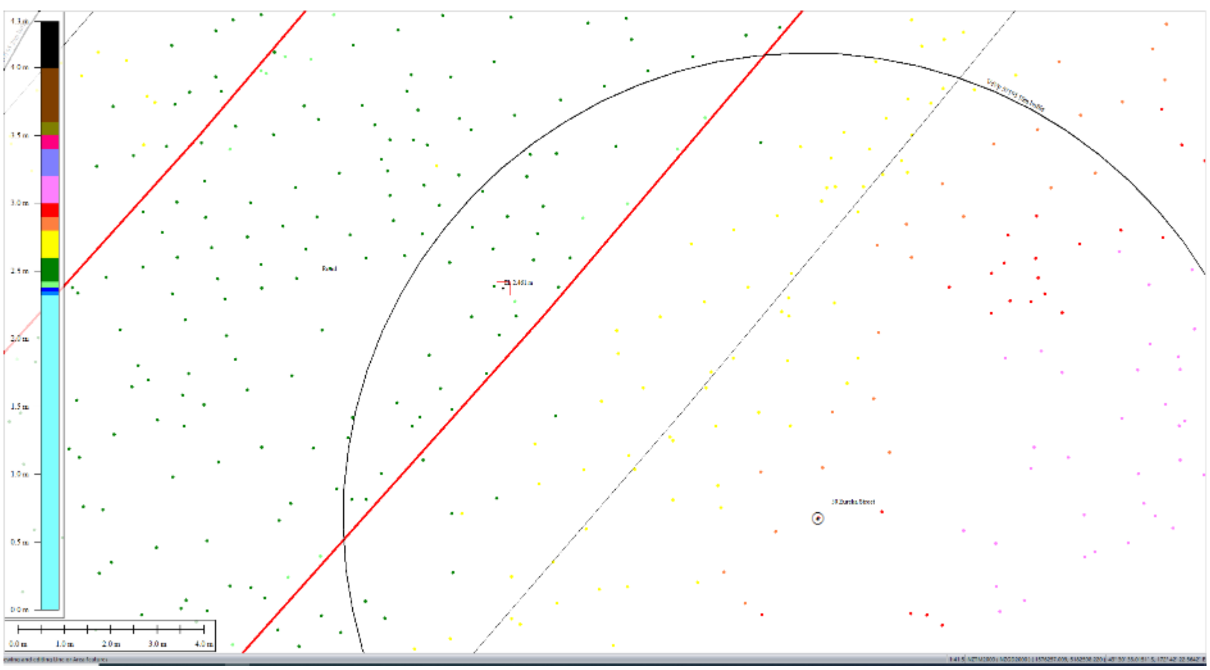

Figure 50: Ground surface elevation averaged over 10-m buffer for Road for May 2011 LiDAR survey.

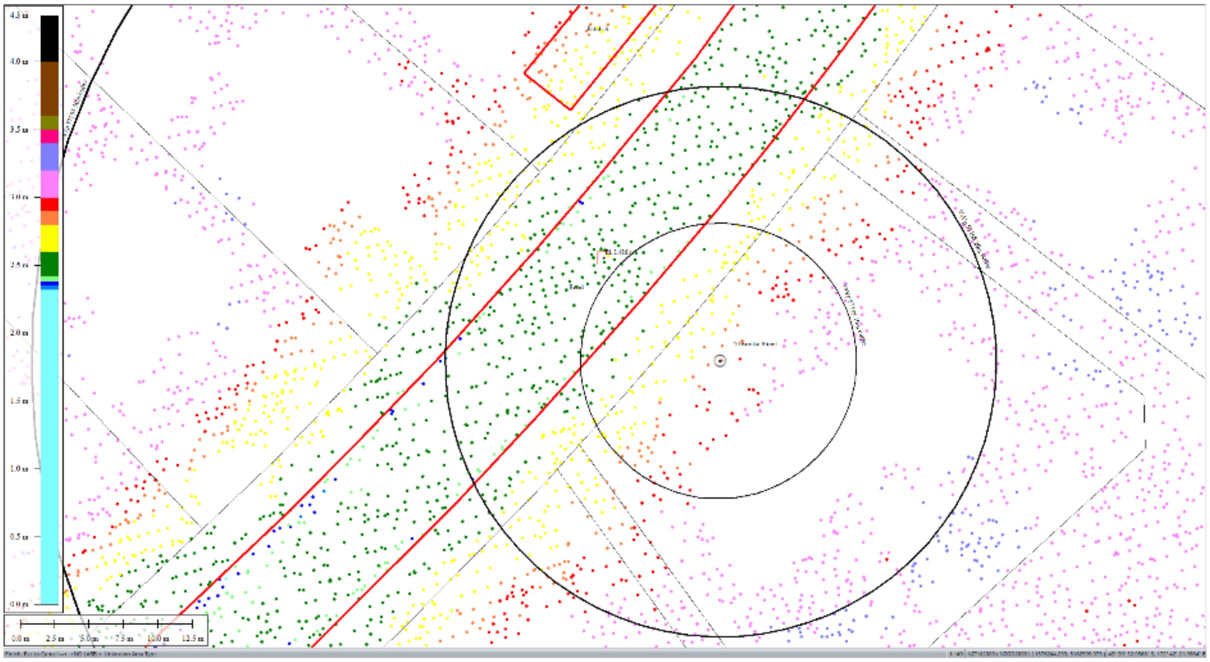

Figure 51: Ground surface elevation averaged over 20-m buffer for Road for May 2011 LiDAR survey.

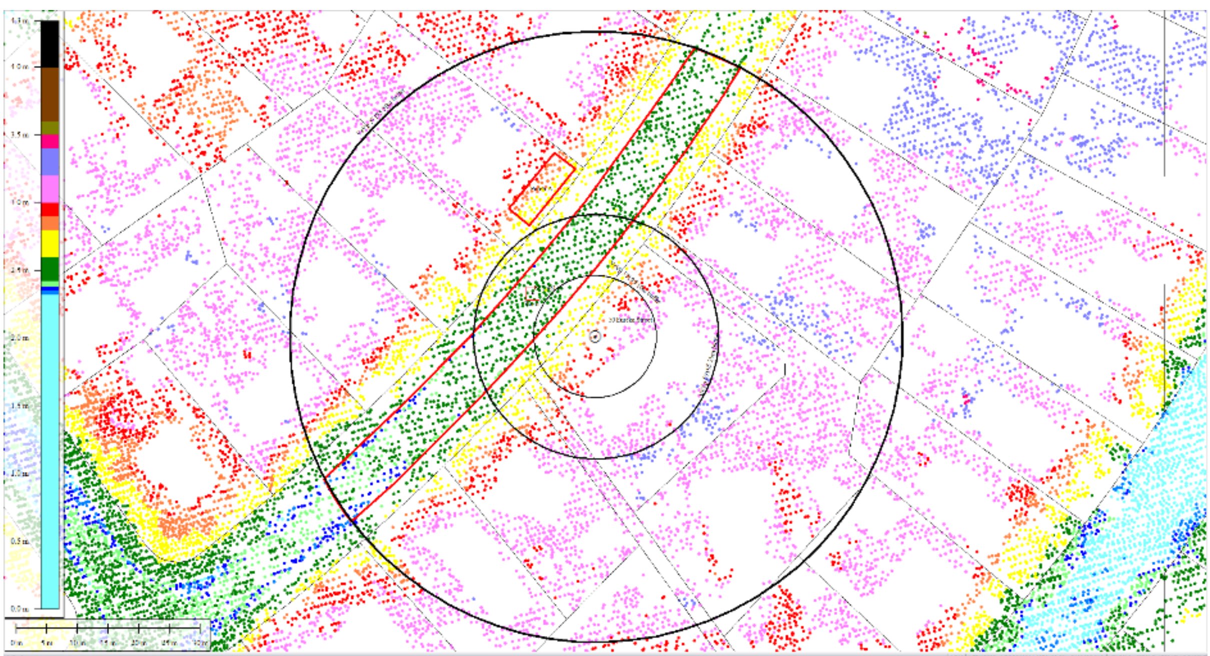

Figure 52: Ground surface elevation averaged over 50-m buffer for Road for May 2011 LiDAR survey.

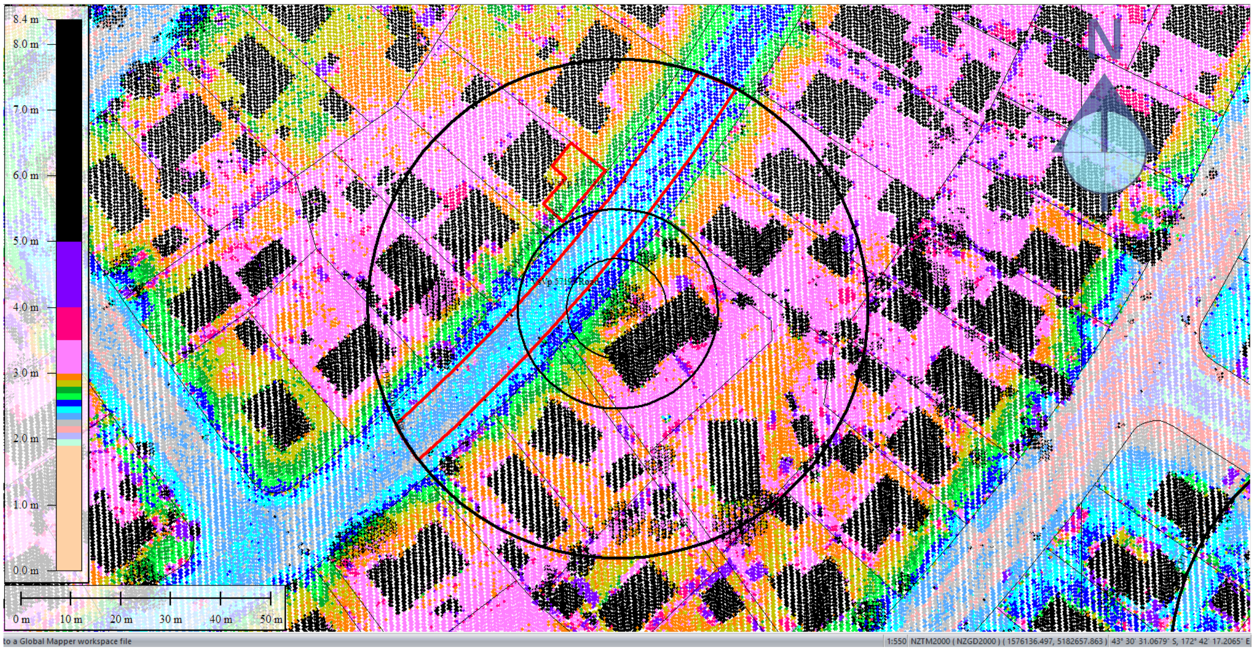

Figure 53: Sep 2011 LiDAR survey.

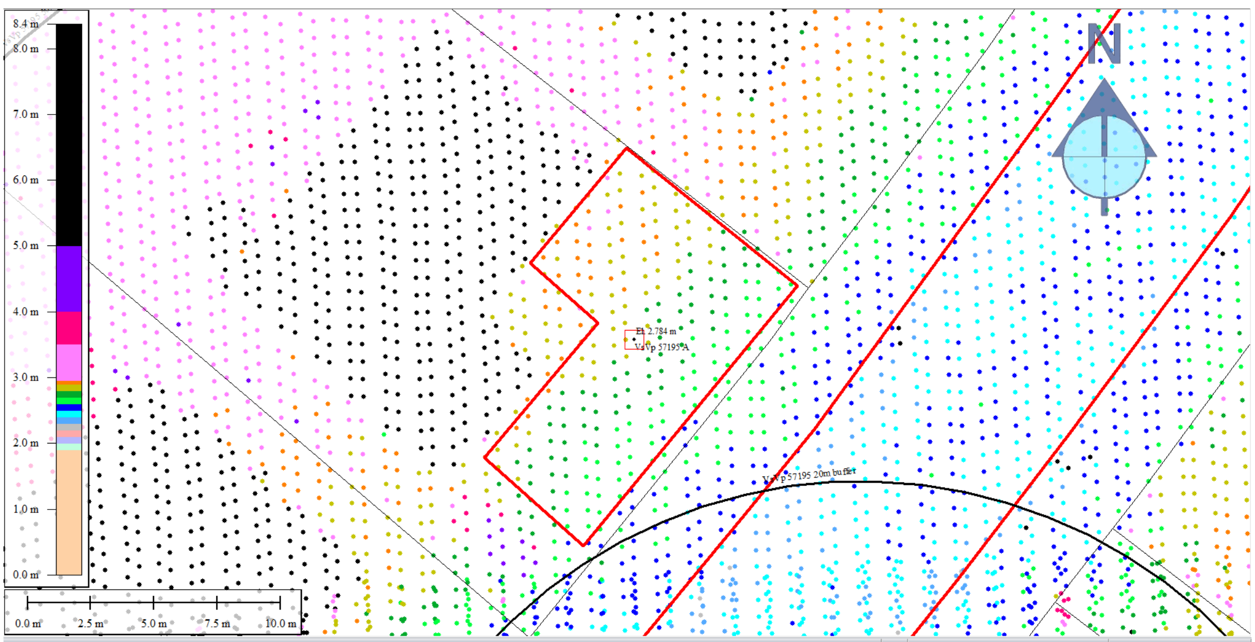

Figure 54: Ground surface elevation averaged over 50-m buffer for Patch A for Sep 2011 LiDAR survey.

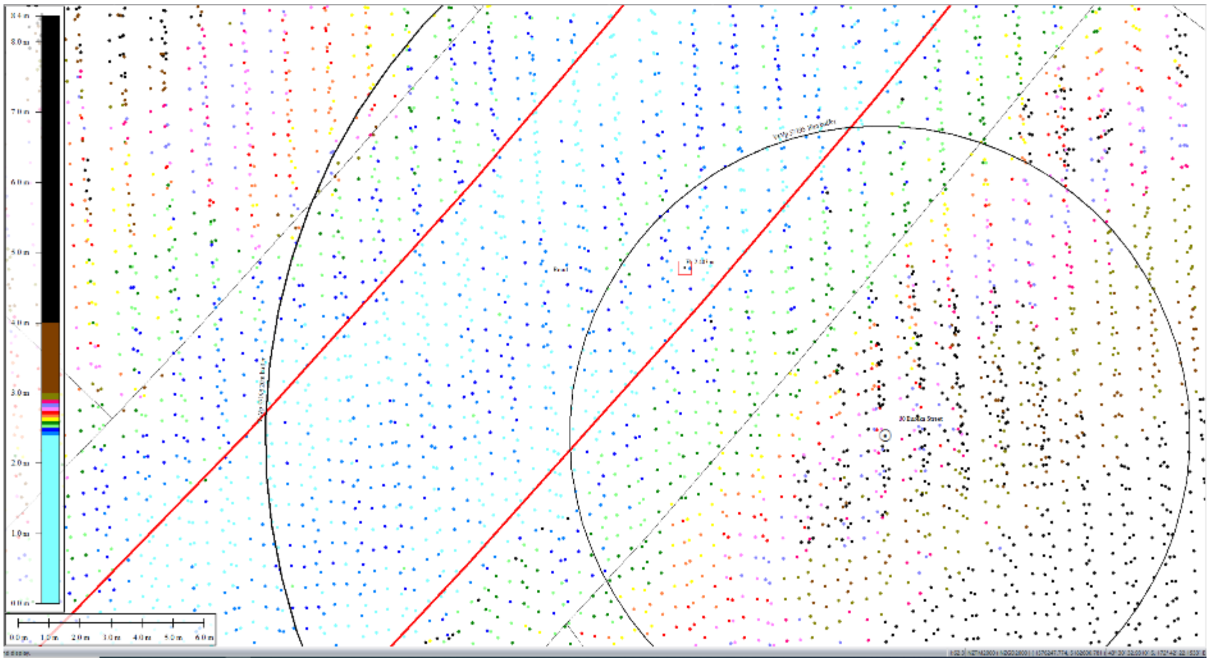

Figure 55: Ground surface elevation averaged over 10-m buffer for Road for Sep 2011 LiDAR survey.

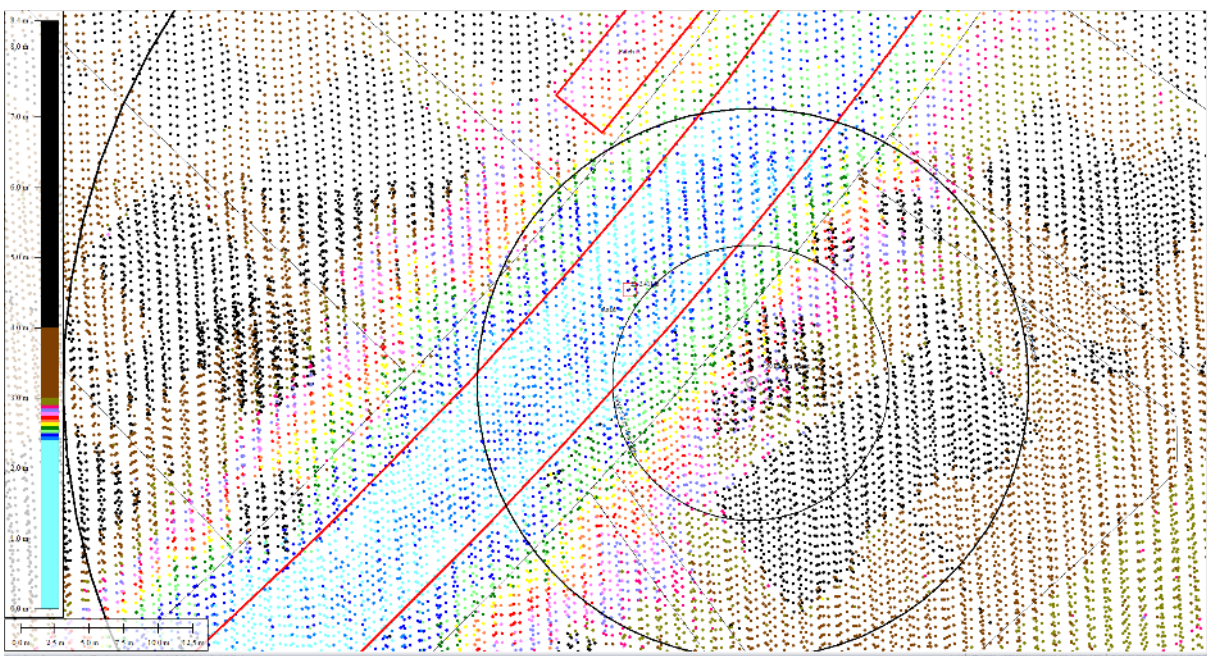

Figure 56: Ground surface elevation averaged over 20-m buffer for Road for Sep 2011 LiDAR survey.

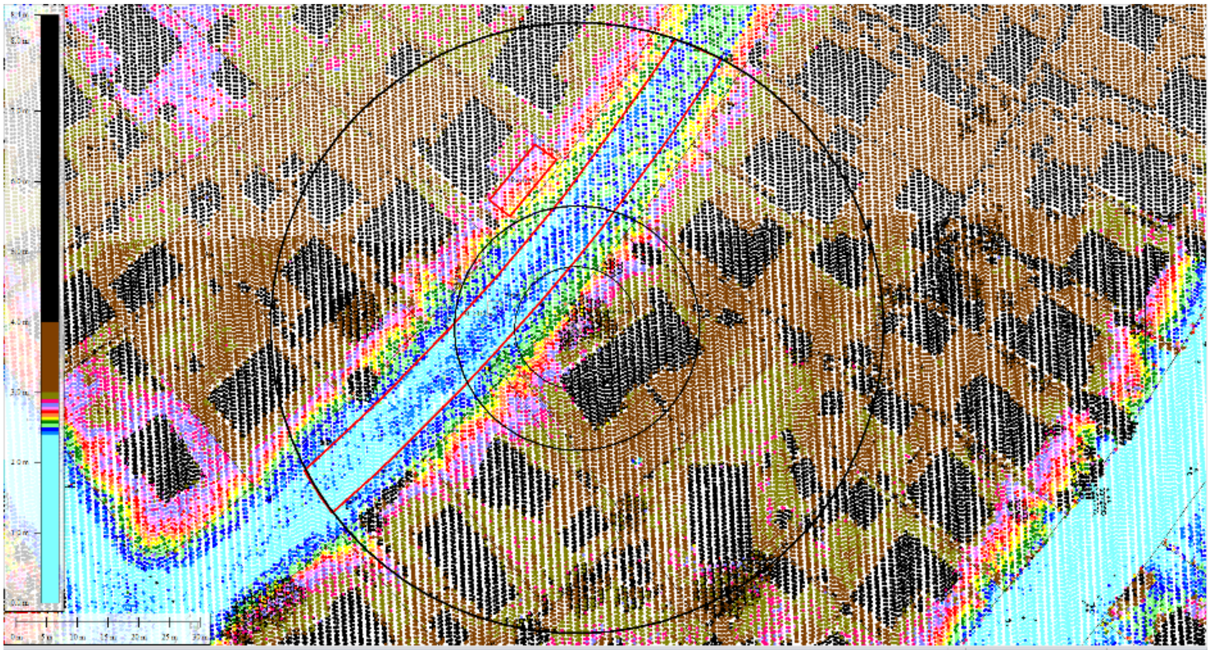

Figure 57: Ground surface elevation averaged over 50-m buffer for Road for Sep 2011 LiDAR survey.

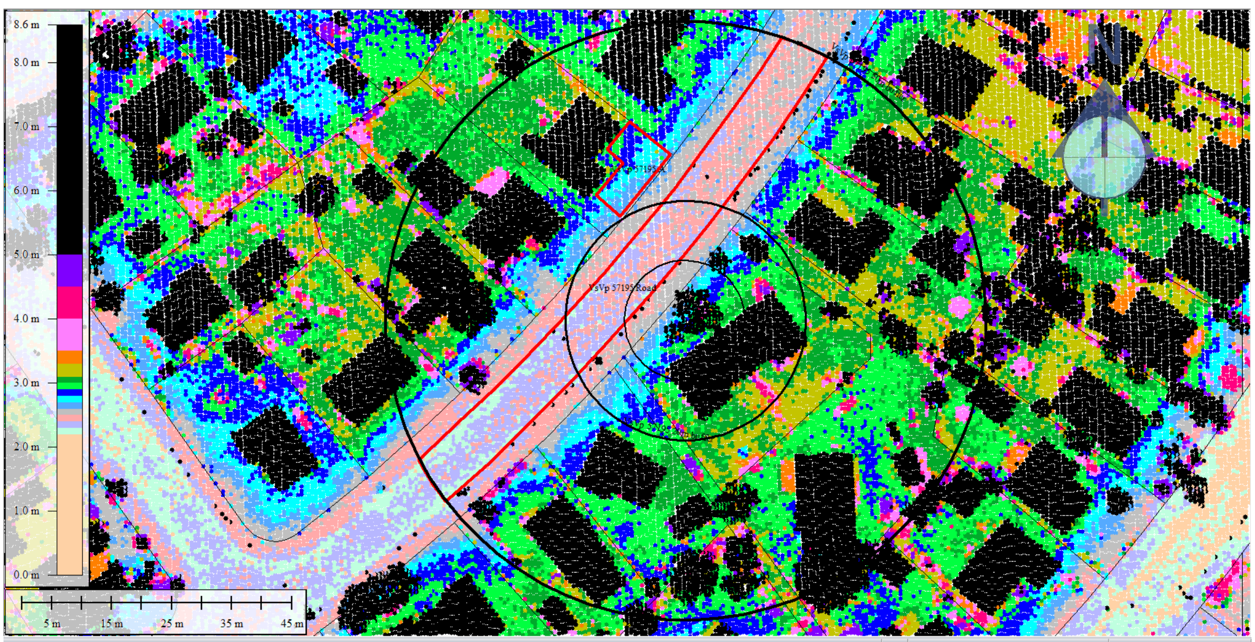

Figure 58: Feb 2012 LiDAR survey.

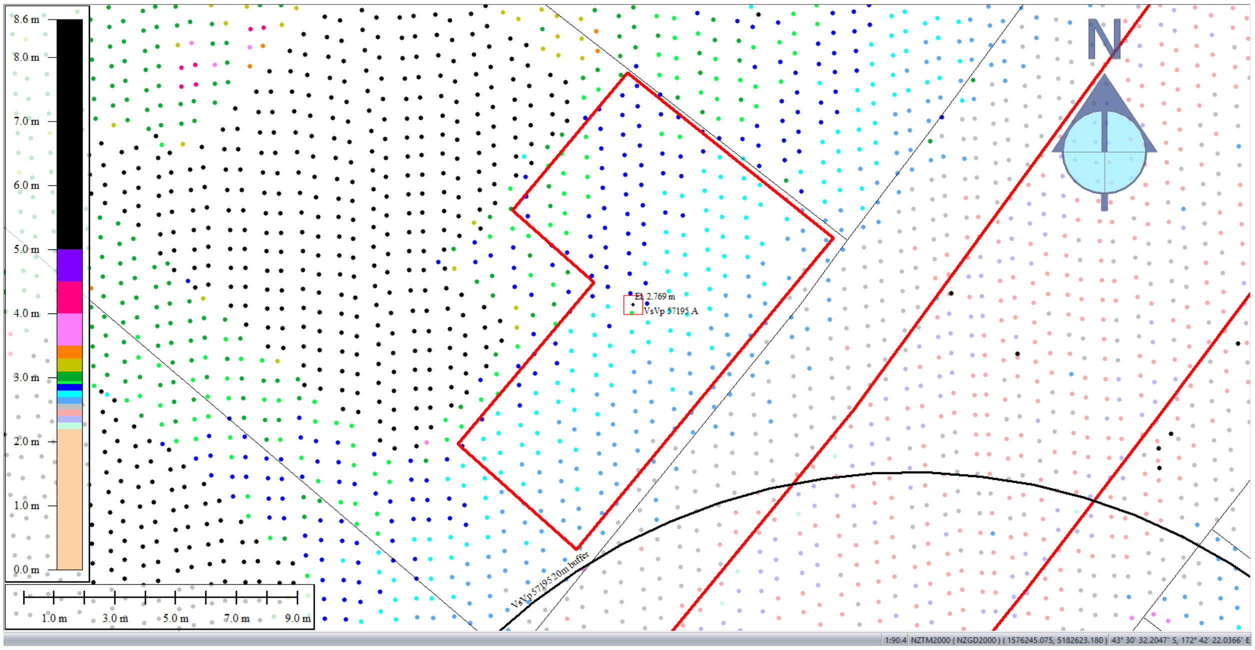

Figure 59: Ground surface elevation averaged over 50-m buffer for Patch A for Feb 2012 LiDAR survey.

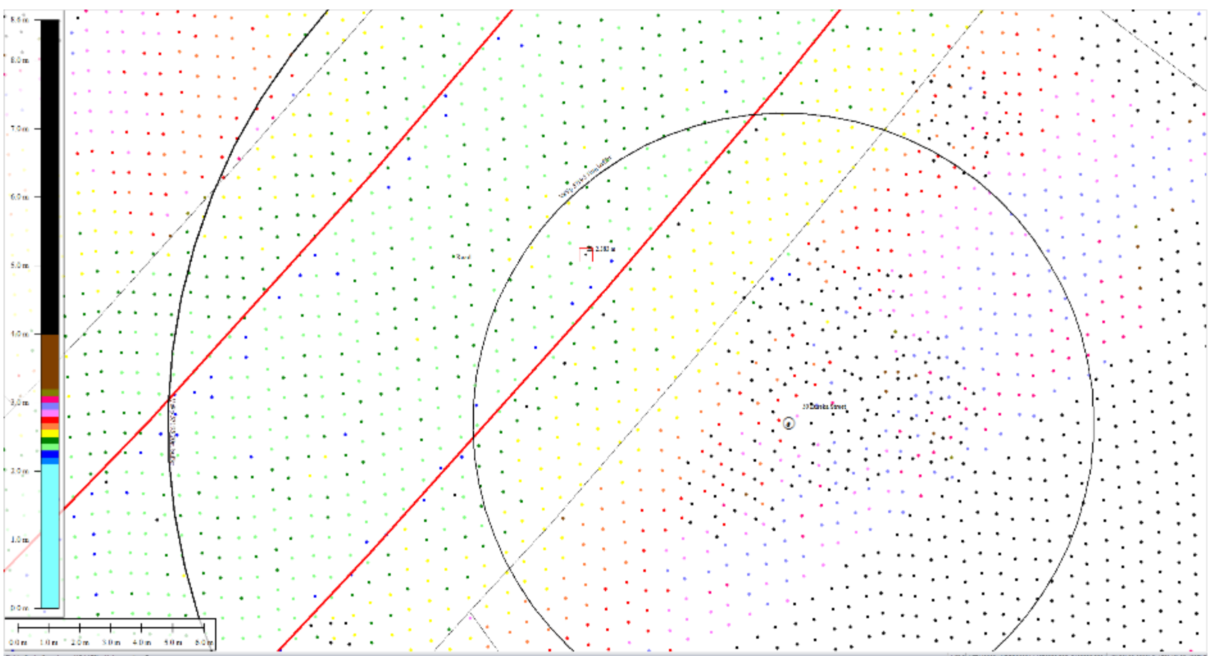

Figure 60: Ground surface elevation averaged over 10-m buffer for Road for Feb 2012 LiDAR survey.

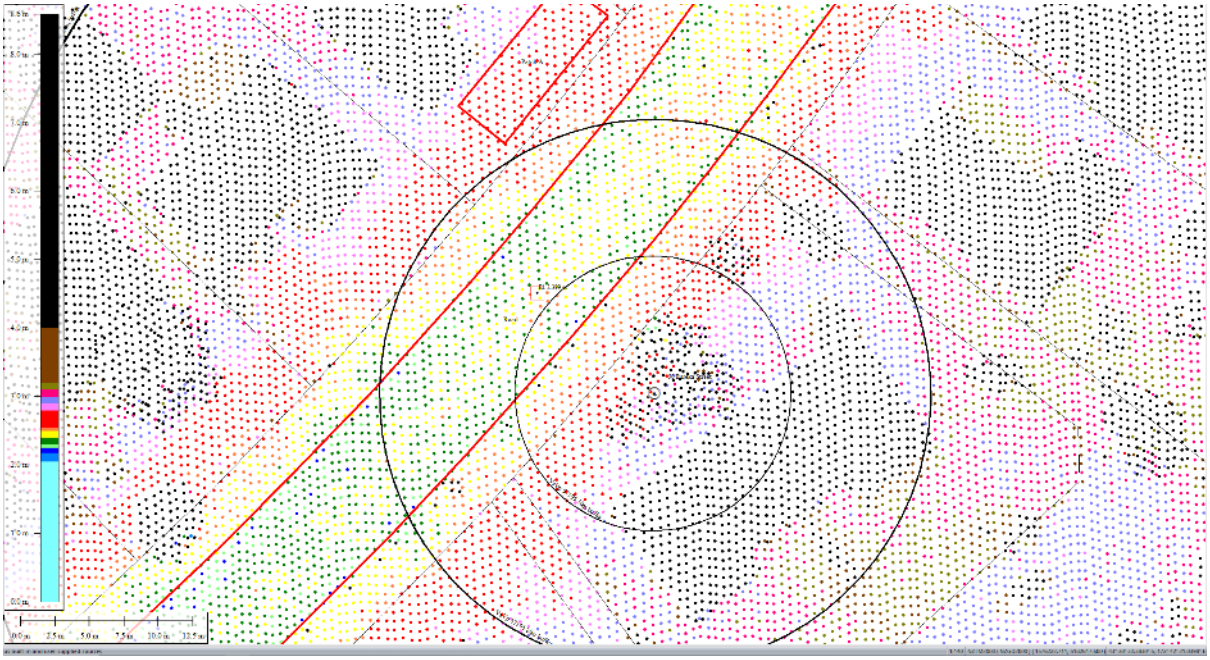

Figure 61: Ground surface elevation averaged over 20-m buffer for Road for Feb 2012 LiDAR survey.

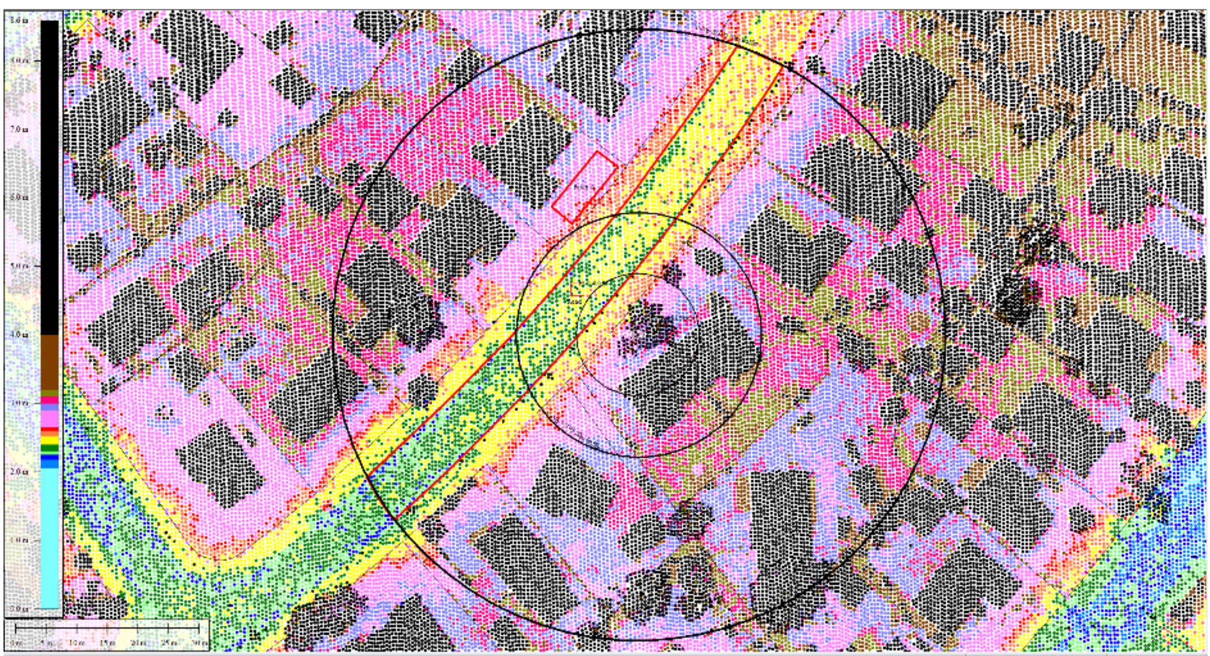

Figure 62: Ground surface elevation averaged over 50-m buffer for Road for Feb 2012 LiDAR survey.

Figure 63: Oct 2015 LiDAR survey.

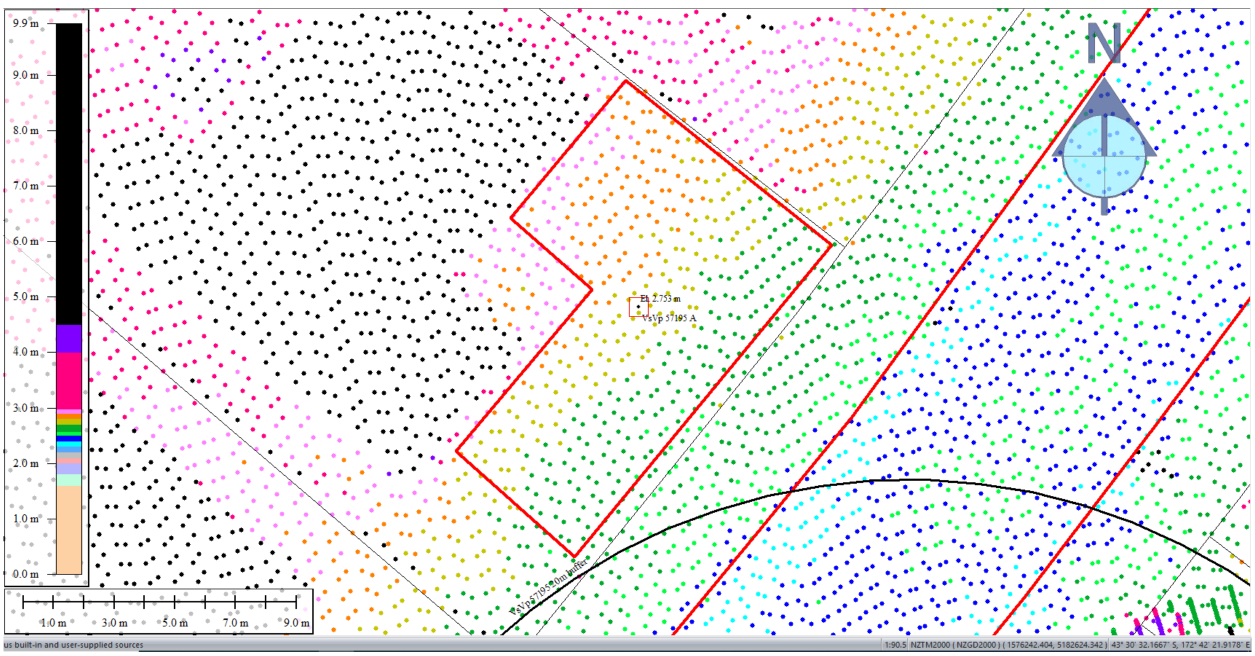

Figure 64: Ground surface elevation averaged over 50-m buffer for Patch A for Oct 2015 LiDAR survey.

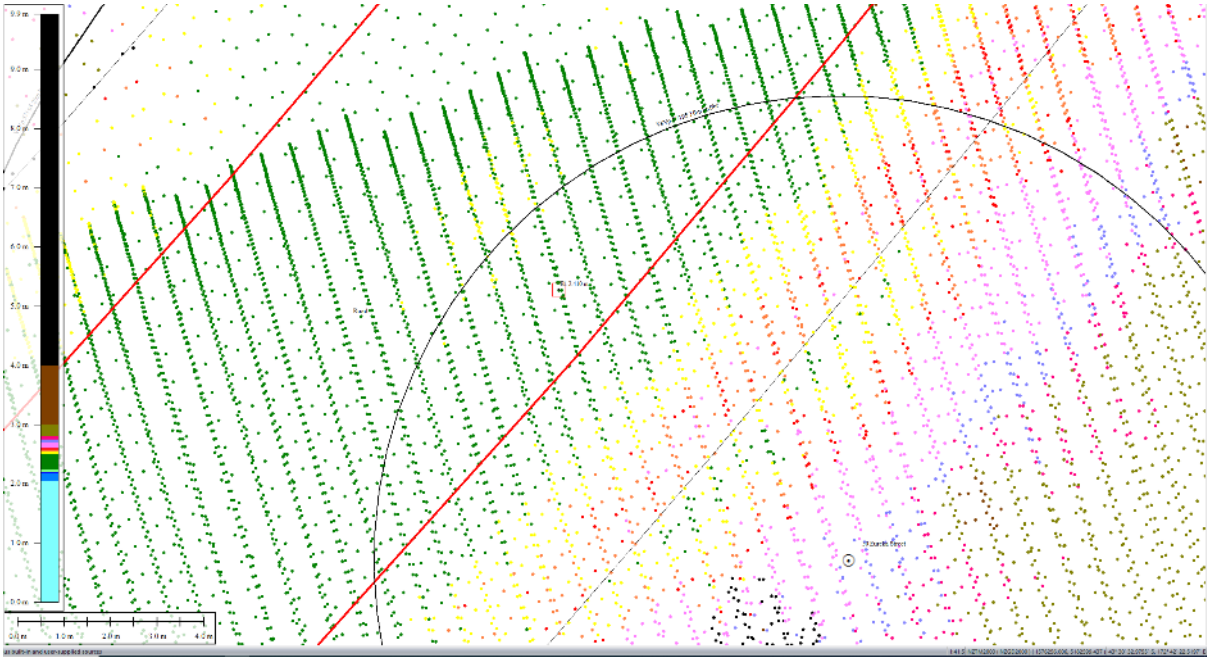

Figure 65: Ground surface elevation averaged over 10-m buffer for Road for Oct 2015 LiDAR survey.

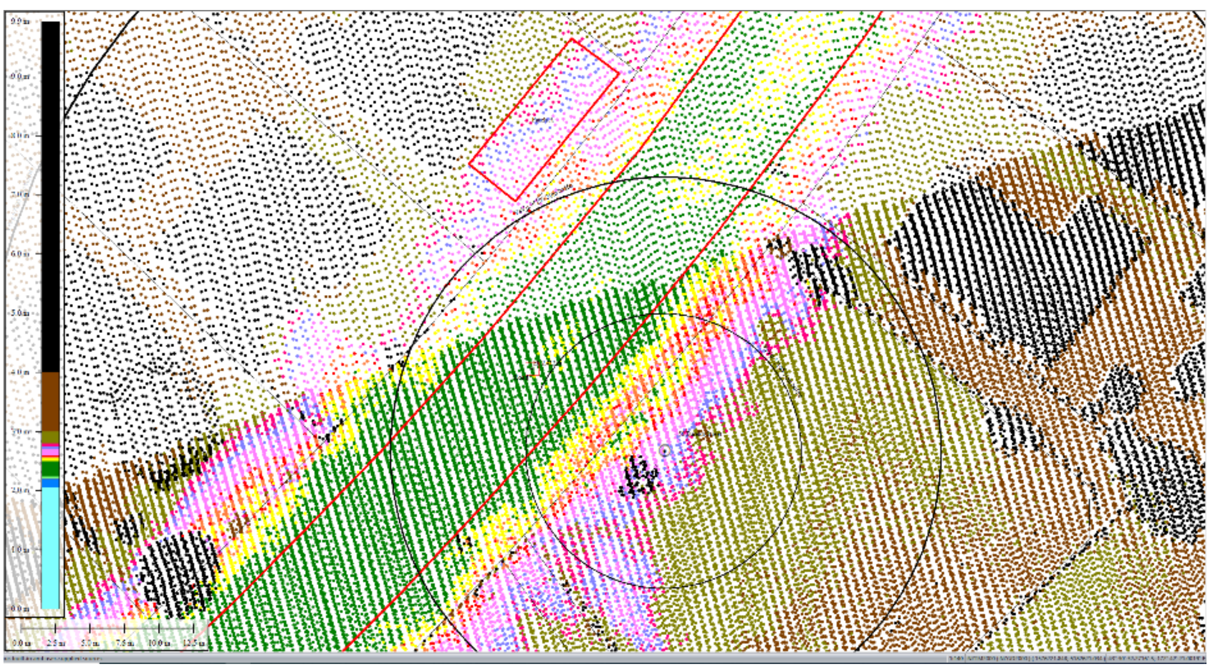

Figure 66: Ground surface elevation averaged over 20-m buffer for Road for Oct 2015 LiDAR survey.

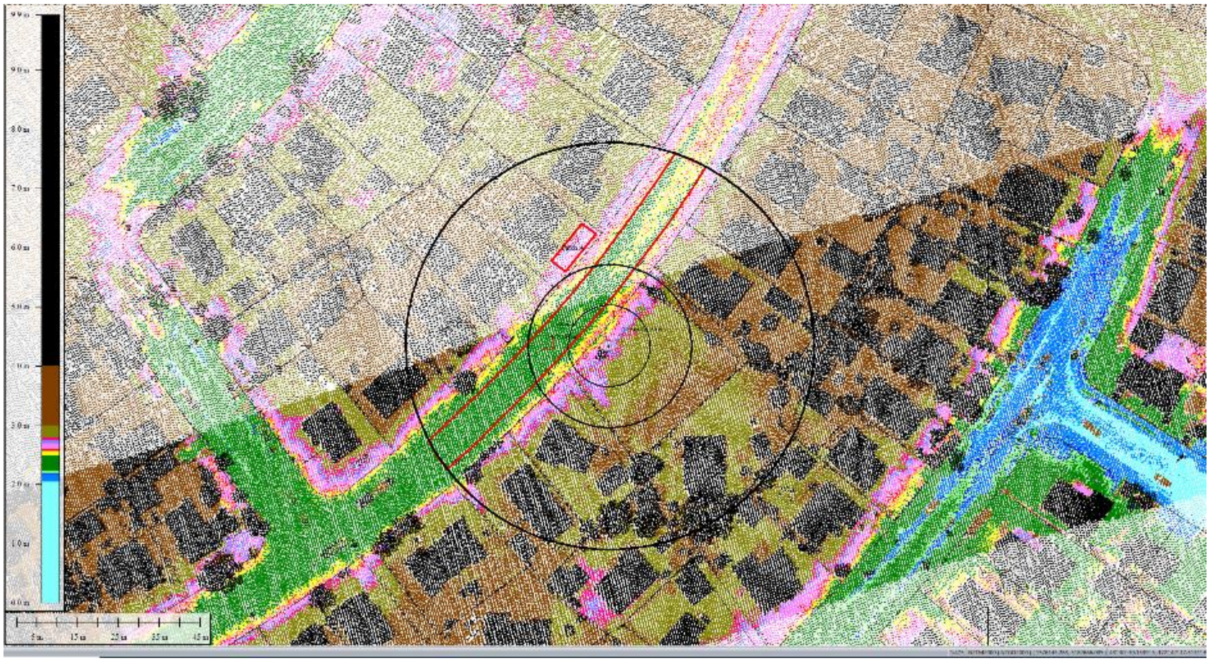

Figure 67: Ground surface elevation averaged over 50-m buffer for Road for Oct 2015 LiDAR survey.

Figure 68: Absence of ejecta at the site for Sep-10 EQ; evidence No. 1.

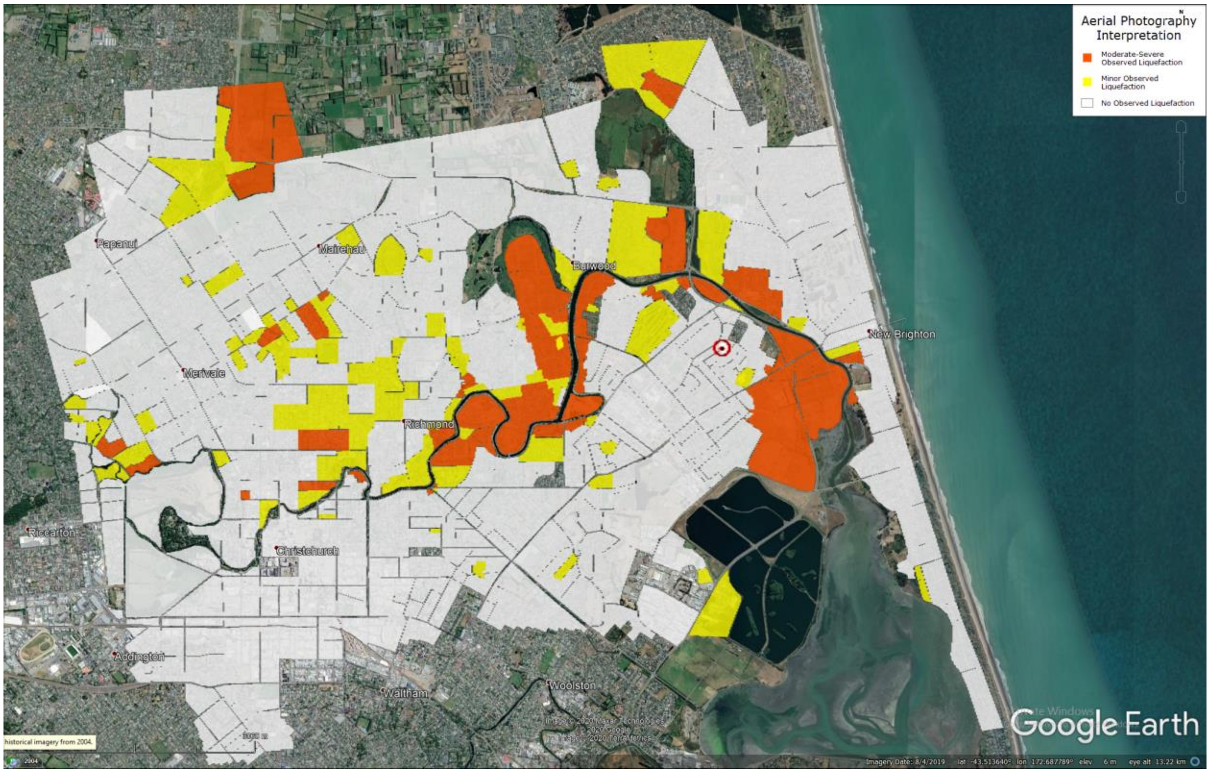

Figure 69: Liquefaction interpreted from aerial photography for Sep-10 EQ as none at the site; evidence No. 2.

Figure 70: Ejecta outline for Feb-11 EQ.

Figure 71: Ejecta at the site for Feb-11 EQ.

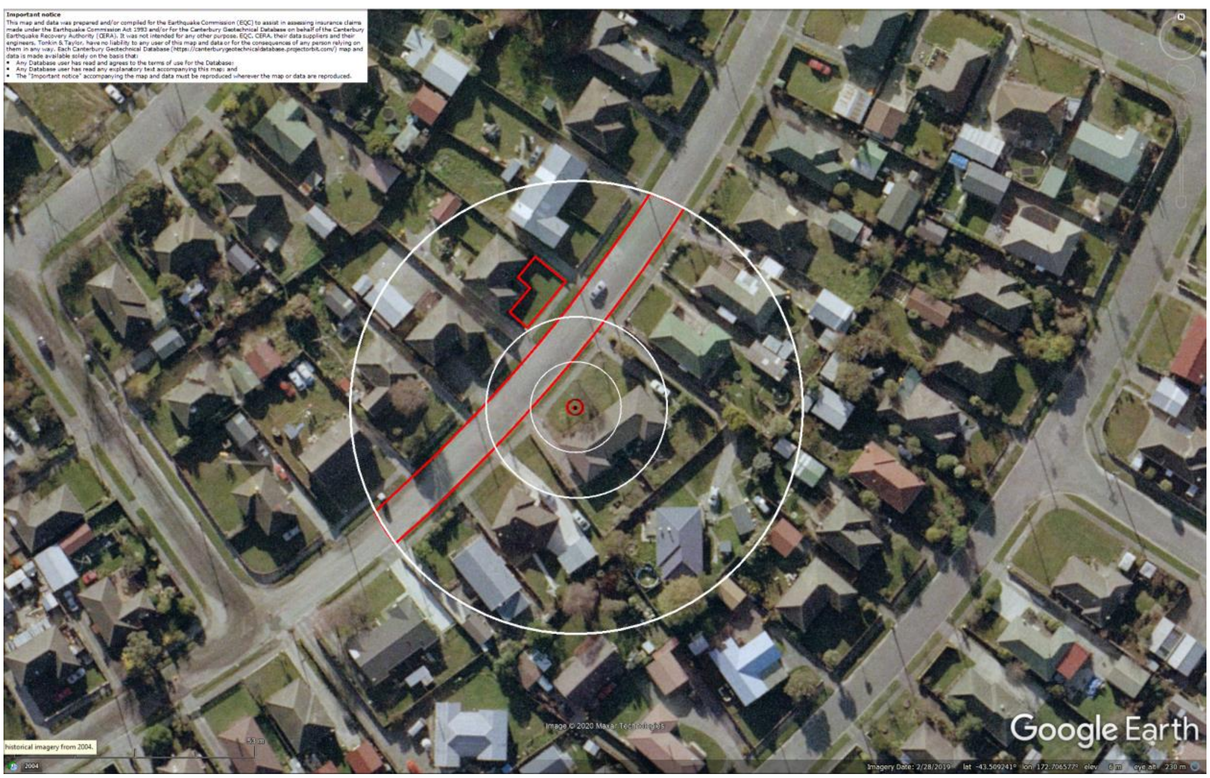

Figure 72: Ejecta outline for Jun-11 EQ.

Figure 73: Absence of ejecta for Dec-11 EQ; evidence No. 1.

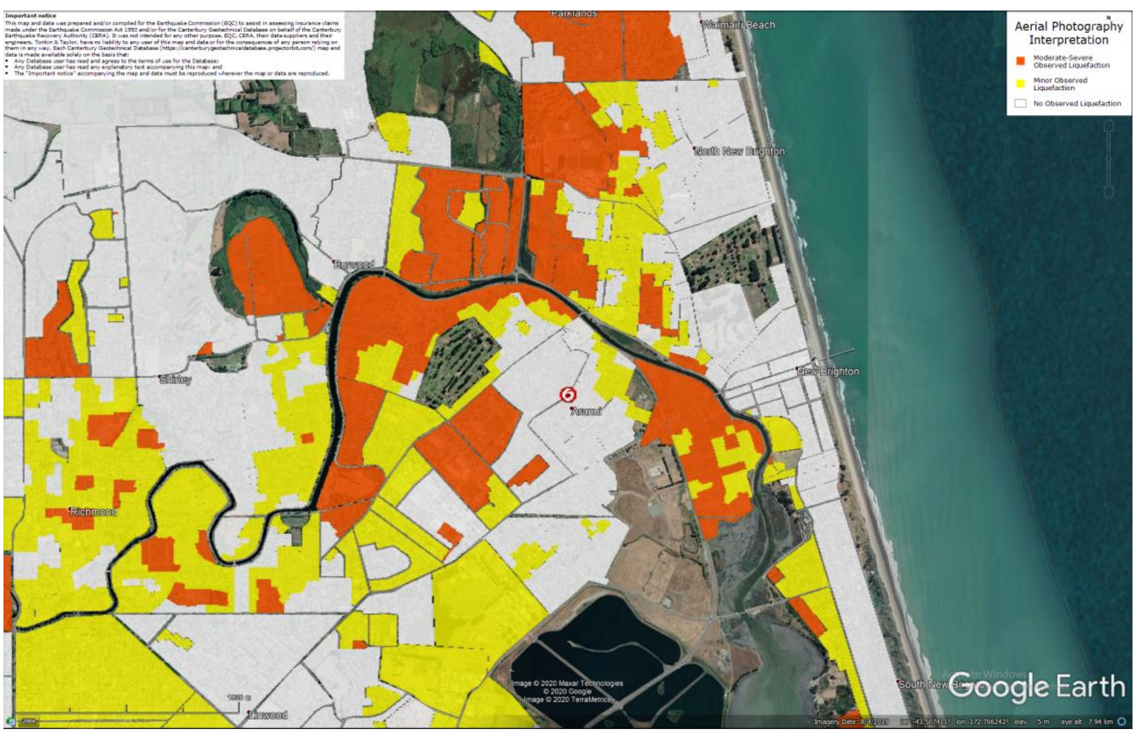

Figure 74: Liquefaction interpreted from aerial photography for Dec-11 EQ; evidence No. 2 supporting absence of ejecta at the site.

Contents of this figure cannot be shared as doing so is restricted by a Non-Disclosure Agreement.

Figure 75: EQC LDAT property inspection notes for Patch A.

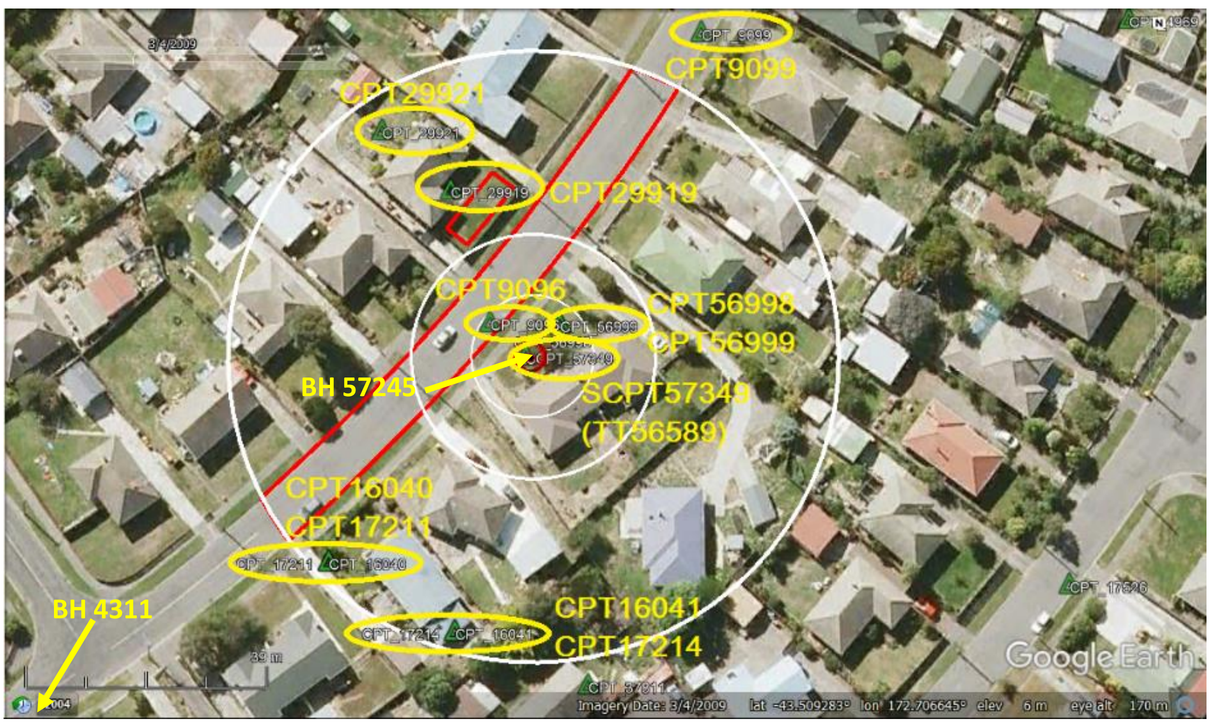

Figure 76: CPT locations at the site.

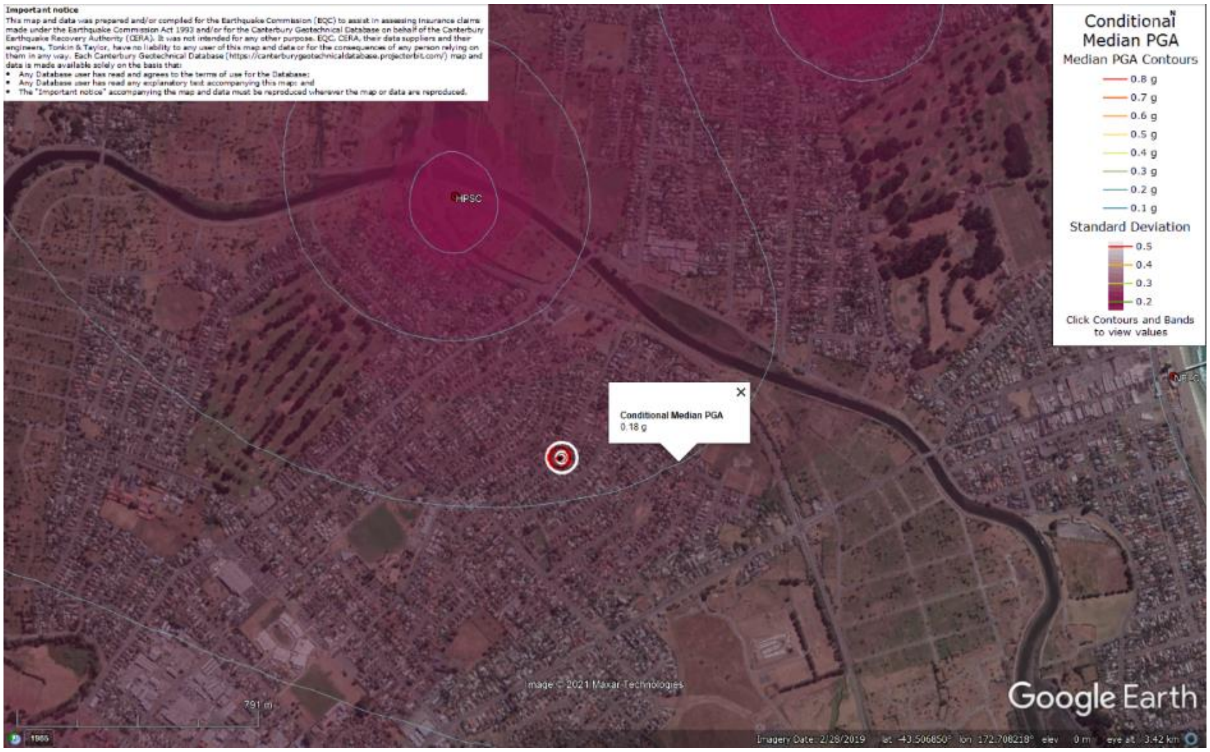

Figure 77: PGA for Sep-10 EQ (st. dev. = 0.275-0.325 ln units).

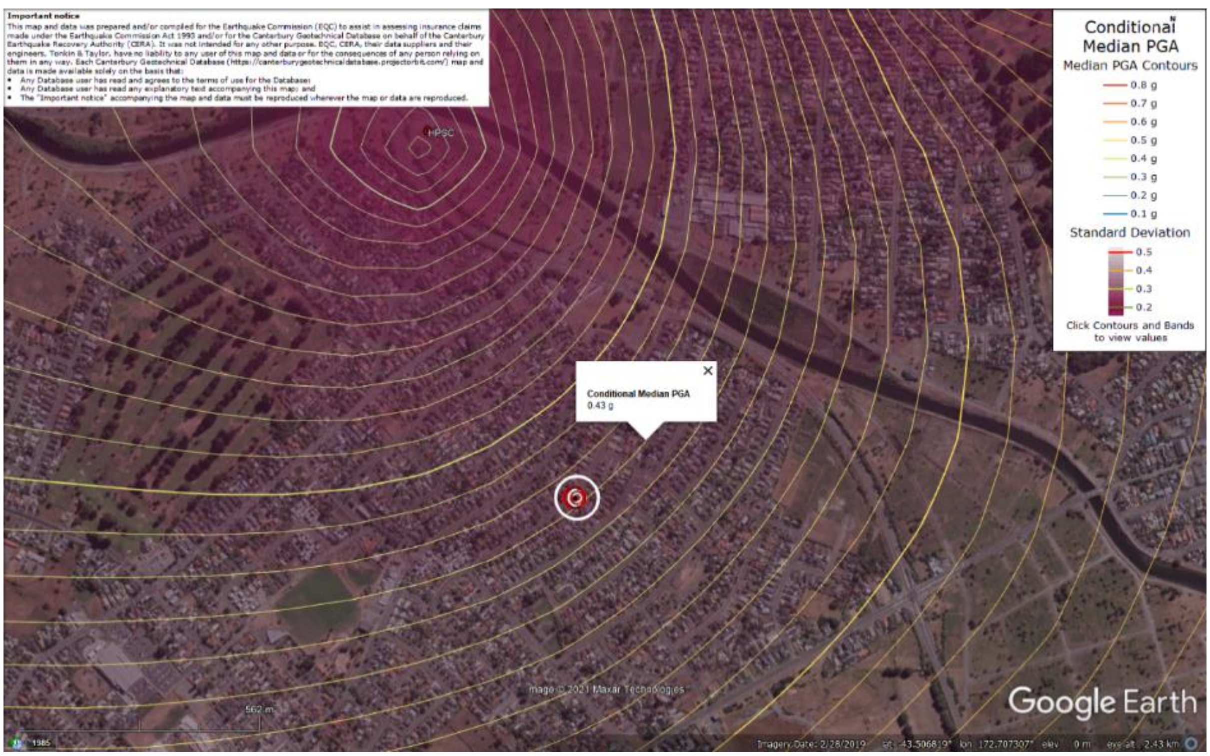

Figure 78: PGA for Feb-11 EQ (st. dev. = 0.300-0.325 ln units).

Figure 79: PGA for Jun-11 EQ (st. dev. = 0.300-0.350 ln units).

Figure 80: PGA for Dec-11 EQ (st. dev. = 0.350-0.375 ln units).

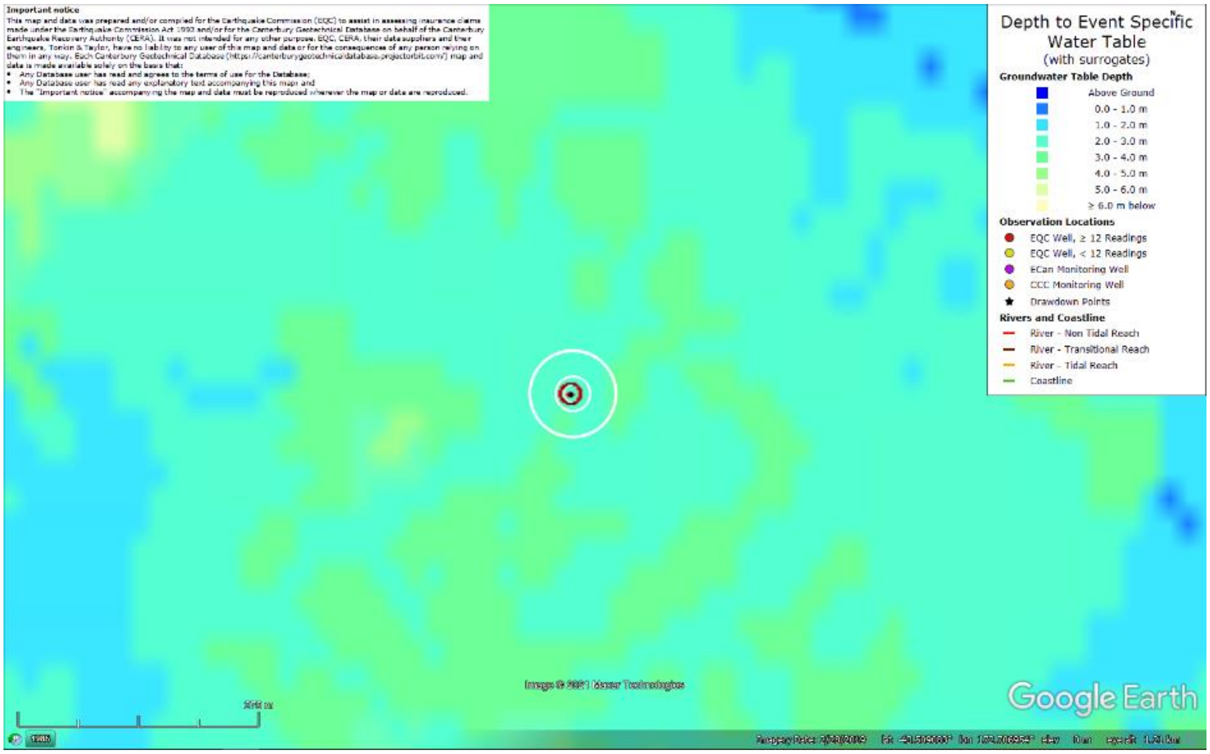

Figure 81: Depth to groundwater table for Sep-10 EQ.

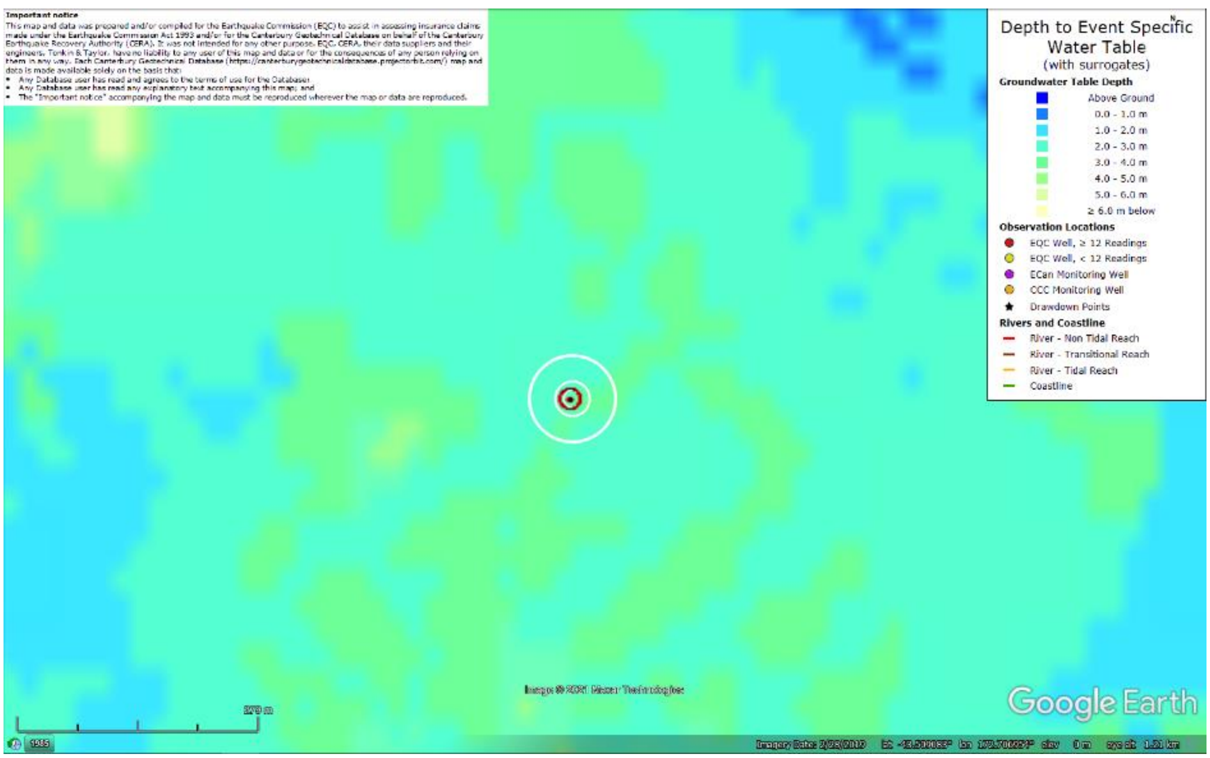

Figure 82: Depth to groundwater table for Feb-11 EQ.

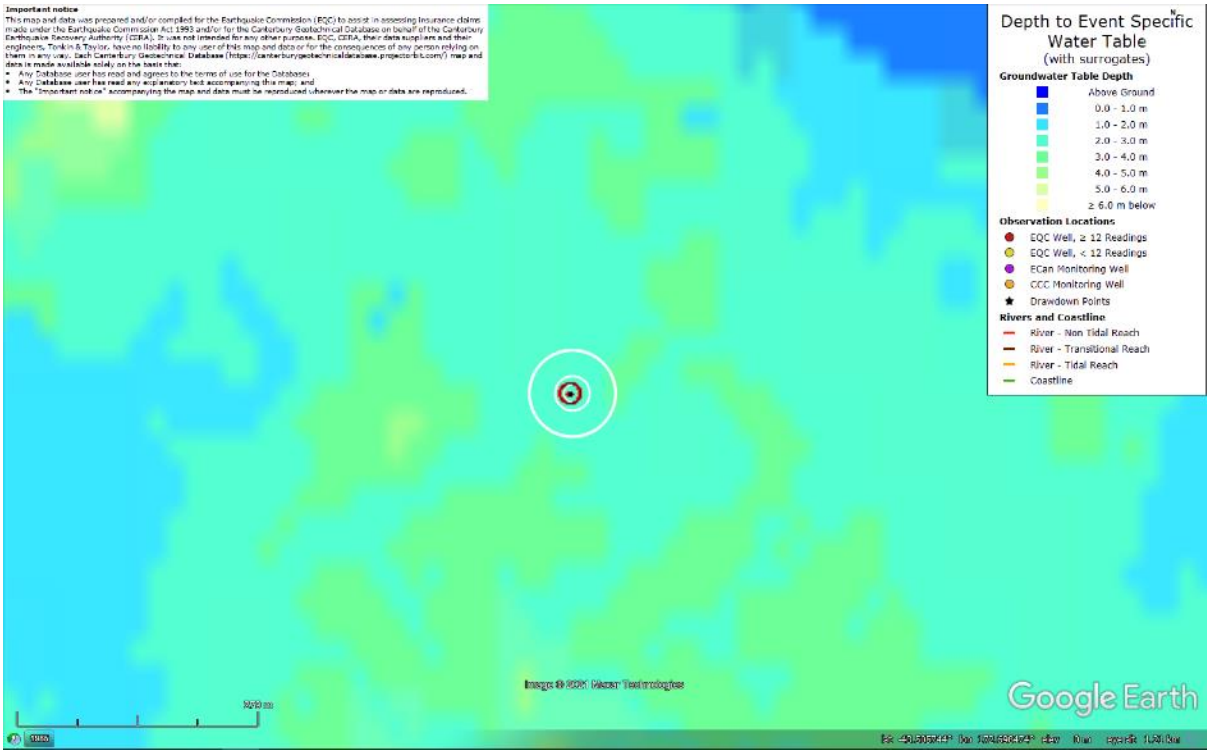

Figure 83: Depth to groundwater table for Jun-11 EQ.

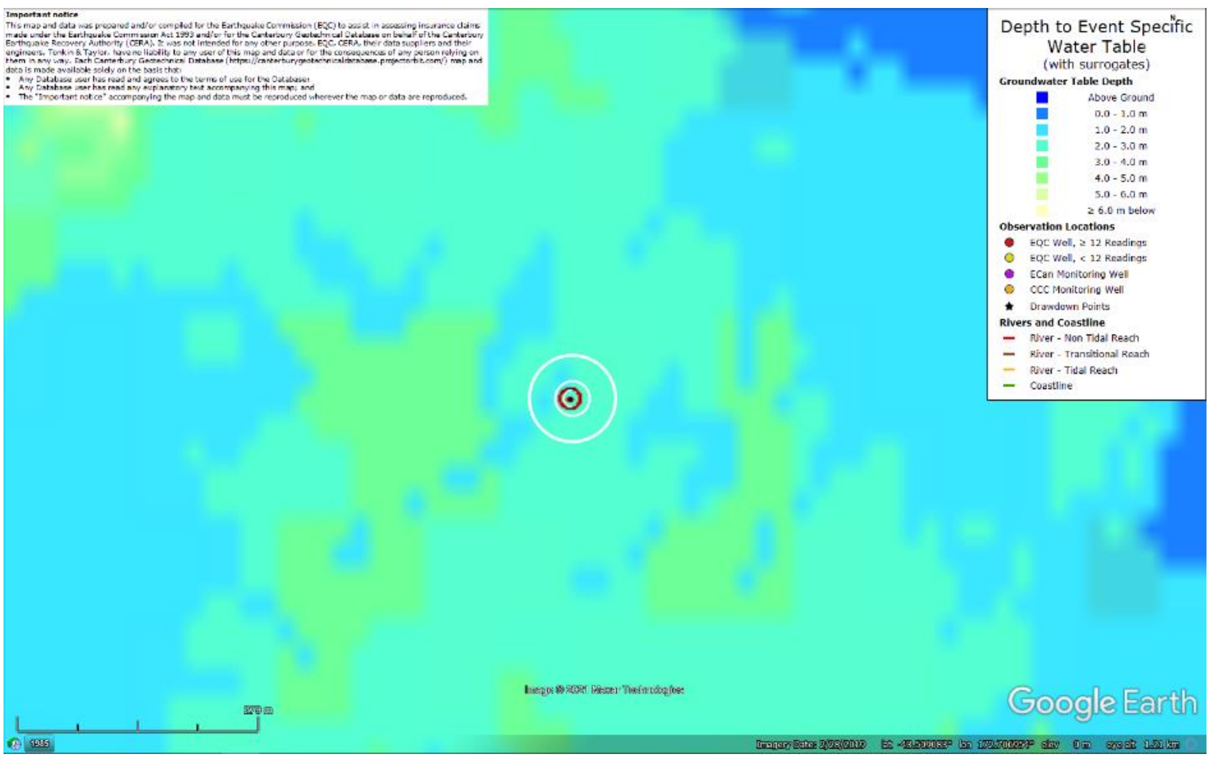

Figure 84: Depth to groundwater table for Dec-11 EQ.

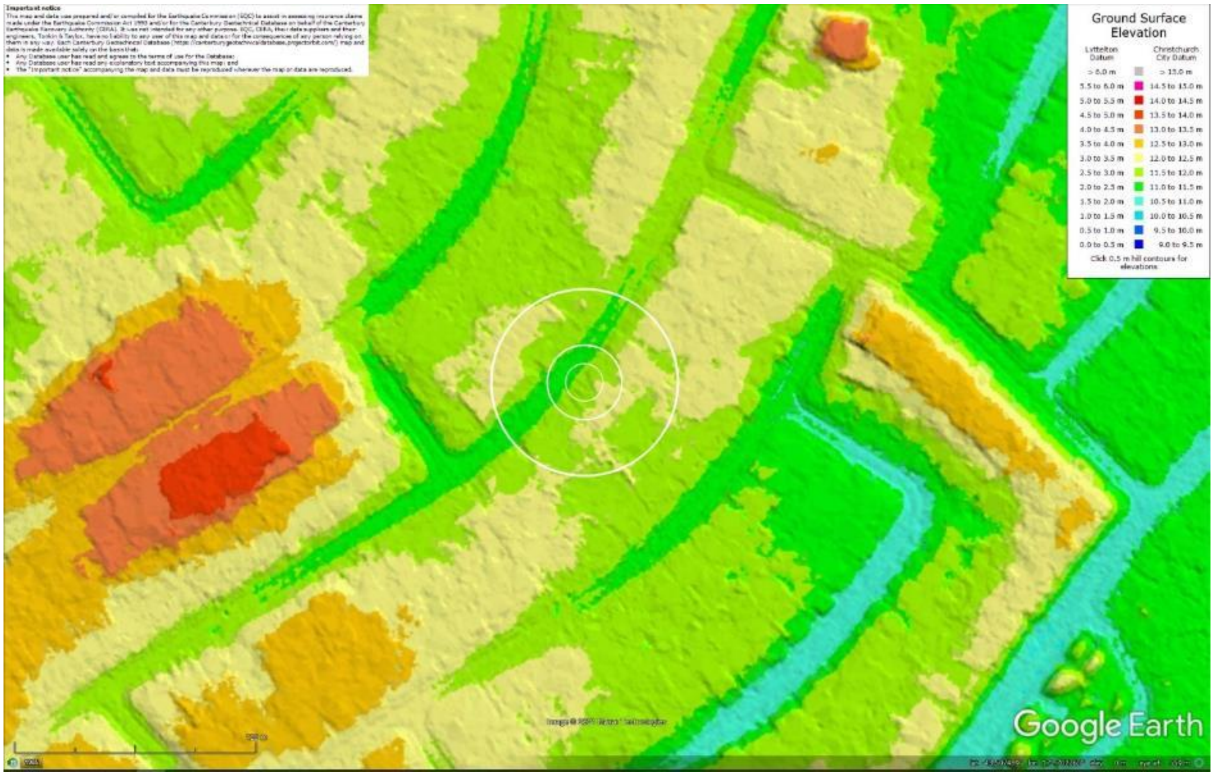

Figure 85: Ground surface elevation according to the Sep-11 LiDAR survey.

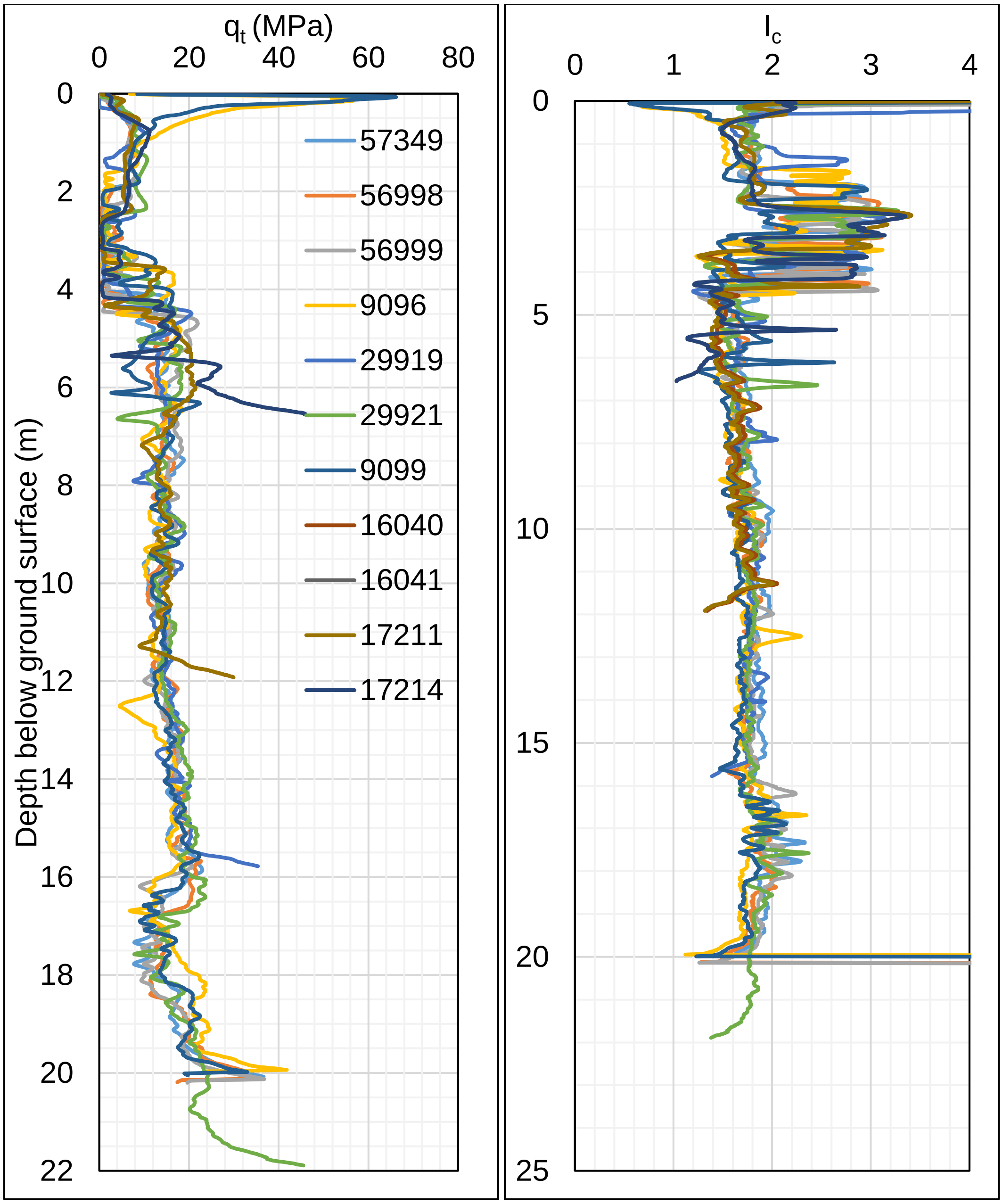

Figure 86: q_t and I_c profiles.

Note 7: The selection of CPTs for the areas considered for settlement assessment (Figure 1) is based on the proximity of the CPTs to the considered areas. In accordance with that, the following table shows CPTs that were used for the volumetric settlement analysis in *Cliq v.3.0.3.2*, a CPT soil liquefaction software developed by GeoLogismiki. (The average volumetric settlements were reported in Table 8.)

Table 12: CPT profiles used in volumetric settlement analysis for areas selected for settlement assessment.

CPT ID No.	Road 10 m-buffer	Road 20-m buffer	Road 50-m buffer	Patch A 50-m buffer
57349	✓	✓	✓	
56998	✓	✓	✓	
56999				
9096	✓	✓	✓	
29919			✓	✓
29921				
16040			✓	
17211				
16041				
17214				
9099*			✓	

Note: * denotes a CPT outside of the 50-m buffer, approximately 10 m away from it.

Table 13: CPT-based results.

EQ Event	Parameter	CPT ID 57349	56998	9096	29919	29921	9099	16040
Sep-10	S_{V1D} (mm)	3	4	6	1	1	2	0
	LSN	1	1	1	0	0	1	0
	LPI	0	0	0	0	0	0	0
	LPI_{ish}	0	0	0	0	0	0	0
	$D_{FS<1}$ (m)	undet.	undet.	undet.	undet.	undet.	undet.	undet.
Feb-11	S_{V1D} (mm)	31	33	113	15	20	101	24
	LSN	8	8	15	4	5	15	4
	LPI	3	3	7	2	2	6	1
	LPI_{ish}	3	3	5	1	1	4	1
	$D_{FS<1}$ (m)	3.06	3.41	2.78	3.80	3.21	2.55	7.23
Jun-11	S_{V1D} (mm)	14	16	27	6	5	16	3
	LSN	4	4	4	2	1	3	1
	LPI	1	1	0	0	0	0	0
	LPI_{ish}	0	0	0	0	0	0	0
	$D_{FS<1}$ (m)	3.52	undet.	12.41	undet.	undet.	5.63	undet.
Dec-11	S_{V1D} (mm)	23	27	63	11	13	53	10
	LSN	7	8	10	3	3	11	2
	LPI	2	2	3	1	1	2	0
	LPI_{ish}	2	2	0	1	1	2	0
	$D_{FS<1}$ (m)	3.22	undet.	2.78	3.80	undet.	2.28	undet.

Notes: $D_{FS<1}$ = Depth to the first liquefiable layer (FS_L<1) that is at least 200-mm thick, as determined by the Boulanger and Idriss (2016) liquefaction-triggering procedure (P_L=50%, C_{FC}=0.13, and $I_{c,cutoff}$ =2.6), and exported from *Cliq v.3.0.3.2*; undet. = the specified soil layer was not detected.

Note 7: Based on the borehole log (BH 57245, Figure 76), the groundwater table is at a depth of 1.7 m below the ground surface. The soil profile consists of (1) poorly graded sand, SP, the Yaldhurst member of the Springston formation, to a depth of 1.95 m, (2) silt, ML, the Yaldhurst member of the Springston formation, to a depth of 2.75 m, (3) sandy silt, ML, of the Christchurch formation to a depth of 3.8 m, and (4) poorly graded sand, SP, of the Christchurch formation to a depth of 11.05 m (the end of the borehole). The nearby borehole (BH 4311, Figure 76) suggests the SP layer of the Christchurch formation extends to a depth of 20 m. The laboratory test results for retrieved soil samples are not available.

Note 8: The ejecta-induced free-field settlement provided in Table 11 is an areal average settlement due to ejecta, which is based on the total settlement assessment area, A_T (provided in Table 9 and repeated in Table 14). However, the considered area was not always covered completely with ejecta; thus, it is important to provide the localized ejecta-induced settlement, too. The localized settlement due to ejecta is estimated using photographic evidence only as

$$S_{E,P\_localized} = \frac{V_E}{A_E}$$

where V_E is the total volume of ejecta within A_T and A_E is the total coverage area of ejecta within A_T. Please note that the areal ejecta-induced settlement provided in Table 14 as S_{E,P_areal} is the same as $S_{E,P}$ in Table 11, which was estimated as

$$S_{E,P\_areal} = S_{E,P} = \frac{V_E}{A_T}$$

where V_E is the total volume of ejecta within A_T and A_T is the total settlement assessment area.

Table 14a: Areal and localized ejecta-induced settlement estimates for Patch A (50-m buffer) based on photographic evidence.

Earthquake Event	A_T (m^2)	A_E (m^2)	V_E (m^3)	S_{E,P_areal} (mm)	$S_{E,P\_localized}$ (mm)
Sep-10	92.0	0	0	0	0
Feb-11	92.0	8.0	0.3-0.6	5±5	60±20
Jun-11	92.0	0	0	0	0
Dec-11	92.0	0	0	0	0

Notes: S_{E,P_areal} = $S_{E,P}$ reported in Table 11 = areal ejecta-induced settlement; $S_{E,P\_localized}$ = localized ejecta-induced settlement; A_T = total settlement assessment area; V_E = total volume of ejecta within A_T; A_E = total area of ejecta within A_T; The estimates of both areal and localized ejecta-induced settlement are rounded to the nearest 5; Final plus/minus values are also rounded to the nearest 5; NA = Not available.

Table 14b: Areal and localized ejecta-induced settlement estimates for Road (10-m buffer) based on photographic evidence.

Earthquake Event	A_T (m^2)	A_E (m^2)	V_E (m^3)	S_{E,P_areal} (mm)	$S_{E,P\_localized}$ (mm)
Sep-10	34.2	0	0	0	0
Feb-11	34.2	29.5	1.0-2.0	45±15	50±15
Jun-11	34.2	0	0	0	0
Dec-11	34.2	0	0	0	0

Notes: S_{E,P_areal} = $S_{E,P}$ reported in Table 11 = areal ejecta-induced settlement; $S_{E,P\_localized}$ = localized ejecta-induced settlement; A_T = total settlement assessment area; V_E = total volume of ejecta within A_T; A_E = total area of ejecta within A_T; The estimates of both areal and localized ejecta-induced settlement are rounded to the nearest 5; Final plus/minus values are also rounded to the nearest 5; NA = Not available.

Table 14c: Areal and localized ejecta-induced settlement estimates for Road (20-m buffer) based on photographic evidence.

Earthquake Event	A_T (m^2)	A_E (m^2)	V_E (m^3)	S_{E,P_areal} (mm)	$S_{E,P\_localized}$ (mm)
Sep-10	258	0	0	0	0
Feb-11	258	183	6.0-12.0	35±10	50±15
Jun-11	258	0	0	0	0
Dec-11	258	0	0	0	0

Notes: S_{E,P_areal} = $S_{E,P}$ reported in Table 11 = areal ejecta-induced settlement; $S_{E,P\_localized}$ = localized ejecta-induced settlement; A_T = total settlement assessment area; V_E = total volume of ejecta within A_T; A_E = total area of ejecta within A_T; The estimates of both areal and localized ejecta-induced settlement are rounded to the nearest 5; Final plus/minus values are also rounded to the nearest 5; NA = Not available.

Table 14d: Areal and localized ejecta-induced settlement estimates for Road (50-m buffer) based on photographic evidence.

Earthquake Event	A_T (m^2)	A_E (m^2)	V_E (m^3)	S_{E,P_areal} (mm)	$S_{E,P\_localized}$ (mm)
Sep-10	782	0	0	0	0
Feb-11	782	553	18.6-37.2	35±10	50±15
Jun-11	782	32.8	0.7-1.4	<5	35±10
Dec-11	782	0	0	0	0

Notes: S_{E,P_areal} = $S_{E,P}$ reported in Table 11 = areal ejecta-induced settlement; $S_{E,P\_localized}$ = localized ejecta-induced settlement; A_T = total settlement assessment area; V_E = total volume of ejecta within A_T; A_E = total area of ejecta within A_T; The estimates of both areal and localized ejecta-induced settlement are rounded to the nearest 5; Final plus/minus values are also rounded to the nearest 5; NA = Not available.

Summary 2:

- **The best estimate of the localized ejecta-induced free-field ground settlement at the 50 Eureka St site for the SEP 2010, FEB 2011, JUN 2011, and DEC 2011 earthquake is 0 mm, 60±20 mm, 0 mm, and 0 mm, respectively.**
- **The best estimate of the localized ejecta-induced free-field ground settlement at the 50 Eureka St site for the SEP 2010, FEB 2011, JUN 2011, and DEC 2011 earthquake is 0 mm, 50±15 mm, 35±10 mm, and 0 mm, respectively.**